WHARLEY PEREIRA DOS SANTOS

PROJECTIONS OF CLIMATE AND LAND USE CHANGES ON WATER EROSION IN THE TOCANTINS-ARAGUAIA BASIN

LAVRAS – MG

2022

WHARLEY PEREIRA DOS SANTOS

PROJECTIONS OF CLIMATE AND LAND USE CHANGES ON WATER EROSION IN THE TOCANTINS-ARAGUAIA BASIN

Tese apresentada à Universidade Federal de Lavras, como parte das exigências do Programa de Pós-Graduação em Ciência do Solo, área de concentração em Recursos Ambientais e Uso da Terra, para obtenção do título de Doutor.

Prof. Dr. Junior Cesar Avanzi

Orientador

Prof. Dr. Nilton Curi

Coorientador

LAVRAS - MG

2022

Ficha catalográfica elaborada pelo Sistema de Geração de Ficha Catalográfica da Biblioteca Universitária da UFLA, com dados informados pelo(a) próprio(a) autor(a).

Santos, Wharley Pereira dos.
Projections of climate and land use changes on water erosion in the Tocantins-Araguaia Basin / Wharley Pereira dos Santos. - 2022.
123 p. : il.

Orientador(a): Junior Cesar Avanzi.
Coorientador(a): Nilton Curi.
Tese (doutorado) - Universidade Federal de Lavras, 2022.
Bibliografia.

1. Water erosion. 2. Climate change. 3. Land use change. I. Avanzi, Junior Cesar. II. Curi, Nilton. III. Título.

WHARLEY PEREIRA DOS SANTOS

PROJECTIONS OF CLIMATE AND LAND USE CHANGES ON WATER EROSION IN THE TOCANTINS-ARAGUAIA BASIN

PROJEÇÕES DAS MUDANÇAS CLIMÁTICAS E DE USO E COBERTURA DO SOLO NA BACIA DO TOCANTINS-ARAGUAIA

Tese apresentada à Universidade Federal de Lavras, como parte das exigências do Programa de Pós-Graduação em Ciência do Solo, área de concentração em Recursos Ambientais e Uso da Terra, para obtenção do título de Doutor.

APROVADA em 29 de abril de 2022.

Dr. Marx Leandro Naves Silva – UFLA/DCS
Dr. Marcelo Ribeiro Viola – UFLA/DRH
Dr. Salvador Franciso Acuña Guzman – UPR
Dr. Paulo Tarso Sanches de Oliveira – UFMS

Prof. Dr. Junior Cesar Avanzi

Orientador

LAVRAS – MG

2022

A Deus, minha família e mestres,

DEDICO

AGRADECIMENTOS

À Universidade Federal de Lavras, especialmente ao Departamento de Ciência do Solo, pela oportunidade.

À Coordenação de Aperfeiçoamento de Pessoal de Nível Superior (CAPES), pela concessão da bolsa de doutorado (o presente trabalho foi realizado com apoio da Coordenação de Aperfeiçoamento de Pessoal de Nível Superior – Brasil (CAPES) – Código de Financiamento 001).

À Fundação de Amparo à Pesquisa do Estado de Minas Gerais (FAPEMIG) e ao Conselho Nacional de Desenvolvimento Científico e Tecnológico (CNPq).

Ao conjunto de professores das diferentes áreas do PPGCS, pelo afeto e dedicação.

Aos professores Junior Cesar Avanzi e Nilton Curi, pela orientação, paciência e disposição para ajudar.

A todos técnicos e demais funcionários do DCS-ESAL/UFLA, em especial à Dirce, Dulce, Doroteo e Maria Alice.

A todos os colegas de departamento.

Aos meus pais Adão e Maria pelo amor e apoio em todas as minhas decisões nas diferentes etapas da minha vida, aos meus irmãos Wellington e Welma e às minhas sobrinhas.

A aqueles que me proporcionaram companheirismo, amor e apoio em todos os momentos difíceis da minha vida.

Muito obrigado!

“O solo é o elo de ligação entre as rochas comuns e a

atmosfera, e entre os restos mortais da Terra

e a continuidade da vida”.

Grenville A.J. Cole, 1913.

RESUMO GERAL

Os cenários de mudanças climáticas, relatados em estudos recentes, aliados ao uso e manejo inadequado do solo, constituem em um agravante fator para sustentabilidade dos agroecossistemas. Esses fatos tendem a acarretar a degradação de recursos naturais como solo, água e florestas, limitando o desenvolvimento sustentável dos sistemas produtivos. Dentre os agravantes, a erosão hídrica decorrente da possibilidade de elevação do potencial erosivo das chuvas e alteração do uso do solo é um fator de relevância em estudos que envolvem mudanças de cenários futuros. Assim, é essencial a modelagem de fatores relacionados à erosão hídrica do solo, principalmente em regiões do Brasil com grande potencial agrícola e hidrelétrico. Objetivou-se então com esse trabalho, avaliar o risco potencial de erosão hídrica sob mudança climática na bacia Tocantins-Araguaia, maior bacia hidrográfica inteiramente brasileira, baseando-se no fator erosividade da chuva –fator R da Equação Universal das Perdas de Solo (USLE – acrônimo em inglês)– simulado para a condição de controle do clima presente próximo e para condições futuras a partir de dados diários de precipitação pluviométrica obtidos de um conjunto de modelos climáticos em dois cenários de mudanças climáticas - RCP4.5 e RCP8.5. Esses cenários são oriundos do quinto Relatório de Avaliação do Painel Intergovernamental sobre Mudanças Climáticas (IPCC – sigla em inglês) e se baseiam em forçantes radiativas para simulação de variáveis climáticas ao longo do século XXI. Além do fator relacionado ao clima, o mapeamento de variáveis relacionadas ao uso e cobertura do solo é de grande importância para a análise das mudanças advindas da expansão da atividade agrícola dentro da bacia Tocantins-Araguaia e o seu impacto sobre as mudanças climáticas. Nesse contexto, cenários futuros de uso e cobertura do solo foram preditos utilizando autômatos celulares e cadeias de Markov (CA-Markov) em duas sub-bacias com grande destaque para a atividade agropecuária dentro da bacia Tocantins-Araguaia. Partindo-se de uma menor escala de planejamento (sub-bacia) para a larga escala, foi avaliado o relacionamento entre o risco potencial de erosão hídrica e o comportamento do NDVI em uma série histórica na bacia Tocantins-Araguaia. Os resultados mostraram como a expansão de áreas de pastagem e agricultura com base em padrões próprios de mudança distribuiu-se na escala de sub-bacia. Esse estudo deixou evidente como as mudanças futuras do uso e cobertura da terra e as predições de erosão hídrica com base em simulações do fator R se interagem em bacias hidrográficas. Os resultados aqui relatados ajudam instituições de pesquisa, governo e agricultores a atuarem juntos frente às mudanças climáticas.

Palavras-chave: Erosão hídrica, uso e cobertura da terra, mudança climática, conservação do solo e da água

GENERAL ABSTRACT

The climate change scenarios, reported in recent studies, combined with the improper use and management of the soil, are an aggravating factor for the sustainability of agroecosystems. These facts tend to lead to the degradation of natural resources such as soil, water and forests, limiting the sustainable development of production systems. Among the aggravating factors, water erosion resulting from the possibility of increasing the erosive potential of rainfall and land use change is a relevant factor in studies involving future scenario changes. Therefore, modeling factors related to soil water erosion is essential, mainly in regions of Brazil with great agricultural and hydroelectric potential. The objective of this study was to evaluate the potential risk of water erosion under climate change in the Tocantins-Araguaia basin, the largest entirely Brazilian watershed, based on the rainfall erosivity factor - R factor of the Universal Soil Loss Equation (USLE). The R-factor was simulated for the condition of control of the near present climate and for future conditions from daily rainfall data obtained from a climate model ensemble in two climate change scenarios - RCP 4.5 and RCP 8.5. These scenarios originate from the fifth Assessment Report of the Intergovernmental Panel on Climate Change (IPCC) and are based on radiative forcing to simulate climate variables throughout the 21st century. In addition to the climate-related factor, the mapping of variables related to land use and land cover is of great importance for the analysis of changes arising from the expansion of agricultural activity within the Tocantins-Araguaia basin and its impact on climate change. In this context, future land use and land cover scenarios were predicted using cellular automata and Markov chain (CA-Markov) in two sub-basins, with the large industries for agriculture and cattle-raising prevailing in Tocantins-Araguaia basin. Working from a smaller scale of planning (sub-basin) to a large scale, the relationship between the potential risk of water erosion and the behavior of the NDVI was evaluated in a historical series in the Tocantins-Araguaia basin. The results showed how the expansion of pasture and agriculture areas based on their own patterns of change has been distributed in the sub-basin scale. This study revealed how future land use and land cover changes and water erosion predictions based on R-factor simulations interact in watersheds. The results reported here help research institutions, government, and farmers to act together facing climate change.

Keywords: Water erosion, land-use and land-cover, climate change, soil and water conservation

SUMÁRIO

PRIMEIRA PARTE – INTRODUÇÃO GERAL

1 INTRODUÇÃO

A avaliação dos impactos que as mudanças climáticas podem produzir em escala regional é determinante para o planejamento de atividades agropecuárias e de proteção ambiental a longo prazo. Modelos Climáticos Globais (MCGs) são utilizados para providenciar informações sobre mudanças climáticas em diferentes cenários de emissões de gases de efeito estufa. São vários os MCGs utilizados ao redor do planeta para a predição climática global e a partir desses modelos surge a necessidade de refinamento de escala para o detalhamento climático regional, originando dessa forma modelos climáticos regionais aninhados aos MCGs (HEWITSON; CRANE, 1996).

As mudanças climáticas estão intrinsicamente relacionadas com as mudanças na cobertura vegetal dos solos de um determinado local (SOUZA et al., 2000; CHU et al, 2019; OJO et al., 2021). Essa relação pode ser negativamente afetada pela exposição da superfície do solo diante das circunstâncias ocasionadas por eventos extremos do clima e do uso e manejo inadequado (SALVADOR; DE BRITO, 2018; SATTLER et al., 2018; TESSEMA et al., 2021). Entre os fatores climáticos, o potencial erosivo das chuvas é o agente deflagrador da erosão hídrica do solo e a redução da cobertura vegetal de proteção contra o impacto das gotas de chuva constitui um agravante.

A organização e o planejamento de atividades agropecuárias devem levar em consideração as projeções de diferentes modelos climáticos. Esses modelos podem ser corrigidos e aplicados em escala regional, simulando dessa forma com boa acurácia os eventos climáticos (TEUTSCHBEIN; SEIBERT, 2012; MARAUN, 2016; OKKAN; KIRDEMIR, 2016; TURCO et al., 2017). Ao longo dos anos, o Painel Intergovernamental sobre Mudanças Climáticas (IPCC, na sigla em inglês) vem lançando novos relatórios sobre mudanças no clima. Acompanhando esses relatórios, os modelos climáticos passaram a permitir um aumento nos níveis de confiança das previsões (MOLINA; ABADAL, 2021). Mesmo assim, as incertezas ainda carecem de ser exploradas e avaliadas em escala regional.

As perdas de solo por erosão hídrica durante a expansão agrícola de uma região, geralmente ocorrem devido a mudanças no uso da terra e nas propriedades do solo ao longo do tempo (VIJITH; HURMAIN; DODGE-WAN, 2018; ABDULKAREEM et al., 2019). Os efeitos negativos dessas mudanças podem ser atenuados através da adoção de práticas conservacionistas e do planejamento da readequação do uso das terras diante de possíveis cenários de mudança no clima.

Localizado entre as regiões norte e centro-oeste do Brasil, a bacia do Tocantins-Araguaia é considerada de grande importância nacional, sendo parte integrante da última fronteira agrícola do país. Com o aumento da pressão exercida por atividades antrópicas, é crescente a preocupação com o manejo sustentável do solo (DONZELI et al., 2006). Assim, a adoção do uso de tecnologias de conservação do solo e da água tende a ser uma alternativa promissora, visando conciliar o desenvolvimento agrícola regional e as políticas socioambientais diante dos desafios climáticos do século XXI.

O mapeamento dos fatores de risco da erosão hídrica é uma ferramenta importante quando se compara a evolução do uso e ocupação do solo dentro de diferentes cenários de mudanças no clima. Com esse objetivo, cabe à pesquisa a primeira etapa rumo ao planejamento sustentável do uso dos recursos água e solo frente à iminência de fenômenos de macro e mesoescala.

1.1 JUSTIFICATIVA

Os estudos que comparam diferentes simulações climáticas por meio da utilização de técnicas estatísticas e modelagem matemática são úteis para o entendimento do comportamento climático em diversos cenários. Devido a essa utilidade, a busca por uma melhor acurácia em resultados obtidos a partir das simulações de modelos climáticos persiste como objetivo principal de pesquisas que preveem condições futuras do clima para alocação de políticas públicas e ambientais. Dentre essas, estão as ligadas ao uso e à conservação do solo e da água.

A bacia Tocantins-Araguaia, por situar-se geograficamente em uma área de expansão agrícola e numa zona de transição entre os biomas Amazônia, Cerrado e Caatinga (ecótonos Amazônia-Cerrado e Cerrado-Caatinga), possui uma elevada vulnerabilidade ao potencial erosivo das chuvas. Apesar do bioma Amazônia ocupar uma pequena área do seu território, a bacia sofre grande influência das massas de ar equatoriais originadas no interior da Amazônia. Isso interfere na dinâmica dos solos e da vegetação ao longo do tempo, uma vez que as mudanças climáticas podem ocasionar retração ou migração de áreas potencialmente agricultáveis dentro da bacia. Uma maior demanda hídrica, maior exposição dos solos, juntamente com o risco potencial de erosão hídrica são fatores resultantes dos eventos extremos das mudanças no clima.

A modelagem e/ou estimativas futuras de fatores relacionados à erosão hídrica do solo justifica-se pela importância dos modelos preditivos e do conhecimento dos cenários de mudanças climáticas que possam impactar no desenvolvimento da agricultura e pecuária.

A análise do potencial erosivo das chuvas em cenários de mudanças climáticas e as mudanças assim condicionadas ao uso e manejo do solo são inovações em estudos do intenso dinamismo solo-planta-atmosfera. Isso reflete como o processo de erosão acelerada dos solos é multidisciplinar no que tange a sua exploração sustentável em agroecossistemas.

1.2 OBJETIVO

O objetivo da pesquisa foi mapear o risco potencial de erosão hídrica sob mudanças climáticas para a bacia Tocantins-Araguaia, baseando-se no fator climático erosividade média da chuva (fator R) simulado para a condição de controle do clima presente próximo e para condições futuras a partir de dados de precipitação diária obtidos dos modelos climáticos Eta-BESM, Eta-CanESM2, Eta-HadGEM2-ES e Eta-MIROC5 nos cenários de mudanças climáticas RCP 4.5 e RCP 8.5. O mapeamento de variáveis relacionadas ao fator de uso e cobertura do solo do modelo Revised Universal Soil Loss Equation (RUSLE) será usado com o objetivo principal de comparação das mudanças obtidas nas últimas décadas a partir da expansão agropecuária em sub-bacias da bacia Tocantins-Araguaia. Serão realizadas simulações futuras de mudança de uso e cobertura do solo e os resultados obtidos serão avaliados de acordo às mudanças do potencial de erosão hídrica nos diferentes cenários climáticos. Aplicar o modelo RUSLE para se verificar potencias perdas de solo futuras em função das alterações climáticas (erosividade) e de uso do solo.

2 REFERENCIAL TEÓRICO

2.1 A erosão hídrica dos solos

O uso e o manejo inadequado do solo têm levado a uma degradação dos recursos naturais disponíveis para a sobrevivência do ser humano. O uso incorreto dos recursos água e solo em atividades agropecuárias vem contribuindo para o desequilíbrio de todo o processo cíclico e dinâmico que envolve o movimento da água na Terra, alterando também os processos que envolvem a fertilização natural do solo e o transporte e armazenamento subterrâneo da água.

Nessas circunstâncias, destaca-se que, conforme o uso do solo, a disponibilidade hídrica pode ser alterada ao longo do tempo. Dessa forma, tem-se uma influência sobre o regime de chuvas em uma determinada região. A expansão agrícola constitui-se no principal fator capaz de impulsionar o desmatamento em florestas tropicais, podendo alterar os padrões de chuva em escalas local, regional e global (SPRACKLEN et al., 2018). Uma vez que parte da floresta é desmatada, superfícies heterogêneas originadas devido a grandes áreas de clareiras podem estabelecer uma circulação convectiva de mesoescala (SOUZA et al, 2000). Consequentemente, as chuvas podem ser alteradas de acordo com a dependente escala de mudanças no uso da terra a partir dos seus padrões heterogêneos, fornecendo respostas ao clima regional (D'ALMEIDA et al, 2007).

A erosão hídrica decorrente do potencial das chuvas é uma das principais causas do empobrecimento dos solos devido ao carreamento dos seus nutrientes pela ação do escoamento superficial gerado pela ação da chuva sob condições desfavoráveis de tipo de solo, relevo, clima e cobertura vegetal disponível. O processo erosivo dá-se através de três eventos consecutivos: desprendimento das partículas do solo pelo impacto das gotas de chuva, arraste e deposição dessas partículas. A complexidade do movimento do solo pela água sofre influência da quantidade, intensidade e duração da chuva, da natureza do solo, da cobertura vegetal e da declividade do terreno. São vários fatores que interagem entre si, dando origem à força erosiva da água. Alguns desses fatores favorecem o movimento do solo, outros, opõe-se a ele (BERTONI; LOMBARDI NETO, 1990)

Em grande parte do planeta, a erosão hídrica situa-se como principal forma de erosão do solo, sendo afetada por muitos fatores naturais e antrópicos (MACHADO; VETTORAZZI, 2003). Nos trópicos úmidos, a erosão acelerada possui agravantes mais sérios que em outras regiões (WEILL; SPAROVEK, 2008). Dessa forma, em agroecossistemas tropicais, ela é o principal processo de degradação da terra, especialmente se o uso do solo for mais intensificado.

No Brasil, a expansão da atividade agrícola tem levado à busca da análise de diferentes cenários de uso do solo, compondo um inventário da erosão. Nesse, a expansão agrícola dentro de áreas de vegetação nativa dos biomas Cerrado e Floresta Amazônica sem a adoção de práticas de conservação do solo e da água constitui o pior cenário para o controle da erosão hídrica (MERTEN; MINELLA, 2013), considerando ainda a complexidade de fatores que conduzem à erosão do solo.

2.2 Modelagem da erosão hídrica

Uma das formas de predizer as perdas de solo por erosão hídrica é através da Equação Universal das Perdas de Solo (EUPS ou USLE – *Universal Soil Loss Equation*), método empírico simples proposto por Wischmeier e Smith (1965, 1978) e desenvolvido nos Estados Unidos. A estimativa do potencial erosivo das chuvas é baseada no fator erosividade da chuva da EUPS, calculado através do uso de índices de erosivade como o EI_{30}. A sua indexação possui relação com as características físicas das chuvas como quantidade, intensidade, intensidade máxima em 30 min, velocidade terminal, diâmetro de gotas e a energia cinética das gotas de chuva (WISCHMEIER; SMITH, 1978).

A EUPS fornece estimativas de perdas de solo, sendo a equação mais utilizada no mundo. Ela prevê a longo prazo a perda média anual de solo (A) associanda à erosão laminar e em sulcos através da interação entre seis fatores condicionados ao clima, solo, topografia, vegetação e manejo (KINNELL, 2010).

Basicamente a EUPS é dada pela fórmula:

$$A = R\ K\ L\ S\ C\ P \quad (1)$$

onde A é a perda média de solo anual (Mg ha^{-1} ano^{-1}) a longo prazo (20 a 30 anos, por exemplo), R é o fator erosividade da chuva (MJ mm ha^{-1} h^{-1} ano^{-1}), K é o fator erodibilidade do solo (Mg h MJ^{-1} mm^{-1}), L e S são fatores topográficos comprimento de encosta (m) e declive (%) (adimensional), C é o fator de uso e manejo do solo (adimensional), e P é o fator de prática de conservação do solo (adimensional).

Os fatores intrínsecos ao meio físico que interferem no processo de erosão hídrica (R, K, L e S) constituem o Potencial Natural de Erosão do Solo (PNE), ou Risco Potencial de Erosão , o qual corresponde às perdas de solo em áreas continuamente desprovidas de cobertura vegetal e sem qualquer intervenção antrópica. É considerada uma metodologia importante para se avaliar o risco de degradação de terras, pois se define como o risco inerente de erosão, independentemente do uso atual da terra ou cobertura vegetal (CORREA et al., 2016).

A equação universal das perdas de solo tendo após algumas modificações com utilização de algoritmos computacionais em uma integração com o Sistema de Informação

Geográfica (SIG ou GIS - *Geographic Information System*), e outras, tais como o cálculo do fator de cobertura do solo e do fator LS, relacionado à topografia do terreno, deu origem a sua forma revisada, a RUSLE (*Revised Universal Soil Loss Equation*) (RENARD et al., 1997).

Os parâmetros utilizados para o cálculo da erosivadade da chuva são escassos e difíceis de serem obtidos, necessitando de medições em séries contínuas de valores de precipitação por um longo período de tempo. Isso torna difícil o cálculo do índice de erosividade em várias localidades do Brasil. Dessa forma, modelos de estimativa da erosividade com a utilização de banco de dados mais acessíveis, como por exemplo a precipitação média mensal e a anual e a utilização de equações de regressão, permitem que localidades que não possuam dados pluviográficos tenham representatividade na compreensão do potencial erosivo das chuvas em uma região de abragência (MELLO et al., 2007; OLIVEIRA et al., 2012; VIOLA et al., 2014).

Estudos conduzidos por Panagos et al. (2022), em escala global concluíram um aumento da erosividade e da precipitação global em média 26,2 a 28,8%, para o ano de 2050 e 27 a 34,3% para o ano de 2070. Segundo os mesmos autores 80 a 85% da superfície terrestre global terá uma tendência crescente na erosividade das chuvas e consequentemente, as mudanças climáticas e o aumento da erosividade das chuvas conduzirão a altas taxas de erosão.

2.3 Mudanças climáticas – cenários e projeções

Os efeitos potenciais de mudanças climáticas podem ser evidenciados em processos erosivos, sendo as variações do índice de erosividade das chuvas o indicador ativo nesses processos. Para se estimar os futuros impactos das mudanças climáticas, utiliza-se a análise de variáveis climáticas interrelacionadas em modelos climáticos globais (MCGs) e a sua combinação com modelos hidrológicos. Devido a sua baixa resolução espacial, inadequada para escalas locais e mesoescalas, modelos climáticos regionais (MCRs) têm sido desenvolvidos para simulações em estudos hidrológicos localizados (TEUTSCHBEIN; SEIBERT, 2012; SORRIBAS et al., 2016; OLIVEIRA et al., 2017).

Em virtude da necessidade de padronização dos experimentos de modelagem por estudos de mudanças climáticas, o quinto Relatório de Avaliação do *Intergovernmental Panel on Climate Change* (IPCC), *Assessment Report Fifth* (AR5 - IPCC, 2013), apresentou novos cenários de concentração de Gases de Efeito Estufa (GEE) a serem utilizados, tendo como base diferentes forçantes radiativas (W/m²) ao longo do século XXI, e obtidos através do CMIP (*Coupled Models Intercomparison Project*) (TAYLOR et al., 2012). Esses cenários servem como base para simular modelos para o comportamento espacial e temporal de diferentes variáveis climáticas, tais como a precipitação pluviométrica.

Através do AR5, estabeleceu-se os Caminhos Representativos de Concentração (RCPs): RCP 2.6, RCP 4.5, RCP 6.0 e RC P8.5 (FIGURA 1). Desses destacam-se estudos dos cenários RCP 4.5 e RCP 8.5 em relação aos cenários do relatório anterior do IPCC (CHOU et al., 2014). Esses valores se relacionam às diferentes forçantes radiativas (W/m^2), as quais equivalem aproximadamente a um nível de emissão de CO_2 em partes por milhão de 490 ppm (concentração de pico até 2100), 650 ppm (valor de concentração estabilizado por volta de 2100), 850 ppm (valor de concentração estabilizado por volta de 2100) e 1.370 ppm (valor de alcance até 2100), respectivamente (IPCC, 2013; RIAHI et al., 2017).

Figura 1 - Forçantes radiativas para os diferentes RCPs até o final do século.

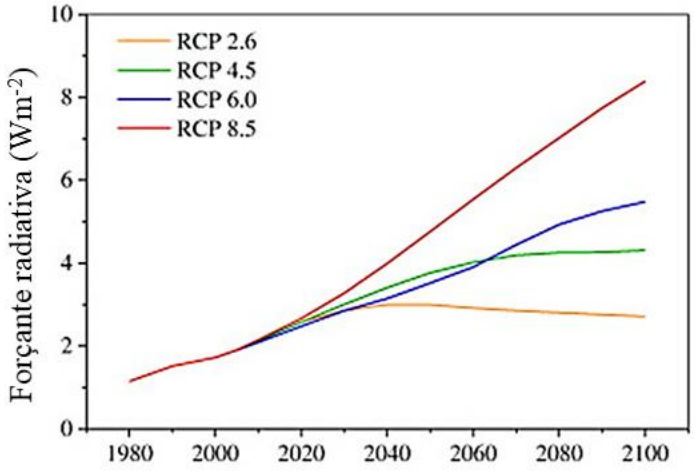

Fonte: IPCC (2013)

Entre os três cenários de mudança climática, o RCP 4.5 é o mais amplamente utilizado. Ele apresenta-se intermediário quanto à rigidez no forçamento radiativo em comparação aos demais cenários do AR5 – IPCC (2013), não sendo tão conservador como o cenário RCP 2.6 e nem tão extremo como o cenário RCP 8.5. Em estudo de projeção climática da erosividade no continente europeu ao longo da primeira metade do século XXI, Panagos et al. (2017) salientam que o cenário RCP 4.5 foi considerado moderado e embora haja incertezas no modelo de predição, áreas com mudanças substanciais podem se destacar. Atualmente o IPCC está em seu sexto ciclo de avaliação (IPCC AR6, 2021) e os resultados usando os modelos brutos CMIP6 já estão sendo disponibilizados na literatura de mudanças climáticas. Entretanto esse ainda carece de informação sobre as melhores técnicas para se combinar os resultados dos modelos

climáticos, diferente da dispersão e média multimodelo que eram utilizados no CMIP5 (HAUSFATHER et al., 2022). Além disso, os cenários climáticos do AR5 ainda permitem uma ampla avaliação do clima sobre toda a América do Sul devido a sua regionalização realizada a partir de modelos climáticos do CMIP5 (CHOU et al., 2014). Uma contribuição para essas predições poderia ser dada através da análise dos efeitos das mudanças climáticas sobre o uso e cobertura da terra, o que poderia balancear ou elevar as tendências de erosão do solo.

2.4 Mudanças de uso e cobertura da terra na bacia Tocantins-Araguaia

No Brasil, o bioma Cerrado na região de expansão da fronteira agrícola, se encontra em um ligeiro processo de destamamento. A maior parte das áreas de Cerrado (mais de 50% dos seus aproximadamente 2 milhões de km²) já sofreram uma transição de vegetação nativa para pastagens e terras agrícolas com produção de valor comercial (KLINK; MACHADO, 2005). A conservação do Cerrado tem atraído uma crescente atenção nacional e estrangeira, pois áreas não agrícolas remanescentes nesse bioma, principalmente na parte sententrional da sua área de abrangência, possuem baixa acessibilidade e poderão ser preferenciáveis mercados futuros de crédito de carbono (LAMBIN et al., 2013).

A bacia Tocantins-Araguaia possui grande relevância por conter grande parte da última fronteira para novos investimentos em agronegócio, conhecida como “MATOPIBA” (englobando os estados do Maranhão, Tocantins, Piauí e Bahia), possuindo frontes de conversão do uso da terra para a agricultura em contínua expansão em áreas de Cerrado e florestas de transição, assim como responsável pela expansão de áreas cultivadas de soja. Dentro dessa região de fronteira agrícola, a vulnerabilidade ambiental por unidade de paisagem apresenta-se alta na maior parte do estado do Tocantins e, de acordo o seu aspecto físico, o leste do seu território, completamente inserido dentro da bacia, possui solos arenosos, altamente susceptíveis a processos erosivos, além dos maiores déficits hídricos, que aumentam em direção à porção sudeste do estado. Esses fatores juntos tornam a região vulnerável às mudanças climáticas (DETZEL et al., 2017).

Diferentes cenários de mudanças climáticas, interferindo no regime hídrico de uma região, podem comprometer a produtividade de culturas a longo prazo, necessitando então de soluções efetivas que venham a mitigar os efeitos negativos sobre a produtividade. A redução da precipitação prevista em diferentes cenários, modelos de safra ou modelos climáticos, principalmente entre os meses de transição entre a estação seca e a chuvosa, no início do plantio consorciado anual no Cerrado, aliada ao desmatamento contínuo, pode ocosionar retornos

negativos para a produtividade agrícola até 2050 (PIRES et al., 2016). Dessa maneira, áreas passíveis de sofrer erosão poderão ter o seu potencial de risco aumentando.

As terras produtoras de grãos e pastagens do bioma Cerrado situadas dentro da bacia estão em situação de risco diante de eventos futuros relacionados às mudanças climáticas. Dentro da região do "MATOPIBA", uma porcentagem dessas terras já se encontra sob fortes sinais de degradação, tendo concentração em áreas de baixa resiliência, com solos arenosos, que apresentam estrutura fraca e baixa fertilidade natural (VIEIRA et al., 2021). O controle da erosão deve ser efetivo em solos tropicais vulneráveis, para isso há a necessidade de planejamento que vise a capacidade de uso da terra diante de tais cenários futuros.

Os impactos das mudanças de uso e cobertura da terra podem ser avaliados em diferentes cenários, os quais quando combinados com as mudanças no clima possibilitam a projeção do efeito combinado da erosividade da chuva e do manejo e cobertura do solo (COLMAN et al., 2019). Partindo-se do pressuposto que essas mudanças de uso e cobertura da terra podem ter reflexos em larga escala, a expansão de terras agrícolas situa-se como um condutor do potencial aumento global da erosão do solo (BORRELLI et al, 2017). Quando as taxas de erosão são avaliadas a partir da sua correlação com as mudanças de uso e cobertura da terra, áreas desmatadas e sujeitas às condições de uso da terra podem apresentar-se dominantes em conjunto com as maiores perdas de solo em bacias hidrográficas (ABDULKAREEM et al., 2019).

Em estudos de parcelas experimentais, Oliveira et al. (2015) encontraram coeficientes de escoamento superficial podendo aumentar de 1%, quando em vegetação nativa de Cerrado, para 20% em solo com vegetação removida. Já as perdas de solo medidas foram de 0,1 a 12,4 Mg ha^{-1} ano^{-1}, quando da remoção da vegetação nativa. Extrapolando essas estimativas para maiores escalas, torna-se perceptível o quão importante é o planejamento do controle da erosão hídrica em áreas de risco do Cerrado.

REFERÊNCIAS

ABDULKAREEM, J. H. *et al.* **Prediction of spatial soil loss impacted by long-term land-use/land-cover change in a tropical watershed.** Geoscience Frontiers, v. 10, n. 2, p. 389-403, 2019.

ALMEIDA, C. O. S. **Erosividade das chuvas no Estado de Mato Grosso**, 83p. Dissertação (Mestrado) – Universidade de Brasília, Brasília, 2009.

BASSETO FÉLIX, V. *et al.* **Estimadores de Semivariância: Uma Revisão.** Ciência e Natura, v. 38, n. 3, 2016.

BENNETT, N. D. *et al.* **Characterising performance of environmental models.** Environmental Modelling & Software, v. 40, p. 1-20, 2013.

BERTONI, J.; LOMBARDI NETO, F. **Conservação do solo.** São Paulo: Ícone, 1990.

BERTONI J. C.; TUCCI, C. E. M. Precipitação. In: TUCCI, C. E. M. **Hidrologia: Ciência e aplicação.** Porto Alegre: UFRGS, p.177-241, 2007.

BORRELLI, P. *et al.* **An assessment of the global impact of 21st century land use change on soil erosion.** Nature communications, v. 8, n. 1, p. 1-13, 2017.

CAMBARDELLA, C. A. *et al.* **Field-scale variability of soil properties in Central Iowa Soils.** Soil Science Society of America Journal, v. 58, n. 2, p. 1501-1511. 1994.

CHOU, S.; LYRA, A. *et al.* **Assessment of climate change over South America under RCP 4.5 and 8.5 downscaling scenarios.** American Journal of Climate Change, 3, p.512–527, 2014.

CHU, H.; VENEVSKY, S.; WU, C.; WANG, M. **NDVI-based vegetation dynamics and its response to climate changes at Amur-Heilongjiang River Basin from 1982 to 2015.** Science of the Total Environment, v. 650, p. 2051-2062, 2019.

COLMAN, C. B. *et al.* **Effects of climate and land-cover changes on soil erosion in Brazilian Pantanal.** Sustainability, v. 11, n. 24, p. 7053, 2019.

CORREA, S. W. *et al.* **Soil erosion risk associated with climate change at Mantaro River basin, Peruvian Andes.** Catena, v. 147, p. 110-124, 2016.

CRESSIE, N.; HAWKINS, D. M. **Robust estimation of the variogram: I.** Journal of the International Association for Mathematical Geology, v. 12, n. 2, p. 115-125, 1980.

D'ALMEIDA, C. *et al.* **The effects of deforestation on the hydrological cycle in Amazonia: a review on scale and resolution.** International Journal of Climatology: A Journal of the Royal Meteorological Society, v. 27, n. 5, p. 633-647, 2007.

DETZEL, V. A. *et al.* **Zoneamento Ecológico-Econômico do Estado do Tocantins.** Prognóstico Ecológico-Econômico do Estado do Tocantins. Secretaria de Planejamento e Orçamento (Seplan). Palmas: Seplan/GIES, vol. I., 370 p, 2017.

DONZELI, P. L. *et al.* **Projeto de Gestão Ambiental Integrada da Região do Bico do Papagaio. Zoneamento Ecológico-Econômico.** Diagnóstico do Risco de Erosão e Perdas de Solo do Norte do Estado do Tocantins. Secretaria do Planejamento e Meio Ambiente (Seplan). Palmas, Seplan/DZE, 42p., ilus. 2006.

HALMY, M. W. A. *et al.* **Land use/land cover change detection and prediction in the north-western coastal desert of Egypt using Markov-CA.** Applied Geography, v. 63, p. 101-112, 2015.

HAUSFATHER, Z. *et al.* **Climate simulations:** Recognize the 'hot model' problem. Nature, v. 605, p. 26–29, 2022.

HEWITSON, B. C.; CRANE, R. G. **Climate downscaling:** techniques and application. Climate Research, v. 7, n. 2, p. 85-95, 1996.

INTERGOVERNMENTAL PANEL ON CLIMATE CHANGE (IPCC): **Climate Change 2013**: The Physical Science Basis. Contribution of Working Group I to the Fifth Assessment

Report of the Intergovernmental Panel on Climate Change [Stocker, T.F., D. Qin, G.-K. Plattner, M. Tignor, S.K. Allen, J. Boschung, A. Nauels, Y. Xia, V. Bex and P.M. Midgley (eds.)]. Cambridge University Press, Cambridge, United Kingdom and New York, NY, USA, 1535 pp. 2013.

IPCC AR6 (Intergovernmental Panel on Climate Change). Summary for Policymakers. In: MASSON-DELMOTTE, V., P. ZHAI, A. PIRANI, S. L. CONNORS, C. PÉAN, S. BERGER, N. CAUD, Y. CHEN, L. GOLDFARB, M. I. GOMIS, M. HUANG, K. LEITZELL, E. LONNOY, J.B.R. MATTHEWS, T. K. MAYCOCK, T. WATERFIELD, O. YELEKÇI, R. YU AND B. ZHOU (Eds). **Climate Change 2021:** The Physical Science Basis. Contribution of Working Group I to the Sixth Assessment Report of the Intergovernmental Panel on Climate Change. Cambridge University Press, 2021, 41 pp.

EASTMAN, J. R. **IDRISI selva.** Worcester, MA: Clark University, 2012.

KINNELL, P. I. A. **Event soil loss, runoff and the Universal Soil Loss Equation family of models:** A review. Journal of hydrology, v. 385, n. 1-4, p. 384-397, 2010.

KLINK, C. A.; MACHADO, R. B. **Conservation of the Brazilian cerrado.** Conservation biology, v. 19, n. 3, p. 707-713, 2005.

LAMBIN, E. F. *et al.* **Estimating the world's potentially available cropland using a bottom-up approach.** Global Environmental Change, v. 23, n. 5, p. 892-901, 2013.

LANDIM, P. M. B. **Krigagem ordinária para situações com tendência regionalizada.** Rio Claro, 2002.

MACHADO, R. E.; VETTORAZZI, C. A. **Simulação da produção de sedimentos para a microbacia hidrográfica do ribeirão dos Marins (SP).** Revista Brasileira de Ciência do Solo, v. 27, n. 1, p. 735–741, 2003.

MARAUN, D. **Bias correcting climate change simulations-a critical review.** Current Climate Change Reports, v. 2, n. 4, p. 211-220, 2016

MATHERON, G. **Traité de géostatistique appliquée**, v. 14. Editions Technip, Paris, 1962.

MELLO, C. R. *et al.* **Erosividade mensal e anual da chuva no Estado de Minas Gerais.** Pesquisa Agropecuária Brasileira, v.42, p.537-545, 2007.

MERTEN, G. H.; MINELLA, J.P.G. **The expansion of Brazilian agriculture:** soil erosion scenarios. International Soil and Water Conservation Research, v. 1, n. 3, p. 37-48, 2013.

MOLINA, T.; ABADAL, E. **The Evolution of Communicating the Uncertainty of Climate Change to Policymakers:** A Study of IPCC Synthesis Reports. Sustainability, v. 13, n. 5, p. 2466, 2021.

NASH, J. E.; SUTCLIFFE, J. V. **River flow forecasting through conceptual models part I—A discussion of principles.** Journal of hydrology, v. 10, n. 3, p. 282-290, 1970.

OJO, S. A. *et al.* **Modelling the relationship between climatic variables and land use/land cover classes in Yewa South Local Government Area of Ogun State, Nigeria.** In: IOP Conference Series: Materials Science and Engineering. IOP Publishing, 2021. p. 012003.

OKKAN, U.; KIRDEMIR, U. **Downscaling of monthly precipitation using CMIP5 climate models operated under RCPs.** Meteorological Applications, v. 23, n. 3, p. 514-528, 2016.

OLIVEIRA JUNIOR, R. C. de. **Índice de erosividade das chuvas na região de Conceição do Araguaia, Pará.** Belém: Embrapa-CPATU, 20p, (Embrapa-CPATU. Boletim de pesquisa, 165), 1996.

OLIVEIRA, P. T. S. *et al*. **Spatial variability of the rainfall erosive potential in the state of Mato Grosso do Sul, Brazil.** Engenharia Agrícola, v.32, p.69-70, 2012.

OLIVEIRA, V. A.; MELLO, C. R.; VIOLA, M. R.; SRINIVASAN, R. **Assessment of climate change impacts on streamflow and hydropower potential in the headwater region of the Grande river basin, Southeastern Brazil.** International Journal of Climatology, 2017.

PANAGOS, P. *et al.* **Towards estimates of future rainfall erosivity in Europe based on REDES and WorldClim datasets.** Journal of Hydrology, v. 548, p. 251-262, 2017.

PANAGOS, P. *et al.* **Global rainfall erosivity projections for 2050 and 2070.** Journal of Hydrology, v. 610, p. 127865, 2022.

PAN, S. *et al.* **Runoff Responses to Climate and Land Use/Cover Changes under Future Scenarios.** Water, v. 9, n. 7, p. 475, 2017.

PIRES, G. F. *et al.* **Increased climate risk in Brazilian double cropping agriculture systems: Implications for land use in Northern Brazil.** Agricultural and Forest Meteorology, v. 228, p. 286-298, 2016.

RAGHAVENDRA, S. N.; DEKA, P. C. **Support vector machine applications in the field of hydrology:** a review. Applied Soft Computing, v. 19, p. 372-386, 2014.

R Core Team. **R: A language and environment for statistical computing.** R Foundation for Statistical Computing, Vienna, Austria, 2017. https://www.R-project.org/.

RENARD, K. G.; FREIMUND, J. R. **Using monthly precipitation data to estimate the R-factor in the revised USLE.** Journal of Hydrology, v.157, p.287-306, 1994.

RENARD, K. G. **Predicting soil erosion by water:** a guide to conservation planning with the revised universal soil loss equation (RUSLE). 1997.

RIAHI, K. *et al.* **The shared socioeconomic pathways and their energy, land use, and greenhouse gas emissions implications:** an overview. Global environmental change, v. 42, p. 153-168, 2017.

SALVADOR, M. A.; DE BRITO, J. I. B. **Trend of annual temperature and frequency of extreme events in the MATOPIBA region of Brazil.** Theoretical and Applied Climatology, v. 133, n. 1, p. 253-261, 2018.

SANG, L. *et al.* **Simulation of land use spatial pattern of towns and villages based on CA–Markov model. Mathematical and Computer Modelling**, v. 54, n. 3-4, p. 938-943, 2011.

SATTLER, D. *et al.* **Pasture degradation in South East Brazil:** status, drivers and options for sustainable land use under climate change. In: Climate Change Adaptation in Latin America. Springer, Cham, 2018. p. 3-17.

SILVA, M. L. N. *et al.* **Índices de erosividade das chuvas da região de Goiânia, GO.** Pesquisa Agropecuária Brasileira, v.32, p.977-985, 1997.

SILVA, A. M. **Rainfall erosivity map for Brazil.** Catena, v.57, p.251-259, 2004.

SORRIBAS, M. V. *et al.* **Projections of climate change effects on discharge and inundation in the Amazon basin.** Climatic change, v. 136, n. 3-4, p. 555-570, 2016.

SOUZA, E. P.; RENNÓ, N. O.; SILVA DIAS, M. A. F. **Convective circulations induced by surface heterogeneities.** Journal of the atmospheric sciences, v. 57, n. 17, p. 2915-2922, 2000.

SPRACKLEN, D. V. *et al.* **The effects of tropical vegetation on rainfall.** Annual Review of Environment and Resources, v. 43, p. 193-218, 2018.

TAYLOR, E. K.; STOUFFER, R. J.; MEEHL, G. A. **A overview of CMIP5 and the experiment design.** Bulletin of American Meteorological Society, v. 93, p. 485-498, 2012.

TESSEMA, K. B.; HAILE, A. T.; NAKAWUKA, P. **Vulnerability of community to climate stress:** An indicator-based investigation of Upper Gana watershed in Omo Gibe basin in Ethiopia. International Journal of Disaster Risk Reduction, v. 63, p. 102426, 2021.

TEUTSCHBEIN, C.; SEIBERT, J. **Bias correction of regional climate model simulations for hydrological climate-change impact studies:** Review and evaluation of different methods. Journal of Hydrology, v. 456, p. 12-29, 2012.

TURCO, M. *et al.* **Bias correction and downscaling of future RCM precipitation projections using a MOS-Analog technique.** Journal of Geophysical Research: Atmospheres, v. 122, n. 5, p. 2631-2648, 2017.

VIEIRA, R. M. S. P. *et al.* **Land degradation mapping in the MATOPIBA region (Brazil) using remote sensing data and decision-tree analysis.** Science of The Total Environment, v. 782, p. 146900, 2021.

VIOLA, M. R. *et al.* **Distribuição e potencial erosivo das chuvas no Estado do Tocantins.** Pesquisa Agropecuária Brasileira, v.49, n.2, p.125-135, 2014.

VIJITH, H.; HURMAIN, A.; DODGE-WAN, D. **Impacts of land use changes and land cover alteration on soil erosion rates and vulnerability of tropical mountain ranges in Borneo.** Remote Sensing Applications: Society and Environment, v. 12, p. 57-69, 2018.

WEILL, M. A. M.; SPAROVEK, G. **Estudo da erosão na microbacia do Ceveiro (Piracicaba, SP):** I-Estimativa das taxas de perda de solo e estudo de sensibilidade dos fatores do modelo EUPS. Revista Brasileira de Ciência do Solo, v. 32, p. 801–814, 2008.

WISCHMEIER, W. H.; SMITH, D. **Predicting rainfall erosion losses from cropland east of the Rocky Mountain.**, 1965.

WISCHMEIER, W. H.; SMITH, D. **Predicting rainfall erosion losses -** a guide to conservation planning. U.S. Department of Agriculture, Agriculture Handbook., n. 537, 1978.

ZARE, M.; PANAGOPOULOS, T.; LOURES, L. **Simulating the impacts of future land use change on soil erosion in the Kasilian watershed, Iran.** Land Use Policy, v. 67, p. 558-572, 2017.

SEGUNDA PARTE – ARTIGOS

ARTIGO 1 Projections of rainfall erosivity in climate change scenarios for the largest watershed within Brazilian territory

Article published in the journal Catena (ISSN: 0341-8162)

https://doi.org/10.1016/j.catena.2022.106225

Authors:

Wharley Pereira dos Santos[a]; Santos, W.P.

Junior Cesar Avanzi[a]*, Avanzi, J.C.

Marcelo Ribeiro Viola[b], Viola, M.R.

Sin Chan Chou[c], Chou, S.C.

Salvador Francisco Acuña-Guzman[ad], Acuña-Guzman, S.F.

Lucas Machado Pontes[e], Pontes, L.M.

Nilton Curi[a]; Curi, N.

[a] *Department of Soil Science, Federal University of Lavras, Lavras, 37200-900, Brazil. E-mail address: wharley.pereira@estudante.ufla.br; junior.avanzi@ufla.br; niltcuri@ufla.br*

[b] *Department of Water Resources and Sanitation, Federal University of Lavras, Lavras, 37200-900, Brazil. E-mail address: marcelo.viola@ufla.br*

[c] *National Institute for Space Research, Cachoeira Paulista, 12630-000, Brazil. E-mail address: chou.chan@inpe.br*

[d] *University of Puerto Rico, Mayagüez Campus. Department of Agricultural and Biosystems Engineering, Mayagüez, 00682, Puerto Rico, USA. E-mail address: salvador.acuna@upr.edu*

[e] *Institute of Astronomy and Geosciences, University of São Paulo, Brazil. E-mail address: lucas.pontesm@gmail.com*

**Corresponding author. Tel.: +55 35 38291639*

E-mail address: junior.avanzi@ufla.br (J.C. Avanzi)

Abstract

Global climate change can potentially threaten agricultural production due to endangered natural resources, such as rainfall patterns. Thus, extreme rainfall events can cause greater rainfall erosivity, consequently, greater soil erosion. Conversely, a reduction in rainfall amount can lead to water scarcity for the agriculture production process. This way, it is a foremost need to model climatic conditions under global climate change scenarios, particularly in places where rainfall data tends to increase. This work aimed to project rainfall erosivity in the major Brazilian watershed, the Tocantins-Araguaia river basin, throughout the 21st century under two Intergovernmental Panel for Climate Change Fifth Assessment Report (IPCC AR5) Scenarios, the Representative Concentration Pathways, RCP4.5 and RCP8.5 scenarios. This study uses the downscaling of four global climate models of the Coupled Model Intercomparison Project (CMIP5) by the Eta regional climate model, used by the Brazilian National Institute for Space Research. The average rainfall erosivity was calculated based on the Modified Fournier Index in three periods of 30-year length throughout the 21st century. Time series of R-factor were analyzed at rain gauge station points overlapping regional model grid cells over the basin for the 1961-2099 period. Projections indicated lower annual average rainfall erosivity values in comparison with historical data. Estimated mean rainfall erosivity values were 10,977.69±526 MJ mm ha^{-1} h^{-1} yr^{-1} for the RCP4.5 scenario, and 10,379.71±723 MJ mm ha^{-1} h^{-1} yr^{-1} for the most pessimistic climate change scenario, RCP8.5. The largest reductions of the mean R-factor reached 5,5% for the multi-model ensemble projections for near future, and 15.4% for the ensemble projections models for long-term, with the greatest decreasing trends under RCP8.5. Reductions greater than 2,000 MJ mm ha^{-1} h^{-1} are expected throughout the 21st century according to multi-model ensemble projections models under RCP8.5 scenario in most of the watershed. Decreasing rainfall erosivity factor in both RCP scenarios was due to a lower rainfall depth. However, the value of rainfall erosivity is still considered high and should be taken into

account in soil conservation practices. Furthermore, the smaller rainfall amount indicates a possible reduction in water availability for crops of longer cycle, and increase in spatial variability of less intense rainfall.

Keywords: water erosion; Amazon and Cerrado biomes; climate change; downscaling; soil and water conservation.

1. INTRODUCTION

The assessment of the impacts that climate change can produce on a regional scale can support the planning and adaptation in the agricultural sector and long-term environmental protection. Global Climate Models (GCM) can provide information on future climate change in different greenhouse gas emission scenarios (IPCC, 2013). Essential climatic variables are used as input data to hydrological models to assess possible impacts of climate change on basin hydrology. However, global models have a coarse spatial resolution, unsuitable for mesoscale hydrological simulations. Regional climate models (RCM) have been applied to increase the resolution of global climate model estimates. This so-called dynamical downscaling produces climate information at the scale appropriate to use in local and regional hydro-climate models (Gorguner et al., 2019; Jin et al., 2018; Oliveira et al., 2017; Sorribas et al., 2016; Teutschbein and Seibert, 2012; 2013).

The erosive potential of heavy rainfall is the triggering agent of soil water erosion. Inappropriate land use and land management combined with the reduction of vegetation cover, which protects against the direct impact of raindrops, tend to increase erosion rates (Morgan, 2005; Zuazo and Pleguezuelo, 2008), especially in the humid tropics (El-Swaify et al., 1982; Labrière et al., 2015; Lal, 1983; Theng, 1991). Extreme climate events have been reported more frequently which increases the rainfall erosive potential (Almagro et al., 2017; Nel et al., 2016; Vallebona et al., 2015; Zhu et al., 2020). Therefore, a large number of studies on climate change have indicated relative changes in rainfall erosivity patterns in several regions, some studies have reported an annual trend of increasing rainfall erosivity (Amanambu et al., 2019; Duulatov et al., 2019; Gafforov et al., 2020; Mello et al., 2015; Mondal et al., 2016; Shiono et al., 2013), while others reported a reduction in rainfall erosivity (Correa et al., 2016; Grillakis et al., 2020). These divergent results in reported rainfall erosivity trends are associated to local conditions and the evaluated future scenarios (Azari et al., 2021; Grillakis et al., 2020; Panagos et al., 2017;

Riquetti et al., 2020); *e.g.*, among the aforementioned studies, Riquetti et al. (2020) reported a strong reduction in the mean annual precipitation and rainfall erosivity throughout the 21st century for the Amazon Forest region.

Potential effects of climate change can be evidenced by variations in rainfall erosivity index, the indicator of active erosion processes. Diodato et al. (2017) monitored and reported that erosive events in a long series of annual rainfall erosivity values may indicate the frequency of extreme precipitation events of short duration in wet periods, which are likely to increase erosion. Furthermore, Ballabio et al. (2017) emphasized that analyses of the spatial and temporal variability of rainfall erosivity based on high temporal resolution precipitation data allows the development of indicators for studies that record intra-annual variation in different locations.

The soil erosion rates are affected by changing rainfall patterns over much of the tropical regions, which are the most susceptible to high levels of soil erosion (Borrelli et al., 2017). In this regard, Riquetti et al. (2020) reported an increasing of future rainfall for the central-south region of South America (crossing Paraguay, northern Argentina, and southern and southeastern Brazil), and another strong reduction for the Brazilian semi-arid region (northeast region), and Amazon region (north region). Souza et al. (2019) highlighted that the region of the State of Tocantins (region of current study) is situated in an important climate transition area (between the Amazon and the semi-arid region). Thus, detailed studies to assess the impact of the climate changes on rainfall erosivity are required.

Rainfall erosivity (R-factor), an index proposed by Wischmeier and Smith (1958), is calculated based on kinetic energy of raindrops through the rainfall intensity, as part of the Universal Soil Loss Equation (USLE) (Wischmeier and Smith, 1978) and its revised version (RUSLE) (Renard et al., 1997). Parameter used to estimate rainfall erosivity, considering higher temporal resolution (<<hourly), are scarce and difficult to access in most of the developing

tropical countries, *i.e.* shortage of available continuous long-term records of rainfall data across tropical regions. The calculation of rainfall erosivity in several locations of Brazil has been hampered by the lack of complete pluviographic data or the short-recorded period to calculate the R-factor. As a further optional methodology for estimating the rainfall erosivity, rainfall intensity indices have been based on annual and monthly rainfall depth, such as the Fournier and modified Fournier indices (Arnoldus, 1980; Fournier, 1956). Therefore, the application of models of rainfall erosivity estimation based on monthly and annual mean rainfall, and regression equations, can help understand the potential erosion by rainfall in regions where no detailed precipitation series data are available (Back et al., 2019; Cardoso et al., 2022; dos Santos Silva et al., 2020; Duulatov et al., 2019; Gafforov et al., 2020; Mello et al., 2007; Oliveira et al., 2012; Viola et al., 2014). An alternative method for rainfall erosivity estimation for locations with coarse resolution rainfall data has been evaluated (Angulo-Martínez and Beguería, 2009; Cardoso et al., 2022; Li et al., 2020; Ma et al., 2014; Men et al., 2008; Oğuz, 2019; Zhang et al., 2002). Oğuz (2019) reported that the modified Fournier index was the closest estimate to rainfall erosivity in Turkey. Rainfall erosivity for African continent was best estimated performing the modified Fournier index using data from satellite-derived rainfall (Vrieling et al., 2010). Although modified Fournier index showed unsuitable for NE Spain (Angulo-Martínez and Beguería, 2009), for Brazilian conditions the modified Fournier index showed to be a suitable method for estimate rainfall erosivity (Cardoso et al., 2022). This index has been used for Brazilian conditions with good correlation with rainfall erosivity (Almeida, 2009; Almeida et al., 2012; Aquino et al., 2012; Cantalice et al., 2009; Martins et al., 2010; Oliveira et al., 2012; Oliveira Junior, 1996; Silva et al., 1997).

In this context, the objective of the study was to evaluate the spatial and temporal rainfall erosivity (R-factor) changes in the Tocantins-Araguaia basin, in Brazil, under future climate change conditions. This study uses daily rainfall dataset from regional climate model outputs

derived from the downscaling of the global climate models: BESM, CanESM2, MIROC5, and HadGEM2-ES, and the greenhouse gas concentration scenarios RCP4.5 and RCP8.5. The future changes are shown in three time-slices of 30 years: 2011-2040, 2041-2070, and 2071-2099, and compared against the historical period between 1961 and 1990. The evaluation of the climate models' historical rainfall over the basin was conducted using the rain gauge observations as reference.

2. MATERIALS AND METHODS

2.1 Study area

The Tocantins-Araguaia basin is located in the central part of Brazil and it drains water from an area of 767,164 km² toward the northern coast (Fig. 1). The Tocantins River is the main river of the basin, and the Araguaia River is the large tributary river to the west. The basin is formed by a large drainage network, in which the Tocantins and Araguaia rivers allow navigation in large extension. The Tocantins-Araguaia basin is considered the second largest one in Brazil, in terms of water availability. The Amazon biome predominates in the northwestern part of the basin, while Cerrado Biome occupies the rest of the basin. The Cerrado biome of the basin is inserted in the so-called MATOPIBA area (acronym for the names of the states of Maranhão, Tocantins, Piaui, and Bahia), which is one of the largest agro-industrial expansion zones in the world, and, therefore, it is strategic to the economic development of the Brazilian economy (Pires et al., 2016). However, anthropogenic activities have raised concerns about environmental management in the region (Donzeli et al., 2006). Geographically located in the transition region between the Cerrado and the Amazon biomes, the basin has high rainfall erosive potential (Trindade et al., 2016).

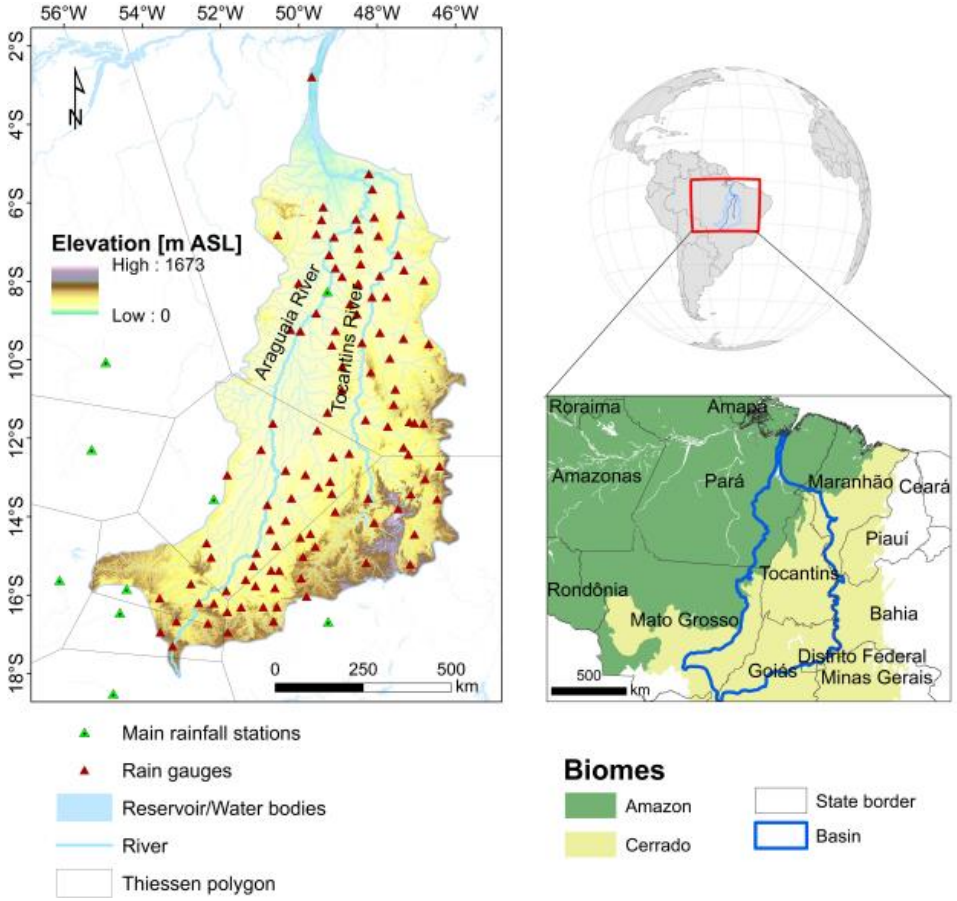

Fig. 1 – The Tocantins-Araguaia basin and the Amazonia (green) and Cerrado (yellow) biomes.

The climate in the region is classified as tropical (Aw), with rainy summer and dry winter (Alvares et al., 2013). The rainy season is between October and April when more than 90% of the total annual precipitation falls. Conversely, dry season ranges from May to September. The precipitation regime is characterized by increased rainfall as the latitude decrease toward the equator. The average total annual precipitation is 1,869 mm in the basin. The annual maximum of 2,565 mm occurs near the Tocantins river mouth, located in the area predominately of Amazon biome.

The Intertropical Convergence Zone (ITCZ) and the South Atlantic Convergence Zone (SACZ) are the two major large-scale meteorological features that strongly influence the basin rainfall. In addition, small-scale weather systems such as convective storms can also contribute to the rainfall. The equatorial air masses that reach the basin produce high rainfall erosivity in

the Amazon-Cerrado transition area. This high rainfall erosivity result in monthly rainfall erosivity rates that exceed the critical value of 500 MJ mm ha^{-1} h^{-1} during the wet season (Viola et al., 2014). Therefore, detailed research and improved models can contribute to provide information for environmental sustainability and mitigation measures and to reduce the negative consequences (economic and social) of soil misuse and environmental resources consumption in the basin.

2.2 Climate data and scenarios

The Fifth Assessment Report of the Intergovernmental Panel on Climate Change (IPCC, 2013) considered Greenhouse Gas emission scenarios based on different levels of radiative forcing throughout the 21st century. These scenarios were referred to as Representative Concentration Pathways. The projections of climate change under these scenarios were provided by global climate models which followed the protocol of the Coupled Model Intercomparison Project Phase 5 (CMIP5) (Taylor et al., 2012).

Global climate models adopt horizontal resolutions that range around 200 km. Climate change projections using these global models are considered coarse for studies in basin scale, especially for studies that extreme values and topographic precipitation are relevant. Downscaling global model output using regional climate models is an approach that provides higher horizontal resolution output based on the dynamics of the climate system. For South America, the highest horizontal resolution (20-km), using the largest number of global climate models (4 global models), the largest number of RCP scenarios (2 scenarios), and for the longest period (from 1961-2099), available at the time of this work were provided by the Eta Model from the Brazilian National Institute for Space Research (Chou et al., 2014a, b). Therefore, this largest dataset is used for this study. The Eta Model is suitable to simulate South America climate due to the reduced errors in the presence of the steep Andes Cordillera (Mesinger et al., 2012; Mesinger et al., 2016). Development of the Eta Model and the validation in multi-decadal

runs have carried out in several works (Pesquero et al., 2010; Chou et al., 2012; Marengo et al., 2012).

The four global climate models, whose resolutions range from about 200 km and 300 km, were downscaled to 20-km resolution. These global climate models are: the Brazilian Earth System Model (BESM) (Nobre et al., 2013); the Canadian Earth System Model, 2nd generation (CanESM2) (Arora et al., 2011); the Hadley Centre Global Environmental Model, version 2 (HadGEM2-ES) (Collins et al., 2011); and the Model for Interdisciplinary Research on Climate, version 5 (MIROC5) (Watanabe et al., 2010). From now on, these downscaling outputs will be referred to as Eta-BESM, Eta-CanESM2, Eta-HadGEM2-ES, Eta-MIROC5, and the respective multi-model ensemble will be also taken into consideration.

Monthly and annual rainfall data sets between 1961 and 1990 were considered as the baseline period of present climate simulations. The projections of the future climate were assessed in three time slices of 30 years in the periods: 2011-2040, 2041-2070, and 2071-2099. These periods are considered centered in the 2020s, 2050s, and 2080s.

Two greenhouse gas scenarios were considered: the moderate concentration scenario (RCP4.5), and the uppermost extreme concentration scenario (RCP8.5). The RCP4.5 consists of a scenario of stabilization of the total radiative forcing at 4.5 W/m² before 2100 (Thomson et al., 2011), whereas the RCP8.5 scenario leads to the radiative forcing of 8.5 W/m^2 at the end of the 21st century (Riahi et al., 2011).

Evaluation of the baseline period show that the downscaling runs reproduce major features in South America Climate, such as the seasonal temperature and precipitation variability, wind climatology (Antico et al., 2021; Chou et al., 2014a). The climatic extreme indices from the downscaling outputs have been evaluated against station observations (Dereczynski et al., 2020). The positive trend of temperature extreme indices were well

reproduced by the model. However, precipitation extreme indices in the basin area have mixed trend signs, but in general, the downscaling reproduce the trends in the 99th percentile of daily precipitation rate and in the 5-day accumulated precipitation. Conversely, for the consecutive dry day's index, the negative trends observed from the gauges were not reproduced by the downscaling outputs.

Bias correction was applied to the downscaling of precipitation produced by the Eta model. The method of bias correction was based on the Quantile-Quantile transformation (Bárdossy and Pegram, 2011).

2.3 Observed rainfall data

Gauge stations with continuous data periods overlapping the CMIP5 historical experiment period (1961–2005) were identified through the Hidroweb portal of the Brazilian National Water and Sanitation Agency (ANA) to evaluate the climate models' baseline period within the Tocantins-Araguaia basin. There were 108 rain gauge stations in the basin (Fig. 1), of which 18 stations had continuous series of daily data for the 1975-1994 period, and 90 stations had continuous series of daily data for the 1985-2005 period (records were selected according to the minimum period required to calculate the R-factor). For evaluation of the mean annual rainfall erosivity, the RCM grid cells closest to the observational rain gauges were extracted and evaluated at point-wise measurements. The gauge records provided a curated set of long-term, historical daily rainfall data. The lack of ground-based stations, with a common data period, unveiled gaps of rainfall measurements in specific 169 regions within the basin, therefore those two different historical series (periods) were selected. All the rain gauge stations were scattered over the drawn Thiessen polygons, according to the methodology also carried out by Almagro et al. (2017) and Mello et al. (2015), *i.e.* polygons generated based on the main weather stations (Fig. 1), –main weather stations are those with rainfall intensity information to calculate rainfall erosivity according to Equations 1 to 3. Precipitation data sets have been used

to validate climate models, and rain gauge datasets remain the most accurate source of rainfall information, regardless of the small-sized rain gauge network over tropical South America (Tapiador et al., 2017). Monthly rainfall datasets were used to determine annual rainfall erosivity for each rain gauge station. Thus, rainfall erosivity estimated from the downscaling outputs were compared against the rainfall erosivity determined from the observations.

2.4 Rainfall erosivity factor calculations

The rainfall erosivity (R-factor) is the most relevant factor when analyzing the impacts of soil water erosion since it is conditioned to the rainfall intensity. The volume and speed of the runoff caused by rainfall depends on its intensity, duration, and frequency. Rainfall intensity is the main variable considered in the calculation of rainfall erosivity. The R-factor is defined as a function of the daily precipitation values, being EI_{30} - total storm energy (E) times the maximum continuous 30-min intensity during the individual storm event (I_{30}). In order to analyze rainfall erosivity measures in the main weather stations (Fig. 1), each erosive rain event was divided into different segments of similar intensities and the rain kinetic energy was calculating as proposed by Wischmeier and Smith (1978) and modified by Foster et al. (1981) through the following equation:

$$e = 0.1191 + 0.0873 \log i \quad (1)$$

where: e is the unit rainfall kinetic energy expressed in MJ ha^{-1} mm^{-1}, and i is the rainfall intensity (mm h^{-1}) within the time segment. The kinetic energy accumulated from each rth segment of the rainfall is given by $E_r = e_r . \upsilon_r$ (MJ ha^{-1}), where υ_r is the rainfall depth (mm) during a period. Thus, the rainfall erosivity index of each erosive storm is given by:

$$EI_{30} = (\sum_{r=1}^{n} E_r) \times I_{30} \quad (2)$$

The average annual rainfall erosivity (MJ mm ha^{-1} h^{-1} year^{-1}) is obtained from averaging the annual sums of individual EI_{30} erosivity indices (Eq. 3):

$$R = \frac{1}{n}\sum_{j=1}^{n}\left[\sum_{k=1}^{m_j}(EI_{30})_k\right]_j \quad (3)$$

where n is the number of years of data, m_j is the number of erosive rainfall events in the year j and $(EI_{30})_k$ is the rainfall erosivity index of the kth event in a given year j. In order to obtain an estimate of the average annual erosivity index, at least a 20-year record of rainfall data is required (Renard et al., 1997). Pluviometric data records are usually used to obtain the R-factor from their relation with the aforementioned erosivity index (da Silva, 2004; Oliveira et al., 2013; Renard and Freimund, 1994). In Brazil, the low availability of hourly and sub-hourly rainfall pluviographic records for observed historical periods in remote and disadvantaged regions is particularly problematic.

Although the rainfall erosivity (Eq. 2) was derived empirically as a model to represent "*... the combined effects of (a) the decreasing infiltration rate during a rain, (b) the geometrically increasing erosion effect of surface flow, and (c) the protection against raindrop splash which is afforded by the film of flowing water*" (Wischmeir and Smith, 1958), it can also underestimate soil losses for long low-intensity rains. Fournier (1960) proposed an index to be correlated to sediment loads in rivers to predict soil losses based on the mean monthly rainfall amounts, however it underestimated rain erosivity (Arnoldus, 1980). Consequently, a Modified Fournier Index (MFI) was proposed (Eq. 4), considering the rainfall amounts of all months in the year (Arnoldus, 1980) to better predict the erosive power of rains throughout the year.

This modified Fournier index has achieved the best results in the calculating of the R-factor in Brazil (Cardoso et al., 2022). Some of the models developed in previous studies from storm event pluviographic records in Brazil were used to compute the R-factor (Table 1).

$$\mathrm{MFI} = \frac{{p_i}^2}{P} \quad (4)$$

$$\mathrm{EI}_{30\ \mathrm{monthly}} = \alpha \mathrm{MFI}^{\beta} \quad \text{or} \quad \mathrm{EI}_{30\ \mathrm{monthly}} = \theta + \alpha \mathrm{MFI}^{\beta} \quad (5)$$

where MFI is the Modified Fournier Index considering modifications performed by Apaydin et al. (2006), p_i is the monthly precipitation amounts of each individual year and P is the total average annual rainfall. In this calculation procedure, the MFI includes the year-to-year variations as well as the within-year variations (Apaydin et al., 2006). The $EI_{30annual}$ was calculated by Eq. 6:

$$EI_{30\ annual} = \sum_{i=1}^{12} \left(EI_{30\ monthly} \right)_i \quad (6)$$

Table 1 - Equations available in the Tocantins-Araguaia basin for determining the rainfall erosivity index (EI_{30}) as a function of the Modified Fournier Index (MFI).

Station	LAT	LONG	Equation	State	Reference
Canarana	13°33'00"S	52°10'12"W	EI_{30}= 317.3978×MFI$^{0.48465}$; R^2= 0.86	Mato Grosso	(Almeida et al., 2012)
Cuiabá	15°37'18"S	56°06'30"W	EI_{30}= 244.47×MFI$^{0.508}$; R^2 = 0.67	Mato Grosso	(Almeida, 2009)
Vera	12°17'24"S	55°17'24"W	EI_{30}= 399.5387×MFI$^{0.4587}$; R^2 = 0.84	Mato Grosso	(Almeida et al., 2012)
Poxoréu	15°50'48"S	54°23'48"W	EI_{30}=272.8656×MFI$^{0.41916}$; R^2 = 0.66	Mato Grosso	(Almeida et al., 2012)
Rondonópolis	16°26'60"S	54°34'00"W	EI_{30}=167.16×MFI$^{0.567}$; R^2 = 0.77	Mato Grosso	(Almeida, 2009)
Coxim	18°30'43.7"S	54°44'10"W	EI_{30}=138.33×MFI$^{0.7431}$; R^2 = 0.91	Mato Grosso do Sul	(Oliveira et al., 2012)
Conceição do Araguaia	8°15'36"S	49°16'12"W	EI_{30} = 321.5 + 36.20×MFI; R^2 = 0.79	Pará	(Oliveira Junior, 1996)
Goiânia	16°40'48"S	49°15'00"W	EI_{30} = 216.15 + 30.69×MFI; R^2 = 0.78	Goiás	(Silva et al., 1997)
Matupá	10°03'36"S	54°55'48"W	EI_{30} = 115.72×MFI$^{0.746}$; R^2 = 0.99	Mato Grosso	(Almeida, 2009)

2.5 Annual erosivity density

In order to assess the patterns of rainfall erosivity in its spatial dynamics, the erosivity density was used. The erosivity density is the ratio of R-factor to precipitation (Kinnell, 2010), and it measures the erosivity per rainfall unit (mm), being expressed as MJ ha^{-1} h^{-1}. In this study, the average annual Erosivity Density (ED) was used, and for each climate model grid point, the ED of a particular year *i* was determined by:

$$ED_i = \frac{R_i}{P_i} \tag{7}$$

The average annual Erosivity Density was calculated for each time-slice of climate model scenarios, and for the baseline period. Smaller values of ED indicated the R-factor was mainly influenced by the rainfall amount, while high values of ED suggested the occurrence of high-intensity rainfall (Panagos et al., 2016).

2.6 Tests for trend detection

2.6.1 Mann-Kendall statistical test

The Mann-Kendall statistical test (Kendall, 1975; Mann, 1945) was used to detect a trend in the rainfall erosivity time series throughout the twenty-first century under the two emission scenarios. This non-parametric statistical test is widely used for detecting trends in hydroclimatic time series (Huang et al., 2013; Mello et al., 2015; Oğuz, 2019; Verstraeten et al., 2006; Vu et al., 2015; Yang and Lu, 2015), and is recommended for general use by the World Meteorological Organization. For the total number of data in the time series indicated by *n*, we computed the statistical variable *S* as follows:

$$S = \sum_{k=1}^{n-1} \sum_{j=k+1}^{n} \text{sign}(x_j - x_k) \tag{8}$$

where: x_j is the value of the jth year, n denotes the number of years, and *sign (x)* is the signal function, as follows:

$$\text{sign}(x) = \begin{cases} 1, & \text{if } x > 0 \\ 0, & \text{if } x = 0 \\ -1, & \text{if } x < 0 \end{cases} \quad (9)$$

For a sample size (n) greater than 10, a normal approximation for the Mann-Kendall test can be used (Adamowski and Bougadis, 2003; Helsel and Frans, 2006). The mean of S is E [S] = 0 and the variance σ^2 was calculated as follows:

$$\sigma^2 = \left\{ n(n-1)(2n+5) - \sum_{j=1}^{p} t_j(t_j-1)(2t_j+5) \right\}/18 \quad (10)$$

where: considering that series can have groups with equal observations, P is the number of groups with equal observations; and t_j is the number of observations equal in group j. Thus, the standardized statistical test Z_{MK} can be calculated as follows:

$$Z = \begin{cases} \frac{S-1}{\sigma}, & \text{if } S > 0 \\ 0, & \text{if } S = 0 \\ \frac{S+1}{\sigma}, & \text{if } S < 0 \end{cases} \quad (11)$$

A positive (negative) value of S indicates an upward (downward) trend. The trend is not significant if $|Z_{MK}|$ is smaller than the standard normal variation $Z_{\alpha/2}$, where α is significant at 5% level. The presence of serial correlation in the time series data may affect trend detection in the non-parametric trend test, then a prewhitening procedure before testing for trends is required. However, the effect of serial correlation on the rejection rate of the null hypothesis is insignificant for large time-series size ($n \geq 50$) and the slope of the trend is high (≥0.01), and is better to use the MK test on the original data (Bayazit and Önöz, 2007; Nkiaka et al., 2017; Önöz and Bayazit, 2012; Yue and Wang, 2002).

2.6.2 Theil-Sen estimator

The Mann-Kendall test provides the detection of statistical significance of the trend, however, it does not provide an estimate of its magnitude. The magnitude of rainfall erosivity is predicted by Sen's slope estimator test (Sen, 1968). Thus, the non-parametric statistical estimator was obtained through the Theil-Sen median slope operator as follows:

$$\boldsymbol{\beta} = \text{median}\left(\frac{Y_i - Y_j}{i - j}\right) \qquad \forall j < i \tag{12}$$

for $1 < j < i < n$, where: β is the Sen's slope (linear change rate), resistant to outliers, Y_i and Y_j denote the variable in years i and j, and n is the number of data. For n years in the time series, $\boldsymbol{\beta}$ is the median of $N = n\,(n - 1)/2$ slope estimates. The β sign indicates the direction of change and its value represents the steepness of change.

Like many other hydrometeorological studies (Almeida et al., 2017; Vu et al., 2018; Zuo et al., 2016), Sen's slope has been used to quantify the true slopes in trend of target variable. Sen's slope estimator was applied to identify the slope for rainfall erosivity over the basin, and it was analyzed spatially.

Analyses of Boxplot with Student's *t*-test of the relative errors (Bennett et al., 2013) and the Levene test included a step to evaluate the suitability of the Eta model precipitation in simulating the variability of the R-factor and the mean values in the basin. This evaluation was carried out by calculating the model precipitation errors in the historical period.

Considering the suitability of the downscaling of the Eta model and the spatialization of the R-factor in the basin, we evaluated the alterations concerning the baseline period (1961-1990) for the short- (2020s), medium- (2050s), and long- (2080s) term periods. For this purpose, average, maximum value, minimum value, standard deviation, and skewness coefficient were used as statistical metrics. The statistical analyses and calculations of the results were carried out in the R (3.5.1) statistical environment (R Core Development Team, 2018).

3. RESULTS

3.1 The rainfall erosivity

3.1.1 Evaluation

Figure 2 depicts the relative errors of the simulated annual average rainfall erosivity derived from downscaling baseline in comparison with estimated rainfall erosivity derived from rain gauge stations, during the baseline period. All downscaling simulations exhibited small relative errors. The Eta-HadGEM2-ES simulation resulted in the smallest median relative error, but it was not significantly different from the Eta-CanESM2 and Eta-MIROC5 simulations, according to the *t*-test.

The Eta-BESM downscaling showed the greatest dispersion in the relative difference between observations and simulations, as shown by the widest boxplot interquartile range (Fig. 2). In addition, about 75% of this downscaling showed smaller relative errors and close to zero, as well as the frequency mostly below the median value. The same error pattern was noticed in the Eta-CanESM2 and Eta-MIROC5 downscalings, but the error distribution was more symmetric around the Eta-MIROC5 model mean value. In general, all four RCM downscalings showed similar results. Nevertheless, the median values of the Eta-HadGEM2-ES model were closer to observations. Around 25% of the relative errors were distributed very close to zero in the third boxplot quartile to this model downscaling (Fig. 2). Based on the Levene test, the variance of the R-factor was not statistically different for all climate simulations and observations for the baseline period.

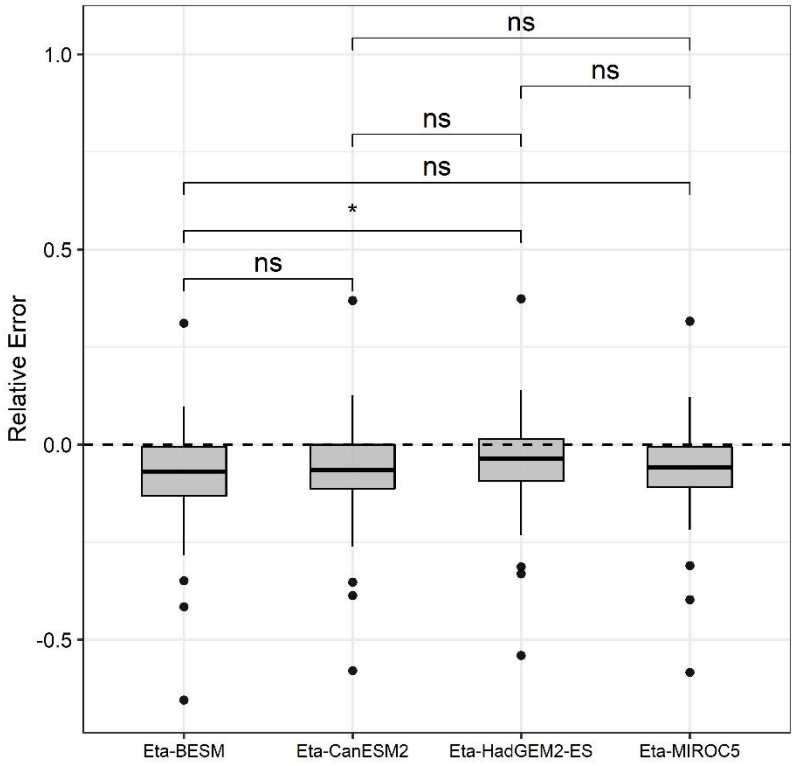

Fig. 2 – Boxplots of the relative errors between the simulated historical average rainfall erosivity derived from downscaling baseline and the rainfall erosivity derived from rain gauge stations. (*) indicates p <0.05; *ns* indicates a non-significant difference.

3.1.2 Projections

The projections of rainfall erosivity showed a substantial decrease from the baseline in the Tocantins-Araguaia basin as illustrated by Figure 3. This was observed through the simulated annual average rainfall erosivity in the entire Tocantins-Araguaia basin as calculated from the downscaling models' output of the historical period (1961-1990), and the future periods. The R-factor values show a spatial gradient reduction in the north-south directions with respect to the baseline climate. The smallest decrease occurred in the extreme north of the basin for the three future time slices.

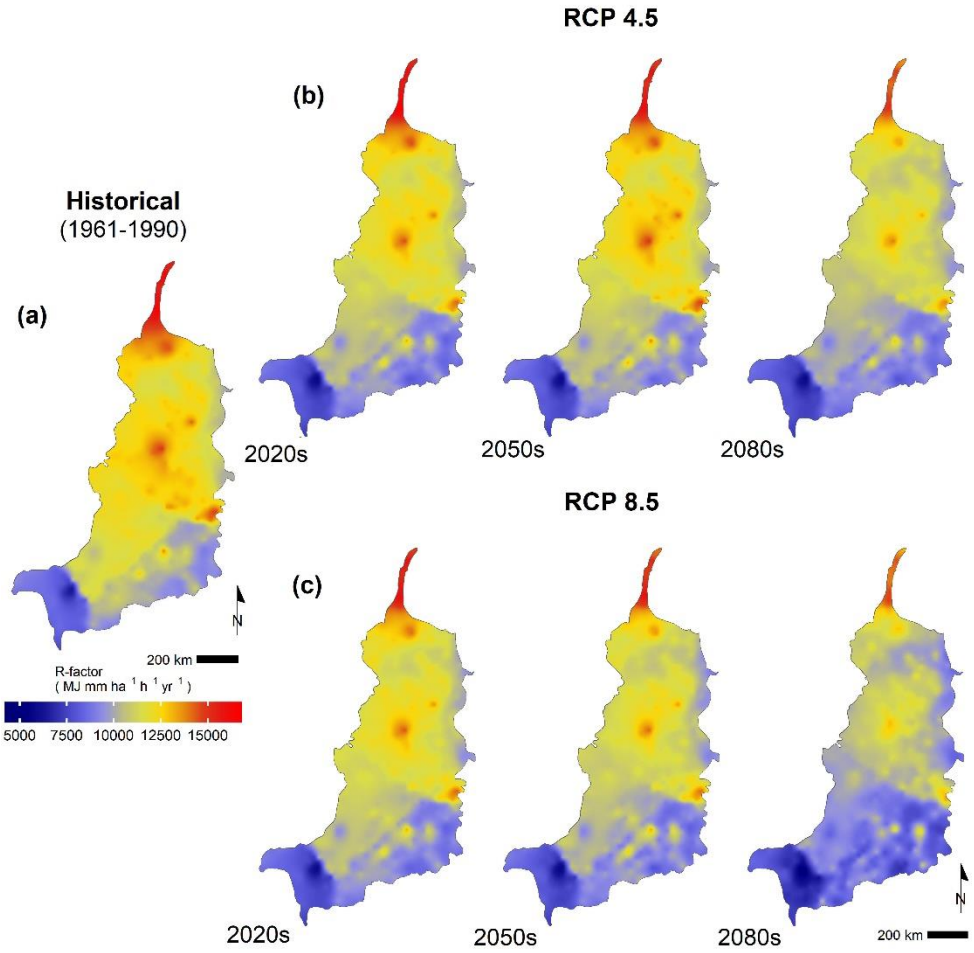

Fig. 3 – Annual average rainfall erosivity in the watershed for short-, medium-, and long- term periods using the multi-model ensemble, under RCP4.5 and RCP8.5 climate scenarios, as well as historical values.

The Modified Fourier Index used in the equations of the R-factor showed that the reduced rainfall indices are determinant on the intensity of rainfall erosivity in South America. As in future trends, the projections only indicated the changes in total precipitation amounts, therefore the analysis of the erosivity density is important to understand the variations, both in the amount and in the intensity of precipitation.

The projected changes in the hydrological processes of the Tocantins-Araguaia watershed indicate longer dry seasons, as well as more frequent and shorter dry spells during

the rainy season. This has also been discussed by Neto et al. (2016) as an effect of climate change that could threaten agroecosystems due to reduced water availability.

The areas of greatest potential of rainfall erosivity are located in the extreme north and northwest of the basin (Fig. 3), which is a region of territorial tension due to many protected natural areas. The projected average values of the R-factor (for all four downscalings) resulted in decreased values under RCP4.5 and RCP8.5 scenarios in the near-term (2011–2040), medium-term (2041–2070) and long-term (2071–2099) periods as compared to the baseline period within the study area (Table 2). Furthermore, the overall yearly R-factor variability was larger in near-, mid-, and long-term future time-slices, considering the mean four downscaling projection. The projected R-factor of all downscaling output, between the range of minimum and maximum values, decrease under both RCP scenarios. The greatest reduction was noticed for the minimum value (Table 3). On multi-model ensemble of the models, the projected mean reduction was 15.41% at the end of the century under the most pessimistic scenario (Table 3). Conversely, the maximum values showed an average increment of 4.46% and 5.03%, in RCP4.5 and RCP8.5 scenarios, respectively (Table 3).

Table 2 - Mean and Standard deviation of rainfall erosivity over baseline and projected periods.

	Baseline	Future scenario	
		RCP4.5	RCP8.5
		($MJ\ mm\ ha^{-1}\ h^{-1}\ yr^{-1}$)	
1961-1990	11507.61 (112.71)	-	-
2011-2040	-	10895.20 (349.71)	10834.09 (878.64)
2041-2070	-	11094.04 (340.10)	10563.89 (462.28)
2071-2099	-	10943.84 (560.83)	9741.14 (744.77)

Table 3 - Percentage change and dispersion measures of projected mean rainfall erosivity in the watershed for short-, medium-, and long-term periods using four RCM downscalings and under two RCP scenarios, as compared to baseline values

		RCP 4.5					**RCP 8.5**				
Model acronym	Period	min	mean	max	sd*	C_s*	min	mean	max	sd	Cs
	2020s	-18.08	-3.40	12.15	5.38	0.48	-2.30	3.72	22.55	3.35	1.36
Eta-BESM	2050s	-14.07	-1.13	10.18	5.53	0.11	-17.23	-3.79	9.63	3.77	-0.09
	2080s	-8.90	0.99	19.41	4.69	0.09	-32.77	-11.86	13.39	6.19	-0.32
	2020s	-15.15	-5.40	7.00	3.33	0.27	-15.31	-6.57	6.48	3.42	0.24
Eta-CanESM2	2050s	-17.53	-6.43	12.85	4.28	0.87	-26.84	-12.75	12.64	5.31	0.61
	2080s	-18.86	-8.54	12.36	4.44	0.90	-41.67	-25.28	3.00	6.27	0.32
	2020s	-26.79	-10.61	1.60	5.11	-0.41	-33.09	-14.14	-0.21	5.85	-0.80
Eta-HadGEM2-ES	2050s	-15.67	-3.53	4.33	3.41	-0.44	-27.73	-11.23	4.13	4.39	-0.78
	2080s	-19.70	-6.33	4.25	3.89	-0.27	-33.35	-16.07	5.47	4.81	-0.11
	2020s	-15.58	-6.01	6.34	3.61	0.04	-23.54	-10.21	0.81	4.97	-0.42
Eta-MIROC5	2050s	-22.74	-7.36	1.75	4.53	-0.57	-19.66	-8.41	5.73	4.31	-0.15
	2080s	-22.59	-9.55	3.73	4.32	0.05	-27.75	-11.64	8.34	5.39	-0.18
	2020s	-14.09	-5.47	2.10	3.34	-0.13	-12.80	-5.91	1.03	2.30	-0.20
Ensemble	**2050s**	-13.70	-3.70	5.88	3.41	-0.24	-18.28	-8.17	6.73	3.45	0.29
	2080s	-14.56	-4.95	5.41	3.31	-0.17	-29.76	-15.41	7.34	4.80	0.06

* sd. standard deviation, Cs. skewness coefficient

Significantly high rainfall erosivity values were computed for the Midwest region of the State of Tocantins, ranging from the Cantão region, into the ecotone between the Cerrado and the Amazon biomes, and towards the center of the State. Considering the separate analyses of each climate model, there were decreases of the R-factor for all periods in both emission scenarios in relation to the baseline period (Table 3). Regarding RCP4.5 (Table 3), the larger average decreases were 10.61% for short-term Eta-HadGEM2-ES; 7.36% for mid-term Eta-MIROC5, and 9.55% for long-term Eta-MIROC5. Meanwhile, concerning RCP8.5 scenario (Table 3), the larger average decreases were 14.14% for short-term Eta-HadGEM2-ES; 12.75% for mid-term Eta-CanESM2, and 25.28% for long-term Eta-CanESM2. Measures of dispersion and asymmetry of the predicted changes in R-factor, for the analyzed term periods and scenarios were realistic since the models were adjusted and validated for the baseline.

The monthly values of rainfall erosivity showed projections of decreased R-factor during the rainy season (Fig. 4), when compared to the baseline. Overall, the smallest decrease was observed in the northern portion of the basin during the wet period. The R-factor showed the greatest decreases in the three time-slices based on the RCP8.5 scenario (Fig. 5). There was a pronounced increase in the long-term for the dry season at downscaling under RCP8.5 scenario (Fig. 4). Meanwhile, decreased rainfall erosivity was estimated in the long-term for the rainy season using the RCP8.5 scenario at the multi-model ensemble in latitudes to the north of 5ºS. It was estimated slightly decreasing rainfall erosivity between February and April, whereas it was estimated a clear rainfall erosivity concentration in March for these lower latitudes. This concentration also was verified in March using long-term simulations under RPC4.5 scenario.

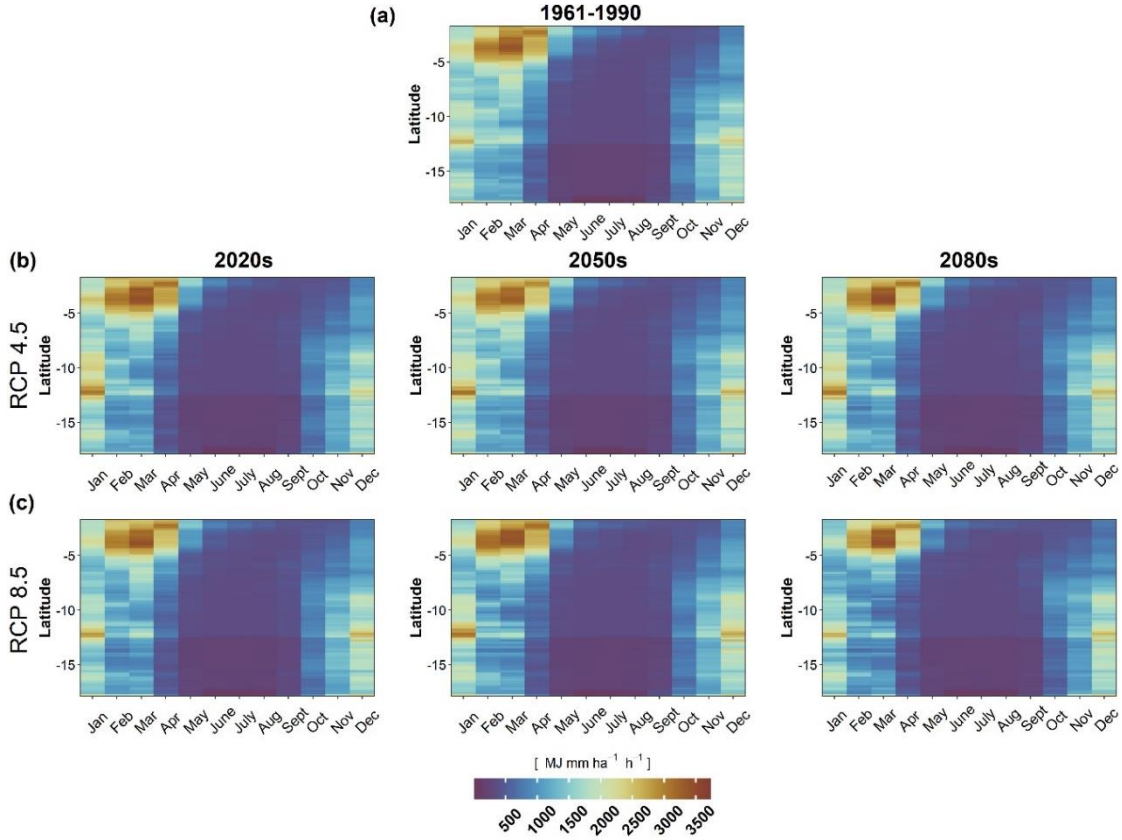

Fig. 4 - Average monthly rainfall erosivity based on the multi-model ensemble projections for the baseline period and future timeslices under RCP4.5 and RCP8.5 scenarios. The vertical axis shows the rainfall erosivity averaged by latitude, and the horizontal axis shows the month of year.

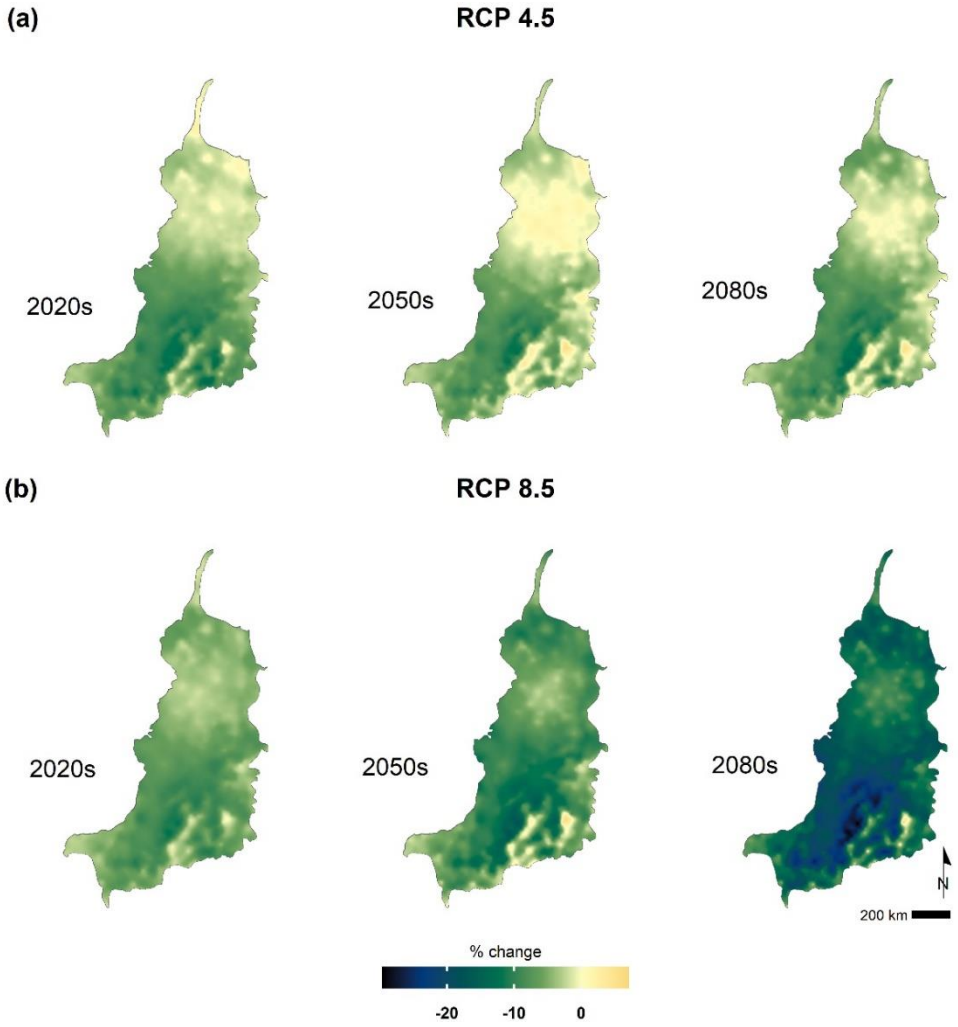

Fig. 5 - Average percentage change as compared to historical values in the rainfall erosivity in the watershed for short-, medium-, and long- term periods under RCP4.5 and RCP8.5 scenarios.

Based on the monthly analysis in the three-time slices, the multi-model ensemble projections exhibited greater sensitivity to changes in rainfall erosivity in the months of highest rainfall indexes. In fact, dry spell during the rainy season may well contribute to reduced rainfall erosivity towards the end of the century. All climate downscalings used in this study agreed consistently upon this regional change (Fig. 4), in which the number of sites less rainfall may contribute significantly to the projection of longer dry seasons, and more frequent short dry spell periods during rainy seasons.

3.2 Annual erosivity density

The average annual distributions of rainfall erosivity density over Tocantins-Araguaia basin for the baseline period and scenario-based projections express the rainfall patterns according to the different simulations of the climate models. Areas with high values of erosivity density indicated that the precipitation is marked by highly erosive events, which distribution is mainly concentrated from southwest to east of the basin (Fig. 6). This annual erosivity density presented values that will indeed exceed 9 MJ ha^{-1} h^{-1} for most of the projections, being characterized as high to very high ED values according to the classification given by Dash et al. (2019) for tropical regions.

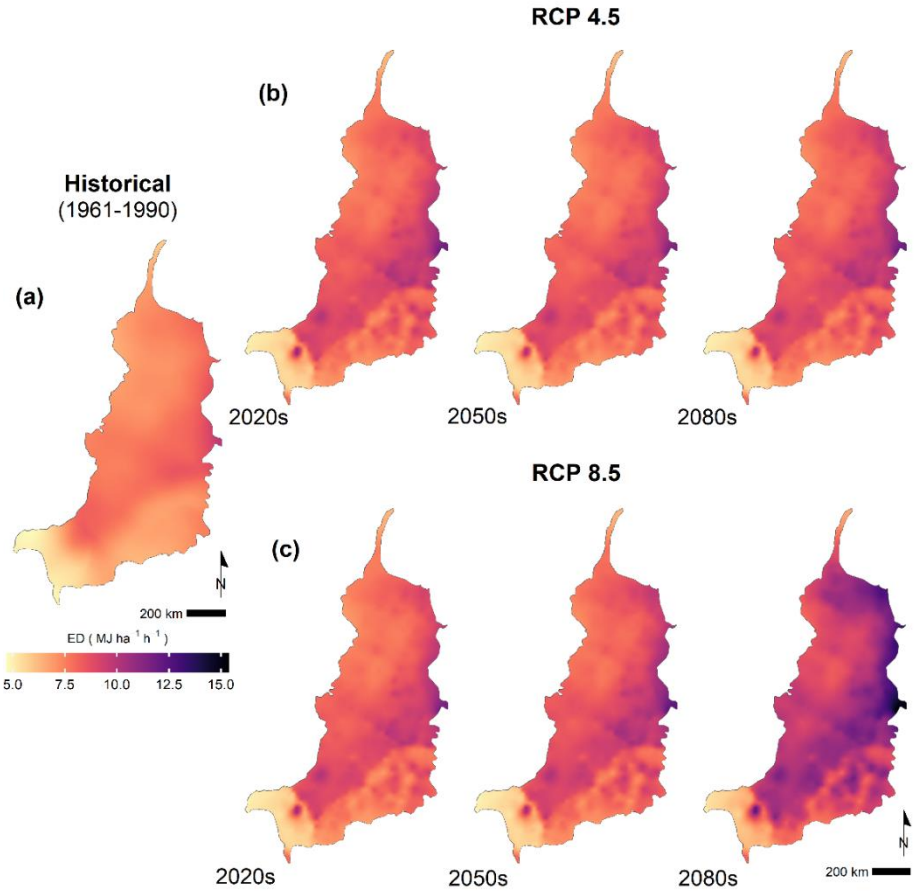

Fig. 6 - Average annual erosivity density in the watershed for short-, medium-, and long- term periods estimated by the multi-model ensemble, under RCP4.5 and RCP8.5 scenarios, as compared to historical values.

From a long-term perspective, a considerable increase for annual erosivity density under the climate change scenario RCP8.5 is expected, according to multi-model ensemble. This finding contrasts to the projected decrease in R-factor values; *viz.* an increase in the annual ED indicates the future presence of high-intensity precipitation events of short duration. This, however, would have little impact to the amount of highly erosive rainfalls throughout the basin. The higher the values of ED, the lesser influence of annual depth precipitation on the annual rainfall erosivity. Thus, the importance of a good statistical fit to calculate the regression model coefficients of this study is commensurate with using reliable data to project future erosive rainfall events via the R-factor.

Long-term increase in average ED in the basin indicated that the decrease amount of precipitation would be more pronounced than the R-factor decrease according to projections. This sensitivity difference among changes in R-factor and rainfall values will become less obvious in the mid-northern portion of the basin where highest values of R-factor were projected. Hence, for the lowest rates of future rainfall erosivity, rainstorms must remain predominant.

3.3 Temporal trends of annual rainfall erosivity

The MK test and the Theil-Sen estimator (Fig. 7) were used to compute spatial patterns of temporal trends for annual rainfall erosivity and their respective magnitudes. The value of the Z statistics identifies trends in the annual rainfall erosivity, being $Z < -1.96$ indicative of a significant negative trend; $-1.96 < Z < 0$ indicative of a negative trend; $0 < Z < 1.96$ indicative of positive trend; and $Z > 1.96$ indicative of a significant positive trend.

Figure 7 shows the trend of simulated annual rainfall erosivity in the watershed throughout the 21st century. Station points show significant or non-significant trends and their respective Sen's slope. The results showed that most of the station points presented a tendency

of decreasing annual rainfall erosivity throughout the 21st century in both, RCP4.5 and RCP8.5 scenarios, at a 95% confidence level. The highest decreasing trend was shown in the worst climate change scenario (RCP8.5), reaching values of the annual decrease of magnitude greater than 20 MJ mm ha^{-1} h^{-1} per year (>2,000 MJ mm ha^{-1} h^{-1} per century), in almost all the extension of the watershed according to multi-model ensemble downscaling climate projections.

Rainfall erosivity trends with the higher decrement at a significant level laid along the Upper and Middle Araguaia river. This was due to reduced rainfall indexes upstream of the basin, leading to decreasing patterns. Furthermore, the process may lead to less rill erosion development in areas susceptible to erosion and consequently of environmental vulnerability. Implementation of soil and water conservational practices are recommended to prevent decreased hydrologic regimes in the future that could challenge agroecosystems downstream.

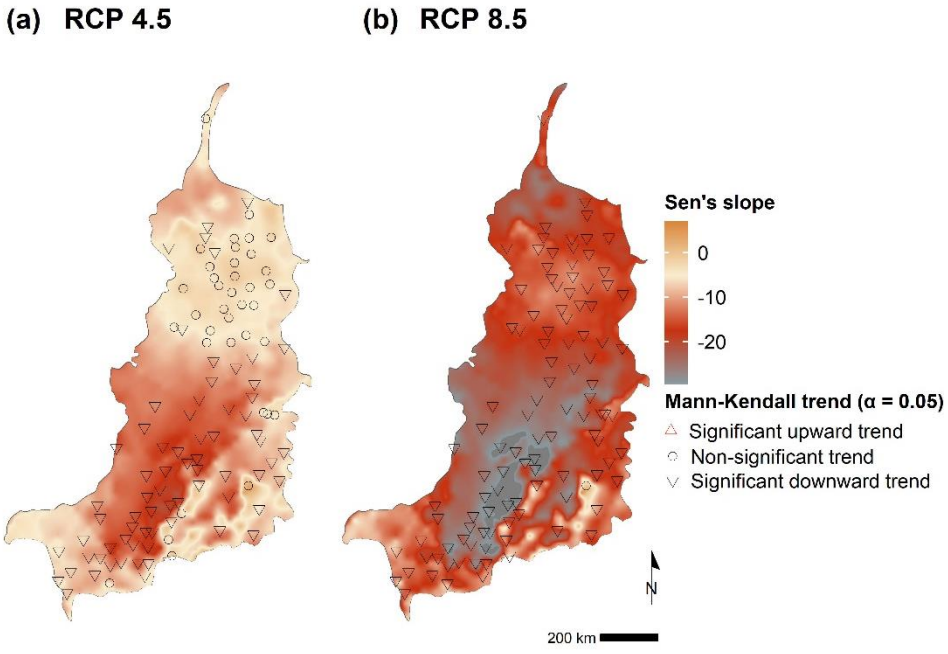

Fig. 7 - Sen's slope (expressed in units $year^{-1}$) and Z-statistics using the MK test at 5% significance level for the average of the multi-model ensemble in the RCP4.5 and RCP8.5 scenarios. The black downward triangles indicate significant decreasing trend, red upward triangles indicate significant increasing trend, and black circles indicate non-significant trend.

Table 4 shows a summary of the average seasonal Mann-Kendall trend and Sen's slope. Trend estimations of reduced R-factor during wet season were significant at an α=0.01, for all downscaling projections using RCP8.5. Meanwhile, for dry season, it was observed a significant trend (α=0.01), for three of the models using RCP8.5. Regarding RCP4.5 scenario, negative trends were estimated for rainy season according to Eta-CanESM2 and Eta-MIROC5 projections at a 0.01 significance level. For the dry season, it could be said reduced R-factor is expected at a 0.05 significance level for most of the downscaling projections using both scenarios; therefore, care should be taken for future climatic water deficit in this watershed. Furthermore, all projections using the worst climate change scenario (RCP8.5) pointed towards reductions during rainy season higher than 14 MJ mm ha^{-1} h^{-1} per year (1,400 MJ mm ha^{-1} h^{-1} per century).

Table 4 - Summary of past and projected R-factor trends for total annual and in the rainy and dry seasons in the Tocantins-Araguaia basin (1961-2099). Mann-Kendall trend test *p*-values < 0.05 are indicated in bold print.

	Z-test			*p*-value			Kendall's tau			Sen's Slope		
Model acronym	Annual	Rainy season	Dry season	Annual	Rainy season	Dry season	Annual	Rainy season	Dry season	Annual	Rainy season	Dry season
						RCP 4.5 emissions scenario						
Eta-BESM	-1.107	-0.783	-2.349	0.268	0.434	**0.019**	-0.063	-0.045	-0.135	-2.803	-2.156	-0.817
Eta-CanESM2	-4.010	-4.112	-1.471	**0.000**	**0.000**	0.141	-0.230	-0.236	-0.084	-12.159	-11.451	-0.603
Eta-HadGEM2-ES	-1.548	-1.399	-2.691	0.122	0.162	**0.007**	-0.089	-0.080	-0.154	-5.069	-4.076	-0.921
Eta-MIROC5	-4.236	-4.126	-3.314	**0.000**	**0.000**	**0.001**	-0.243	-0.236	-0.190	-13.612	-13.002	-1.052
						RCP 8.5 emissions scenario						
Eta-BESM	-4.494	-4.297	-3.026	**0.000**	**0.000**	**0.002**	-0.257	-0.246	-0.173	-14.802	-14.034	-1.140
Eta-CanESM2	-8.205	-8.249	-3.795	**0.000**	**0.000**	**0.000**	-0.470	-0.472	-0.217	-30.000	-28.947	-1.534
Eta-HadGEM2-ES	-4.764	-4.753	-0.969	**0.000**	**0.000**	0.333	-0.273	-0.272	-0.056	-15.132	-14.450	-0.408
Eta-MIROC5	-4.858	-4.472	-5.368	**0.000**	**0.000**	**0.000**	-0.278	-0.256	-0.307	-16.346	-14.594	-1.632

4. DISCUSSION

Future scenarios revealed that for the Tocantins-Araguaia basin, a reduction in rainfall erosivity is expected throughout the 21st century. This reduction in rainfall erosivity will occur due to the decrease in the amount of precipitation in the region, however extreme events will continue to occur (high value of the annual Erosivity Density). Thus, the reduction in rainfall erosivity will be much more influenced by the reduction in the amount of rainfall than by its intensity. Marengo et al. (2022) reported that MATOPIBA has already been changing towards a drier and warmer climate since 1980, being stronger over the State of Tocantins. For the future trend, the Global Circulation Models projected an accumulated reduction in precipitation in the Amazon region, reaching -40% (Riquetti et al., 2020).

Decrease in average amount of precipitation in the Tocantins-Araguaia Basin is closely related to the large-scale deforestation of the Amazon rainforest (Chou et al., 2014a; Lawrence and Vandecar, 2015) due to the influence of the high moisture flows in this region, which regulates the climate across the rest of Brazil (Marengo et al., 2022). Unlike other tropical regions in Southeast Asia or Central Africa, the Amazonia responds strongly to global warming, and its effects are exacerbated by deforestation, *i.e.*, a decline in rainfall frequency, and an expected shift in seasonality will occur as warmer daytime temperatures become common (Lawrence and Vandecar, 2015). Conversely, other tropical watersheds in Malaysia have shown an increasing trend in annual rainfall erosivity, as reported by Nasidi et al. (2021). In addition, an increase and decrease in rainfall erosivity are expected in areas of the Lower Niger Basin in West Africa (Amanambu et al., 2019), and the Huai Luang watershed in Thailand (Pheerawat and Udmale, 2017), respectively, mainly driven by the amount of precipitation in these tropical regions.

Climate change is expected to cause several negative impacts on agriculture (Jägermeyr et al., 2021), such as reduced annual precipitation (de Jong et al. 2018; Lyra et al., 2018; Pousa

et al., 2019), more frequent short-duration, but intense rainfall events, and regionalized water scarcity. In a regional scale, the reduction of erosive rainfall may be a positive factor in terms of soil erosion control; nevertheless, better water management practices should be adopted to support the expansion of agricultural production in this watershed. Adaptation measures to mitigate the effects of climate change need to be taken into action by all stakeholders. Seasonal hazardous climate events will become more frequent, *i.e.* water scarcity and wildfire vulnerability (dry season), and flash flooding (wet season). Thus, an interdisciplinary scientific approach is required to identify the challenges ahead and assure sustainable adaptation strategies to the ongoing, and never ending, climate change conditions. Changing rain patterns and trends in rainfall erosivity in the Tocantins-Araguaia basin are of greater concern, mainly in agricultural areas due to socio-economic and environmental impacts, in Southern Pará and Northern Tocantins (Bico do Papagaio region). In the Bico do Papagaio region, where rainy season extends to autumn, the expected seasonal increase in rainfall erosivity according to some models can lead to rural vulnerability under rising climate risk. Trends in rainfall erosivity due to climate change attract the interest of policy-makers and the great public, particularly when dealing with the poverty net and rural population distribution. Furthermore, it has already been addressed how climate change is pressuring the wide and fragile protected areas in the Amazon biome (Nobre et al., 2016).

The projections of reduced rainfall erosivity result in the positive outcome of less soil losses in the areas already endangered due to anthropogenic activities such as the expansion of crop and livestock and replacing native vegetation in the Brazilian Savannah (Cerrado) and Brazilian rainforest (Amazon) biomes. The reduced soil losses may translate in less load of soil nutrients and sediments into downstream water bodies. Therefore, the expansion of agroecosystems under soil conservation practices can ensure that reduced rainfall erosivity values support sustainable land management within the watershed. Our findings of potential

changes in rainfall erosivity in the Tocantins-Araguaia basin, as a result of future declining and variable rainfall, are in accordance with other research groups. Palomino-Lemus et al. (2018, 2017) reported a marked decrease in the amounts of rainfall, using climate change projections towards the end of the 21st century in Central and Southeastern Brazil. The block of the passage of frontal systems (a region where the Tocantins-Araguaia basin borders the La Plata Basin) will be submitted to negative anomalies in precipitation under RCP4.5 scenario (Mourão et al., 2016), being conditioned by a weakening of the SACZ. Likewise, reduced precipitation on the Eastern equatorial Amazon is expected as a result of warmer sea surface temperatures in the Atlantic ITCZ (Fu et al., 2001), *i.e.* reduced low-level moisture convergence is associated with decreased convection over the region. Additionally, other mechanisms are known to control the water vapor transport through the Amazon, being strongly affected by the reduction of the Amazon rainforest cover, *viz.* anthropogenic deforestation reduces local evapotranspiration and consequently impacts negatively on tropospheric water vapor, convection and climate (Agudelo et al., 2019; Sherwood et al., 2010). Besides the effects of human activities on the land, weather anomalies will continue to govern precipitation events –intensity, duration and frequency– (Borges et al., 2018; de Carvalho et al., 2013), as well as rainfall erosivity (dos Santos Silva et al., 2020). According to Ho et al. (2016), the average annual rainfall for ensemble mean of climate models decreases at the end of the 21st century under the RCP4.5 scenario in the watershed. On the interannual analysis, it is also expected an increase in the dry season period with the greatest reduction in rainfall in October, which can delay the sowing period in the region. The space-time variations of rainfall of the Tocantins-Araguaia hydrographic region are most susceptible to the meteorological anomaly in the Pacific (El Niño Southern Oscillation - ENSO) and Atlantic (Atlantic dipole) oceans (Loureiro et al., 2015). Those phenomena are associated with a decreasing trend in rainfall into the watershed, through heterogeneous and irregular spatial behavior. The climate aggressiveness during high-intensity pluviometric events

can be explained by the concentration of maximum rainfall at the northern of the watershed, which supports the occurrence of high rainfall erosivity events.

The monitoring of pronounced dry periods is important for agriculture in the region (Anderson et al., 2016). Moreover, longer droughts may favor wildfires which impact negatively on soil physical quality, as soil may become more vulnerable to erosion processes (DeLong et al., 2018). Thus, it is of foremost importance to advance the understanding of climate-soil-temporal systems for agricultural sustainability while preparing for future climatic conditions (Mäkinen et al., 2017). Other authors have discussed further consequences of climate change, and its impacts on the hydrological cycle. Reduction in average rainfall has also been projected for Northeastern Brazil; drier conditions will impact negatively on hydroelectric production and might require expansion on irrigated agricultural areas (de Jong et al., 2018). Almagro et al. (2017) also reported decreased rainfall in areas between the northeast and north of Brazil. This stretch pointed out as the last Brazilian agricultural frontier, encompasses parts of the states of Maranhão, Tocantins, Piauí, and Bahia. A strong tendency to implement high productivity agricultural systems has been observed within this region. Thus, anthropogenic activities, such as modifications on land use and soil coverage in the Amazon and Cerrado biomes, have brought ecological pressure upon the area (Spera et al., 2016). To the east of the Tocantins-Araguaia basin, an important agricultural expansion area (Western Bahia) is expected to generate socioeconomical conflicts in the region due to intense irrigation growth, while a significant decrease in rainfall (up to 12%) is expected (Pousa et al., 2019). Such large climate variability, with an increase in the drought period and the occurrence of extreme precipitation events, can adversely affect the driest areas susceptible to erosion processes.

The estimated impacts of climate change on rainfall erosivity are relevant for the assessment of hydrological ecosystem services at different spatial and temporal scales. Climate changes and anthropogenic pressures, such as expansion of urban areas, and agricultural

activities are already impacting hydrological services in various regions of Brazilian biomes; perhaps, even beyond natural ecosystem resilience, *e.g.*, water supply (Sone et al., 2019; Taffarello et al., 2017), or natural occurring sediment and nutrient transport to support vital aquatic ecosystems (Casagrande et al., 2021; Maia et al., 2018; Sone et al., 2019). For large river basins, it needs to be emphasized the complexity of using hydrological modeling as a decision-making tool based on heterogeneous data (resolution, time continuity, defective equipment, among others), and assessment models with different levels of uncertainty (calibration, validation, number of water-related processes) (Johnston and Smakhtin, 2014; Tafarello et al., 2017; van de Sand et al., 2014).

Ultimately, results suggest potential or expected trends of reduced annual R-factor towards the end of the 21st century, under climate change scenarios and regional conditions. Nonetheless, rainfall erosivity should not be treated as an isolated variable. Research institutions, government, and farmers should act together facing climate change. Therefore, public policies, at the local or regional level, should address today problems to achieve sustainable agro-alimentary systems. Likewise, projections of reduced rainfall erosion potential, in the Tocantins-Araguaia basin, reinforces the need to analyze other environmental factors that may lead to diverse future challenges, *e.g.* water scarcity.

5. CONCLUSIONS

Through the Mann-Kendall test and the analysis of the Theil-Sen estimator, we can confirm the general trend of decreasing rainfall erosivity values in the Tocantins-Araguaia river basin for both RCP scenarios. The RCP8.5 scenario projected the worse drought conditions, according to the Eta-CanESM2 and Eta-MIROC5 dowsncaling outputs. In most of the watershed, projected annual rainfall erosivity reduced more than 20 MJ mm ha^{-1} h^{-1} per year, which corresponds to over 2,000 MJ mm ha^{-1} h^{-1} throughout the 21st century.

The monthly values of the R-factor, during all three timeslices of the century, were concentrated in the rainy season, with the projections under RCP8.5 scenario being the most sensitive to the reduction of rainfall erosivity. The dry season decreased in all years of the century under the RCP8.5 scenario in most of the projections.

Projected precipitation towards the end of the century may lead to less erosive rains, in contrast to the trend of greater erosion caused by the change in land use (Cardoso, 2021). Nevertheless, the expansion of agricultural activity in this watershed should include best management practices for soil and water conservation. Further research studies are required to ensure agroecosystems sustainability under climatic change conditions and ever-growing stressed agricultural environments.

ACKNOWLEDGMENTS

The authors would like to acknowledge the CNPq process 476803/2013-6 and CAPES code 001 for the financial support of research funds and fellowships associated with the research groups involved. S.C. Chou is partially funded by CNPq 306757/2017-6. The authors also wish to thank the Eta climate group from the Brazilian National Institute for Space Research (INPE) for the availability of the Eta RCM outputs. The climate change projections datasets can be accessed from https://projeta.cptec.inpe.br and CORDEX-ESGF.

6. REFERENCES

Adamowski, K., Bougadis, J., 2003. Detection of trends in annual extreme rainfall. Hydrol. Process. 17, 3547–3560. https://doi.org/10.1002/hyp.1353

Agudelo, J., Arias, P.A., Vieira, S.C., Martínez, J.A., 2019. Influence of longer dry seasons in

the Southern Amazon on patterns of water vapor transport over northern South America and the Caribbean. Clim. Dyn. 52, 2647–2665. https://doi.org/10.1007/s00382-018-4285-1

Almagro, A., Oliveira, P.T.S., Nearing, M.A., Hagemann, S., 2017. Projected climate change impacts in rainfall erosivity over Brazil. Sci. Rep. 7, 8130. https://doi.org/10.1038/s41598-017-08298-y

Almeida, C.O.S., 2009. Erosividade das chuvas no estado de Mato Grosso. Diss. Mestr. em Ciências Agrárias. Universidade de Brasília.

Almeida, C.O.S., Amorim, R.S.S., Eltz, F.L.F., Couto, E.G., Jordani, S.A., 2012. Erosividade da chuva em municípios do Mato Grosso: distribuição sazonal e correlações com dados pluviométricos. Rev. Bras. Eng. Agrícola e Ambient. 16, 142–152. https://doi.org/10.1590/s1415-43662012000200003

Almeida, C.T., Oliveira-Júnior, J.F., Delgado, R.C., Cubo, P., Ramos, M.C., 2017. Spatiotemporal rainfall and temperature trends throughout the Brazilian Legal Amazon, 1973–2013. Int. J. Climatol. 37, 2013–2026. https://doi.org/10.1002/joc.4831

Alvares, C.A., Stape, J.L., Sentelhas, P.C., De Moraes Gonçalves, J.L., Sparovek, G., 2013. Köppen's climate classification map for Brazil. Meteorol. Zeitschrift 22, 711–728. https://doi.org/10.1127/0941-2948/2013/0507

Amanambu, A.C., Lia, L., Egbinola, C.N., Obarein, O.A., Mupenzi, C., Chen, D., 2019. Spatio-temporal variation in rainfall-runoff erosivity due to climate change in the Lower Niger Basin, West Africa. Cantena. 172, 324–334. https://doi.org/10.1016/j.catena.2018.09.003

Anderson, M.C., Zolin, C.A., Sentelhas, P.C., Hain, C.R., Semmens, K., Yilmaz, M.T., Gao,

F., Otkin, J.A., Tetrault, R., 2016. The Evaporative Stress Index as an indicator of agricultural drought in Brazil: An assessment based on crop yield impacts. Remote Sens. Environ. 174, 82–99. https://doi.org/10.1016/j.rse.2015.11.034

Angulo-Martínez, M., Beguería, S., 2009. Estimating rainfall erosivity from daily precipitation records: A comparison among methods using data from the Ebro Basin (NE Spain). J. Hydrol. 379, 111–121. https://doi.org/10.1016/j.jhydrol.2009.09.051.

Apaydin, H., Erpul, G., Bayramin, I., Gabriels, D., 2006. Evaluation of indices for characterizing the distribution and concentration of precipitation: A case for the region of Southeastern Anatolia Project, Turkey. J. Hydrol., 328, 726–732. https://doi.org/10.1016/j.jhydrol.2006.01.019.

Aquino, R.F., Silva, M.L.N., Freitas, D.A.F., Curi, N., Mello, C.R., Avanzi, J.C., 2012. Spatial

variability of the rainfall erosivity in Southern region of Minas Gerais State, Brazil. Ci. Agrotec. 36, 533–542. https://doi.org/10.1590/S1413-70542012000500006

Antico, P.L., Chou, S.C. & Brunini, C.A., 2021: The foehn wind east of the Andes in a 20-year climate simulation. Meteorol Atmos Phys vol 132, no.3, 317-330. https://doi.org/10.1007/s00703-020-00752-3

Arnoldus, H.M.J., 1980. An approximation of the rainfall factor in the Universal Soil Loss Equation. An Approx. rainfall factor Univers. Soil Loss Equation. 127–132.

Arora, V.K., Scinocca, J.F., Boer, G.J., Christian, J.R., Denman, K.L., Flato, G.M., Kharin, V. V., Lee, W.G., Merryfield, W.J., 2011. Carbon emission limits required to satisfy future representative concentration pathways of greenhouse gases. Geophys. Res. Lett. 38, 3–8. https://doi.org/10.1029/2010GL046270

Azari, M., Oliaye, A., Nearing, M.A., 2021. Expected climate change impacts on rainfall erosivity over Iran based on CMIP5 climate models. J. Hydrol., 593, 125826. https://doi.org/10.1016/j.jhydrol.2020.125826.

Back, Á.J., Gonçalves, F.N., Fan, F.M., 2019. Spatial, seasonal, and temporal variations in rainfall aggressiveness in the south of Brazil. Eng. Agric. 39, 466–475. https://doi.org/10.1590/1809-4430-Eng.Agric.v39n4p466-475/2019

Ballabio, C., Borrelli, P., Spinoni, J., Meusburger, K., Michaelides, S., Beguería, S., Klik, A., Petan, S., Janeček, M., Olsen, P., Aalto, J., Lakatos, M., Rymszewicz, A., Dumitrescu, A., Tadić, M.P., Diodato, N., Kostalova, J., Rousseva, S., Banasik, K., Alewell, C., Panagos, P., 2017. Mapping monthly rainfall erosivity in Europe. Sci. Total Environ. 579, 1298–1315. https://doi.org/10.1016/j.scitotenv.2016.11.123

Bárdossy, A., Pegram, G., 2011. Downscaling precipitation using regional climate models and circulation patterns toward hydrology. Water Resour. Res. 47, 1–18. https://doi.org/10.1029/2010WR009689

Bayazit, M., Önöz, B., 2007. To prewhiten or not to prewhiten in trend analysis? Hydrol. Sci. J. 52, 611–624. https://doi.org/10.1623/hysj.52.4.611

Bennett, N.D., Croke, B.F.W., Guariso, G., Guillaume, J.H.A., Hamilton, S.H., Jakeman, A.J., Marsili-libelli, S., Newham, L.T.H., Norton, J.P., Perrin, C., Pierce, S.A., Robson, B., Seppelt, R., Voinov, A.A., Fath, B.D., 2013. Characterising performance of environmental models. Environ. Model. Softw. 40, 1–20. https://doi.org/10.1016/j.envsoft.2012.09.011

Borges, P.D.A., Bernhofer, C., Rodrigues, R., 2018. Extreme rainfall indices in Distrito Federal , Brazil : Trends and links with El Niño southern oscillation and Madden – Julian oscillation. Int. J. Climatol. 38, 4550–4567. https://doi.org/10.1002/joc.5686

Borrelli, P., Robinson, D.A., Fleischer, L.R., Lugato, E., Ballabio, C., Alewell, C., Meusburger, K., Modugno, S., Schütt, B., Ferro, V., Bagarello, V., Van Oost, K., Montanarella, L., Panagos, P., 2017. An assessment of the global impact of 21st century land use change on soil erosion. Nat. Commun. 8, 2013. https://doi.org/10.1038/s41467-017-02142-7

Cantalice, J.R.B., Bezerra, S.A., Figueira, S.B., Inácio, E.S.B., Silva, M.D.R.O., 2009. Linhas isoerosivas do estado de Pernambuco – 1ª aproximação. Caatinga 22, 75–80.

Cardoso, D.P., 2021. Rainfall erosivity estimation via several methods, and water erosion modeling at Peixe Angical Reservoir - TO. 105p. Doctoral dissertation. Federal University of Lavras, Lavras.

Cardoso, D.P., Avanzi, J.C., Ferreira, D.F., Acuña-Guzman, S.F., Silva, M.L.N., Pires, F.R., Curi, N., 2022. Rainfall erosivity estimation: Comparison and statistical assessment among methods using data from Southeastern Brazil. Rev. Bras. Ci. Solo, 46, e0210122, https://doi.org/10.36783/18069657rbcs20210122

Casagrande, M.F.S., Furlan, L.M., Moreira, C.A., Rosa, F.T.G., Rosolen, V., 2021. Non-invasive methods in the identification of hydrological ecosystem services of a tropical isolated wetland (Brazilian study case), Environ. Challenges. 5, 100233, https://doi.org/10.1016/j.envc.2021.100233.

Chou, S.C., Lyra, A., Mourão, C., Dereczynski, C., Pilotto, I., Gomes, J., Bustamante, J., Tavares, P., Silva, A., Rodrigues, D., Campos, D., Chagas, D., Sueiro, G., Siqueira, G., Marengo, J., 2014a. Assessment of Climate Change over South America under RCP 4.5 and 8.5 Downscaling Scenarios. Am. J. Clim. Chang. 03, 512–527. https://doi.org/10.4236/ajcc.2014.35043

Chou, S.C., Lyra, A., Mourão, C., Dereczynski, C., Pilotto, I., Gomes, J., Bustamante, J., Tavares, P., Silva, A., Rodrigues, D., Campos, D., Chagas, D., Sueiro, G., Siqueira, G., Nobre, P., Marengo, J., 2014b. Evaluation of the Eta Simulations Nested in Three Global Climate Models. Am. J. Clim. Chang. 03, 438–454. https://doi.org/10.4236/ajcc.2014.35039

Chou, S.C., Marengo, J.A., Lyra, A.A., Sueiro, G., Pesquero, J.F., Alves, L.M., Kay, G., Betts, R., Chagas, D.J., Gomes, J.L., Bustamante, J.F., Tavares, P., 2012. Downscaling of South America present climate driven by 4-member HadCM3 runs. Clim. Dyn. 38, 635–653. https://doi.org/10.1007/s00382-011-1002-8

Collins, W.J., Bellouin, N., Doutriaux-Boucher, M., Gedney, N., Halloran, P., Hinton, T., Hughes, J., Jones, C.D., Joshi, M., Liddicoat, S., Martin, G., O'Connor, F., Rae, J., Senior, C., Sitch, S., Totterdell, I., Wiltshire, A., Woodward, S., 2011. Development and evaluation of an Earth-System model – HadGEM2. Geosci. Model Dev. 4, 1051–1075. https://doi.org/10.5194/gmd-4-1051-2011

Correa, S.W., Mello, C.R., Norton, L.D., Curi, N., Chou, S.C., 2016. Soil erosion risk associated with climate change at Mantaro River basin, Peruvian Andes. Catena 147, 110–124. https://doi.org/10.1016/j.catena.2016.07.003

da Silva, A.M., 2004. Rainfall erosivity map for Brazil. Catena 57, 251–259. https://doi.org/10.1016/j.catena.2003.11.006

Dash, C.J., Das, N.K., Adhikary, P.P., 2019. Rainfall erosivity and erosivity density in Eastern Ghats Highland of east India. Nat. Hazards 97, 727–746. https://doi.org/10.1007/s11069-019-03670-9

de Carvalho, J.R.P., Assad, E.D., Evangelista, S.R.M., Pinto, H. da S., 2013. Estimation of dry spells in three Brazilian regions — Analysis of extremes. Atmos. Res. 132, 12–21.

https://doi.org/doi.org/10.1016/j.atmosres.2013.04.003

de Jong, P., Tanajura, C.A.S., Sánchez, A.S., Dargaville, R., Kiperstok, A., Torres, E.A., 2018. Hydroelectric production from Brazil's São Francisco River could cease due to climate change and inter-annual variability. Sci. Total Environ. 634, 1540–1553. https://doi.org/10.1016/j.scitotenv.2018.03.256

DeLong, S.B., Youberg, A.M., DeLong, W.M., Murphy, B.P., 2018. Post-wildfire landscape change and erosional processes from repeat terrestrial lidar in a steep headwater catchment, Chiricahua Mountains, Arizona, USA. Geomorphology 300, 13–30. https://doi.org/10.1016/j.geomorph.2017.09.028

Dereczynski, C., Chou, S.C., Lyra, A., Sondermann, M., Regoto, P., Tavares, P.,Chagas, D., Gomes, J.L., Rodrigues, D.C., Skansi, M.M.. Downscaling of climate extremes over South America – Part I: Model evaluation in the reference climate. Weather and Climate Extremes. p. 100273, 2020. DOI: 10.1016/j.wace.2020.100273

Diodato, N., Borrelli, P., Fiener, P., Bellocchi, G., Romano, N., 2017. Discovering historical rainfall erosivity with a parsimonious approach: A case study in Western Germany. J. Hydrol. 544, 1–9. https://doi.org/10.1016/j.jhydrol.2016.11.023

Donzeli, P.L., Morais, J.F.L., Dias, R.R., Pereira, E.Q., Santos, L.F. dos, 2006. Projeto de Gestão Ambiental Integrada da Região do Bico do Papagaio. Zoneamento Ecológico-Econômico. Diagnóstico do Risco de Erosão e Perdas de Solo do Norte do Estado do Tocantins. Palmas.

dos Santos Silva, D.S., Blanco, C.J.C., dos Santos Junior, C.S., Martins, W.L.D., 2020. Modeling of the spatial and temporal dynamics of erosivity in the Amazon. Model. Earth Syst. Environ. 6, 513–523. https://doi.org/10.1007/s40808-019-00697-6

Duulatov, E., Chen, X., Amanambu, A.C., Ochege, F.U., Orozbaev, R., Issanova, G., Omurakunova, G., 2019. Projected Rainfall erosivity over central asia based on CMIP5 climate models. Water. 11, 897. https://doi.org/10.3390/w11050897

El-Swaify, S.A., Dangler, E.W., Armstrong, C.L., 1982. Soil erosion by water in the tropics. Research Extension Series 024, College of Tropical Agriculture and Human Resources, University of Hawaii, Honolulu.

Foster, G.R., McCool, D.K., Renard, K.G., Moldenhauer, W.C., 1981. Conversion of the universal soil loss equation to SI metric units. J. Soil Water Conserv. 36, 355–359.

Fournier, F., 1956. The effect of climatic factors on soil erosion estimates of solids transported in suspension in runoff. [S.l.] Assoc. Hydrol. Ent. Public.

Fournier, F., 1960. Climat et Erosion, 1st ed. Presses Universitaires de France. Paris, France.

Fu, R., Dickinson, R.E., Chen, M., Wang, H., 2001. How do tropical sea surface temperatures influence the seasonal distribution of precipitation in the equatorial Amazon? J. Clim. 14, 4003–4026. https://doi.org/10.1175/1520-0442(2001)014<4003:HDTSST>2.0.CO;2

Gafforov, K.S., Bao, A., Rakhimov, S., Liu, T., Abdullaev, F., Jiang, L., Durdiev, K., Duulatov, E., Rakhimova, M., Mukanov, Y., 2019. The Assessment of Climate Change on Rainfall-Runoff Erosivity in the Chirchik–Akhangaran Basin, Uzbekistan. Sustainability. 12, 3369. https://doi.org/10.3390/su12083369

Gorguner, M., Kavvas, M.L., Ishida, K., 2019. Assessing the impacts of future climate change on the hydroclimatology of the Gediz Basin in Turkey by using dynamically downscaled CMIP5 projections. Sci. Total Environ. 648, 481–499. https://doi.org/10.1016/j.scitotenv.2018.08.167

Grillakis, M.G., Polykretis, C., Alexakis, D.D., 2020. Past and projected climate change

impacts on rainfall erosivity: Advancing our knowledge for the eastern Mediterranean island of Crete. Catena. 193, 104625. https://doi.org/10.1016/j.catena.2020.104625

Helsel, D.R., Frans, L.M., 2006. Regional Kendall test for trend. Environ. Sci. Technol. 40, 4066–4073. https://doi.org/10.1021/es051650b

Ho, J.T., Thompson, J.R., Brierley, C., 2016. Projections of hydrology in the Tocantins-Araguaia Basin, Brazil: uncertainty assessment using the CMIP5 ensemble. Hydrol. Sci. J. 61, 551–567. https://doi.org/10.1080/02626667.2015.1057513

Huang, J., Zhang, J., Zhang, Z., Xu, C.Y., 2013. Spatial and temporal variations in rainfall erosivity during 1960-2005 in the Yangtze River basin. Stoch. Environ. Res. Risk Assess. 27, 337–351. https://doi.org/10.1007/s00477-012-0607-8

IPCC, 2013. Climate Change 2013: The Physical Science Basis. Contribution of Working Group I to the Fifth Assessment Report of the Intergovernmental Panel on Climate Change. Cambridge University Press, Cambridge, United Kingdom and New York, NY, USA.

Jägermeyr, J., Müller, C., Ruane, A.C., Elliott, J., Balkovic, J., Castillo, O., Faye, B., Foster, I., Folberth, C., Franke, J.A., Fuchs, K., Guarin, J.R., Heinke, J., Hoogenboom, G., Iizumi, T., Jain, A.K., Kelly, D., Khabarov, N., Lange, S., Lin, T.S., Liu, W., Mialyk, O., Minoli, S., Moyer, E.J., Okada, M., Phillips, M., Porter, C., Rabin, S.S., Scheer, C., Schneider, J.M., Schyns, J.F., Skalsky, R., Smerald, A., Stella, T., Stephens, H., Webber, H., Zabel, F., Rosenzweig, C., 2021. Climate impacts on global agriculture emerge earlier in new generation of climate and crop models. Nat Food 2, 873–885. https://doi.org/10.1038/s43016-021-00400-y

Jin, L., Whitehead, P.G., Appeaning Addo, K., Amisigo, B., Macadam, I., Janes, T., Crossman, J., Nicholls, R.J., McCartney, M., Rodda, H.J.E., 2018. Modeling future

flows of the Volta River system: Impacts of climate change and socio-economic changes. Sci. Total Environ. 637–638, 1069–1080. https://doi.org/10.1016/j.scitotenv.2018.04.350

Johnston, R., Smakhtin, V., 2014. Hydrological Modeling of Large river Basins: How Much is Enough? Water Resour. Manag. 28, 2695–2730. https://doi.org/10.1007/s11269-014-0637-8

Kendall, M.G., 1975. Rank Correlation Methods, 4th ed. Charles Griffin, London.

Kinnell, P.I.A., 2010. Event soil loss, runoff and the Universal Soil Loss Equation family of models: A review. J. Hydrol. 385, 384–397. https://doi.org/10.1016/j.jhydrol.2010.01.024

Labrière, N., Locatelli, B., Laumonier, Y., Freycon, V., Bernoux, M., 2015. Soil erosion in the humid tropics: A systematic quantitative review. Agric. Ecosyst. Environ. 203, 127–139. https://doi.org/10.1016/j.agee.2015.01.027

Lal, R., 1983. Soil erosion in the humid tropics with particular reference to agricultural land development and soil management, in: Keller, R. (Ed.), Hydrology of Humid Tropical Regions with Particular Reference to the Hydrological Effects of Agriculture and Forestry Practice (Proceedings of the Hamburg Symposium, August 1983). IHAS Publication, Wallingford, UK, pp. 221–239.

Lawrence, D., Vandecar, K., 2015. Effects of tropical deforestation on climate and agriculture. Nat. Clim. Chang. 5, 27–36. https://doi.org/10.1038/nclimate2430

Li, X., Li, Z., Lin, Y., 2020. Suitability of TRMM Products with Different Temporal Resolution (3-Hourly, Daily, and Monthly) for Rainfall Erosivity Estimation. Remote Sens. 12, 3924. https://doi.org/10.3390/rs12233924.

Loureiro, G.E., Fernandes, L.L., Ishihara, J.H., 2015. Spatial and temporal variability of

rainfall in the Tocantins-Araguaia hydrographic region. Acta Sci. - Technol. 37, 89–98. https://doi.org/10.4025/actascitechnol.v37i1.20778

Lyra, A., Tavares, P., Chou, S.C., Sueiro, G., Dereczynski, C., Sondermann, M., Silva, A., Marengo, J., Giarolla, A., 2018. Climate change projections over three metropolitan regions in Southeast Brazil using the non-hydrostatic Eta regional climate model at 5-km resolution. Theor Appl Climatol 132, 663–682. https://doi.org/10.1007/s00704-017-2067-z

Ma, X., He, Y., Xu, J., van Noordwijk, M., Lu, X., 2014. Spatial and temporal variation in rainfall erosivity in a Himalayan watershed. Catena 121, 248–259. https://doi.org/10.1016/j.catena.2014.05.017.

Maia, A.G., Miyamoto, B.C.B., Garcia, J.R., 2018. Climate Change and Agriculture: Do Environmental Preservation and Ecosystem Services Matter?. Ecol. Econ. 152, 27–39. https://doi.org/10.1016/j.ecolecon.2018.05.013.

Mäkinen, H., Kaseva, J., Virkajärvi, P., Kahiluoto, H., 2017. Agricultural and Forest Meteorology Shifts in soil – climate combination deserve attention. Agric. For. Meteorol. 234–235, 236–246. https://doi.org/10.1016/j.agrformet.2016.12.017

Mann, H.B., 1945. Nonparametric tests against trend. Soc. Econom. J. Econom. 13, 245–259. https://doi.org/10.2307/1907187

Marengo, J.A., Chou, S.C., Kay, G., Alves, L.M., Pesquero, J.F., Soares, W.R., Santos, D.C., Lyra, A.A., Sueiro, G., Betts, R., Chagas, D.J., Gomes, J.L., Bustamante, J.F., Tavares, P., 2012. Development of regional future climate change scenarios in South America using the Eta CPTEC/HadCM3 climate change projections: Climatology and regional analyses for the Amazon, São Francisco and the Paraná River basins. Clim. Dyn. 38, 1829–1848. https://doi.org/10.1007/s00382-011-1155-5

Marengo, J.A., Jimenez, J.C., Espinoza, J.C., Cunha, A.P., Aragão, L.E.O., 2022. Increased climate pressure on the agricultural frontier in the Eastern Amazonia–Cerrado transition zone. Sci. Rep. 12, 1–10. https://doi.org/10.1038/s41598-021-04241-4

Martins, S.G., Avanzi, J.C., Silva, M.L.N., Curi, N., Norton, L.D., Fonseca, S., 2010. Rainfall erosivity and rainfall return period in the experimental watershed of Aracruz, in the Coastal Plain of Espirito Santo, Brazil. Rev. Bras. Ci. Solo 34, 999–1004. https://doi.org/10.1590/S0100-06832010000300042

Mello, C.R. de, Ávila, L.F., Viola, M.R., Curi, N., Norton, L.D., 2015. Assessing the climate change impacts on the rainfall erosivity throughout the twenty-first century in the Grande River Basin (GRB) headwaters, Southeastern Brazil. Environ. Earth Sci. 73, 8683–8698. https://doi.org/10.1007/s12665-015-4033-3

Mello, C.R. De, Sá, M.A.C. De, Curi, N., Mello, J.M. de, Viola, M.R., Silva, A.M. Da, 2007. Erosividade mensal e anual da chuva no Estado de Minas Gerais. Pesqui. Agropecuária Bras. 42, 537–545. https://doi.org/10.1590/S0100-204X2007000400012

Men, M., Yu, Z., Xu, H., 2008. Study on the spatial pattern of rainfall erosivity based on geostatistics in Hebei Province, China. Front. Agric. China 2, 281–289. https://doi.org/10.1007/s11703-008-0042-2.

Mesinger, F., Chou, S.C., Gomes, J.L., Jovic, D., Bastos, P., Bustamante, J.F., Lazic, L., Lyra, A.A., Morelli, S., Ristic, I., Veljovic, K., 2012. An upgraded version of the Eta model. Meteorol. Atmos. Phys. 116, 63–79. https://doi.org/10.1007/s00703-012-0182-z

Mesinger, F., Veljovic, K., Chou, S.C., Gomes, J., Lyra, A., 2016. The Eta Model: Design, Use, and Added Value, in: Hromadka, T., Rao, P. (Eds.), Topics in Climate Modeling. Intech, Rijeka, pp. 137–156. https://doi.org/10.5772/64956

Mondal, A., Khare, D., Kundu, S., 2016. International Soil and Water Conservation Research Change in rainfall erosivity in the past and future due to climate change in the central part of India. Int. Soil Water Conserv. Res. 4, 186–194. https://doi.org/10.1016/j.iswcr.2016.08.004

Morgan, R.P.C., 2005. Soil Erosion & Conservation, 3rd ed. Blackwell Publishing, Oxford.

Mourão, C., Chou, S.C., Marengo, J., 2016. Downscaling Climate Projections over La Plata Basin. Atmos. Clim. Sci. 06, 1–12. https://doi.org/10.4236/acs.2016.61001

Nasidi, N.M., Wayayok, A., Abdullah, A.F., Kassim, M.S.M., 2021. Spatio-temporal dynamics of rainfall erosivity due to climate change in Cameron Highlands, Malaysia. Model. Earth Syst. Environ. 7, 1847–1861. https://doi.org/10.1007/s40808-020-00917-4

Nel, W., Hauptfleisch, A., Sumner, P.D., Boojhawon, R., Rughooputh, S.D.D.V., Dhurmea, K.R., 2016. Intra-event characteristics of extreme erosive rainfall on Mauritius. Phys. Geogr. 37, 264–275. https://doi.org/10.1080/02723646.2016.1189756

Neto, A.R., da Paz, A.R., Marengo, J.A., Chou, S.C., 2016. Hydrological Processes and Climate Change in Hydrographic Regions of Brazil. J. Water Resour. Prot. Water Resour. Prot. 8, 1103–1127. https://doi.org/10.4236/jwarp.2016.812087

Nkiaka, E., Nawaz, N.R., Lovett, J.C., 2017. Analysis of rainfall variability in the Logone catchment, Lake Chad basin. Int. J. Climatol. 37, 3553–3564. https://doi.org/10.1002/joc.4936

Nobre, C.A., Sampaio, G., Borma, L.S., Castilla-Rubio, J.C., Silva, J.S., Cardoso, M., 2016. Land-use and climate change risks in the amazon and the need of a novel sustainable development paradigm. Proc. Natl. Acad. Sci. U. S. A. 113, 10759–10768. https://doi.org/10.1073/pnas.1605516113

Nobre, P., Siqueira, L.S.P., De Almeida, R.A.F., Malagutti, M., Giarolla, E., Castelã O, G.P., Bottino, M.J., Kubota, P., Figueroa, S.N., Costa, M.C., Baptista, M., Irber, L., Marcondes, G.G., 2013. Climate simulation and change in the brazilian climate model. J. Clim. 26, 6716–6732. https://doi.org/10.1175/JCLI-D-12-00580.1

Oğuz, I., 2019. Rainfall erosivity in North-Central Anatolia in Turkey. Appl. Ecol. Environ. Res. 17, 2719–2731. https://doi.org/10.15666/aeer/1702_27192731

Oliveira Junior, R.C. de., 1996. Índice de erosividade das chuvas na região de Conceição do Araguaia, Pará. Belém.

Oliveira, P.T.S., Rodrigues, D.B.B., Sobrinho, T.A., Carvalho, D.F. de, Panachuki, E., 2012. Spatial varibility of the rainfall erosive potencial in the State of Mato Grosso do Sul, Brazil. Eng. Agrícola 32, 69–79. https://doi.org/10.1590/S0100-69162012000100008

Oliveira, P.T.S., Wendland, E., Nearing, M.A., 2013. Rainfall erosivity in Brazil: A review. Catena 100, 139–147. https://doi.org/10.1016/j.catena.2012.08.006

Oliveira, V.A., Mello, C.R., Viola, M.R., Srinivasan, R., 2017. Assessment of climate change impacts on streamflow and hydropower potential in the headwater region of the Grande river basin, Southeastern Brazil. Int. J. Climatol. https://doi.org/10.1002/joc.5138

Önöz, B., Bayazit, M., 2012. Block bootstrap for Mann-Kendall trend test of serially dependent data. Hydrol. Process. 26, 3552–3560. https://doi.org/10.1002/hyp.8438

Palomino-Lemus, R., Córdoba-Machado, S., Gámiz-Fortis, S.R., Castro-Díez, Y., Esteban-Parra, M.J., 2018. High-resolution boreal winter precipitation projections over tropical America from CMIP5 models. Clim. Dyn. 51, 1773–1792. https://doi.org/10.1007/s00382-017-3982-5

Palomino-Lemus, R., Córdoba-Machado, S., Gámiz-Fortis, S.R., Castro-Díez, Y., Esteban-

Parra, M.J., 2017. Climate change projections of boreal summer precipitation over tropical America by using statistical downscaling from CMIP5 models. Environ. Res. Lett. 12. https://doi.org/10.1088/1748-9326/aa9bf7

Panagos, P., Ballabio, C., Borrelli, P., Meusburger, K., 2016. Spatio-temporal analysis of rainfall erosivity and erosivity density in Greece. Catena 137, 161–172. https://doi.org/10.1016/j.catena.2015.09.015

Panagos, P., Ballabio, C., Meusburger, K., Spinoni, J., Alewell, C., Borrelli, P., 2017. Towards estimates of future rainfall erosivity in Europe based on REDES and WorldClim datasets. J. Hydrol. 548, 251–262. https://doi.org/10.1016/j.jhydrol.2017.03.006

Pesquero, J.F., Chou, S.C., Nobre, C.A., Marengo, J.A., 2010. Climate downscaling over South America for 1961-1970 using the Eta Model. Theor. Appl. Climatol. 99, 75–93. https://doi.org/10.1007/s00704-009-0123-z

Pheerawat, P., Udmale, P., 2017. Impacts of climate change on rainfall erosivity in the Huai Luang watershed, Thailand. Atmosphere (Basel). 8. https://doi.org/10.3390/atmos8080143

Pires, G.F., Abrahão, G.M., Brumatti, L.M., Oliveira, K.J.C., Costa, M.H., Liddicoat, S., Kato, E., Ladle, R.J., 2016. Increased climate risk in Brazilian double cropping agriculture systems: Implications for land use in Northern Brazil. Agric. For. Meteorol. 228–229. https://doi.org/10.1016/j.agrformet.2016.07.005

Pousa, R., Costa, M.H., Pimenta, F.M., Fontes, V.C., Brito, V.F.A. de, Castro, M., 2019. Climate Change and Intense Irrigation Growth in Western Bahia, Brazil: The Urgent Need for Hydroclimatic Monitoring. Water 11, 933. https://doi.org/10.3390/w11050933

R Core Team, 2018. R: A language and environment for statistical computing. R Foundation for Statistical Computing.

Renard, K.G., Foster, G.R., Weesies, G., McCool, D., Yoder, D., 1997. Predicting Soil Erosion by Water: A Guide to Conservation Planning with the Revised Universal Soil Loss Equation (RUSLE), Agriculture Handbook. Washington, DC, USA.

Renard, K.G., Freimund, J.R., 1994. Using monthly precipitation data to estimate the R-factor in the revised USLE. J. Hydrol. 157, Pages 287-306.

Riahi, K., Rao, S., Krey, V., Cho, C., Chirkov, V., Fischer, G., Kindermann, G., Nakicenovic, N., Rafaj, P., 2011. RCP 8.5-A scenario of comparatively high greenhouse gas emissions. Clim. Change 109, 33–57. https://doi.org/10.1007/s10584-011-0149-y

Riquetti, N.B., Mello, C.R., Beskow, S., Viola, M.R., 2020. Rainfall erosivity in South America: Current patterns and future perspectives. Sci. Total Environ. 724, 138315. https://doi.org/10.1016/j.scitotenv.2020.138315

Sen, P.K., 1968. Estimates of the Regression Coefficient Based on Kendall ' s Tau. J. Am. Stat. Assoc. 63, 1379–1389. https://doi.org/10.2307/2285891

Sherwood, S.C., Roca, R., Weckwerth, T.M., Andronova, N.G., 2010. Tropospheric water vapor, convection, and climate. Rev. Geophys. 48, 29. https://doi.org/10.1029/2009RG000301

Shiono, T., Ogawa, S., Miyamoto, T., Kameyama, K., 2013. Expected impacts of climate change on rainfall erosivity of farmlands in Japan. Ecol. Eng. 61, 678–689. https://doi.org/10.1016/j.ecoleng.2013.03.002

Silva, M.L.N., De Freitas, P.L., Blancaneaux, P., Curi, N., 1997. Índices de erosividade das chuvas da região de Goiânia, GO. Pesqui. Agropecu. Bras. 32, 977–985.

Sone, J.S., Gesualdo, G.C., Zamboni, P.A.P., Vieira, N.O.M., Mattos, T.S., Carvalho, G.A., Rodrigues, D.B.B., Sobrinho, T.A., Oliveira, P.T.S., 2019. Water provisioning improvement through payment for ecosystem services. Sci. Total Environ. 655, 1197–1206. https://doi.org/10.1016/j.scitotenv.2018.11.319

Sorribas, M.V., Paiva, R.C.D., Melack, J.M., Bravo, J.M., Jones, C., Carvalho, L., Beighley, E., Forsberg, B., Costa, M.H., 2016. Projections of climate change effects on discharge and inundation in the Amazon basin. Clim. Change 136, 555–570. https://doi.org/10.1007/s10584-016-1640-2

Souza, F.H.M., Viola, M.R., Avanzi, J.C., Giongo, M., Vieira Filho, M., 2019. thornthwaite's climate regionalization for the State of Tocantins, Brazil. Floresta. 49, 783–792. http://dx.doi.org/10.5380/rf.v49i4.59188

Spera, S.A., Galford, G.L., Coe, M.T., Macedo, M.N., Mustard, J.F., 2016. Land-use change affects water recycling in Brazil's last agricultural frontier. Glob. Chang. Biol. 22, 3405–3413. https://doi.org/10.1111/gcb.13298

Taffarello, D., Calijuria, M.C., Viani, R.A.G., Marengo, J.A., Mendiondo, E.M., 2017. Hydrological services in the Atlantic Forest, Brazil: An ecosystem-based adaptation using ecohydrological monitoring. Clim. Serv. 8, 1–16. https://doi.org/10.1016/j.cliser.2017.10.005

Tapiador, F.J., Navarro, A., Levizzani, V., García-Ortega, E., Huffman, G.J., Kidd, C., Kucera, P.A., Kummerow, C.D., Masunaga, H., Petersen, W.A., Roca, R., Sánchez, J.L., Tao, W.K., Turk, F.J., 2017. Global precipitation measurements for validating climate models. Atmos. Res. 197, 1–20. https://doi.org/10.1016/j.atmosres.2017.06.021

Taylor, K.E., Stouffer, R.J., Meehl, G.A., 2012. An overview of CMIP5 and the experiment design. Bull. Am. Meteorol. Soc. 93, 485–498. https://doi.org/10.1175/BAMS-D-11-

00094.1

Teutschbein, C., Seibert, J., 2012. Bias correction of regional climate model simulations for hydrological climate-change impact studies: Review and evaluation of different methods. J. Hydrol. 456–457, 12–29. https://doi.org/10.1016/j.jhydrol.2012.05.052

Teutschbein, C., Seibert, J., 2013. Is bias correction of regional climate model (RCM) simulations possible for non-stationary conditions? Hydrol. Earth Syst. Sci., 17, 5061–5077. https://doi.org/10.5194/hess-17-5061-2013.

Theng, B.K.G., 1991. Soil science in the tropics-the next 75 years. Soil Sci. 151, 76–90. https://doi.org/10.1097/00010694-199101000-00010

Thomson, A.M., Calvin, K. V., Smith, S.J., Kyle, G.P., Volke, A., Patel, P., Delgado-Arias, S., Bond-Lamberty, B., Wise, M.A., Clarke, L.E., Edmonds, J.A., 2011. RCP4.5: A pathway for stabilization of radiative forcing by 2100. Clim. Change 109, 77–94. https://doi.org/10.1007/s10584-011-0151-4

Trindade, A.L.F., Oliveira, P.T.S. de, Anache, J.A.A., Wendland, E., 2016. Variabilidade espacial da erosividade das chuvas no Brasil. Pesqui. Agropecu. Bras. 51, 1918–1928. https://doi.org/10.1590/s0100-204x2016001200002

Vallebona, C., Pellegrino, E., Frumento, P., Bonari, E., 2015. Temporal trends in extreme rainfall intensity and erosivity in the Mediterranean region: a case study in southern Tuscany, Italy. Clim. Change 128, 139–151. https://doi.org/10.1007/s10584-014-1287-9

van de Sand, I., Mwangi, J.K., Namirembe, S., 2014. Can payments for ecosystem services contribute to adaptation to climate change? Insights from a watershed in Kenya. Ecol. Soc., 19 (1), p. 47, https://doi.org/10.5751/ES-06199-190147

Verstraeten, G., Poesen, J., Demarée, G., Salles, C., 2006. Long-term (105 years) variability

in rain erosivity as derived from 10-min rainfall depth data for Ukkel (Brussels, Belgium): Implications for assessing soil erosion rates. J. Geophys. Res. Atmos. 111, 1–11. https://doi.org/10.1029/2006JD007169

Viola, M.R., Avanzi, J.C., de Mello, C.R., Lima, S. de O., Alves, M.V.G., 2014. Distribuição e potencial erosivo das chuvas no Estado do Tocantins. Pesqui. Agropecu. Bras. 49, 125–135. https://doi.org/10.1590/S0100-204X2014000200007

Vrieling, A., Sterk, G., Jong, S.M. de, 2010. Satellite-based estimation of rainfall erosivity for Africa. J. Hydrol. 395, 235–241. https://doi.org/10.1016/j.jhydrol.2010.10.035.

Vu, M.T., Raghavan, S. V., Pham, D.M., Liong, S.Y., 2015. Investigating drought over the Central Highland, Vietnam, using regional climate models. J. Hydrol. 526, 265–273. https://doi.org/10.1016/j.jhydrol.2014.11.006

Vu, T.M., Raghavan, S. V., Liong, S.Y., Mishra, A.K., 2018. Uncertainties of gridded precipitation observations in characterizing spatio-temporal drought and wetness over Vietnam. Int. J. Climatol. 38, 2067–2081. https://doi.org/10.1002/joc.5317

Watanabe, M., Suzuki, T., O'Ishi, R., Komuro, Y., Watanabe, S., Emori, S., Takemura, T., Chikira, M., Ogura, T., Sekiguchi, M., Takata, K., Yamazaki, D., Yokohata, T., Nozawa, T., Hasumi, H., Tatebe, H., Kimoto, M., 2010. Improved climate simulation by MIROC5: Mean states, variability, and climate sensitivity. J. Clim. 23, 6312–6335. https://doi.org/10.1175/2010JCLI3679.1

Wischmeier, W.H., Smith, D.D., 1978. Predicting rainfall erosion losses —a guide to conservation planning., U.S. Department of Agriculture, Agriculture Handbook. Washington, DC.

Wischmeier, W.H., Smith, D.D., 1958. Rainfall energy and its relationship to soil loss. Eos,

Trans. Am. Geophys. Union 39, 285–291. https://doi.org/10.1029/TR039i002p00285

Yang, F., Lu, C., 2015. Spatiotemporal variation and trends in rainfall erosivity in China's dryland region during 1961-2012. Catena 133, 362–372. https://doi.org/10.1016/j.catena.2015.06.005

Yue, S., Wang, C.Y., 2002. Applicability of prewhitening to eliminate the influence of serial correlation on the Mann-Kendall test. Water Resour. Res. 38, 4-1-4–7. https://doi.org/10.1029/2001wr000861

Zhang, W.-B., Xie, Y., Liu, B.-Y., 2002. Rainfall erosivity estimation using daily rainfall amounts. Sci. Geogr. Sin. 22, 705–711.

Zhu, Q., Yang, X., Ji, F., Liu, D.L., Yu, Q., 2020. Extreme rainfall, rainfall erosivity, and hillslope erosion in Australian Alpine region and their future changes. Int. J. Climatol. 40, 1213–1227. https://doi.org/10.1002/joc.6266

Zuazo, V.H.D., Pleguezuelo, C.R.R., 2008. Soil-erosion and runoff prevention by plant covers. A review. Agron. Sustain. Dev. 28, 65–86. https://doi.org/10.1051/agro:2007062

Zuo, D., Xu, Z., Yao, W., Jin, S., Xiao, P., Ran, D., 2016. Assessing the effects of changes in land use and climate on runoff and sediment yields from a watershed in the Loess Plateau of China. Sci. Total Environ. 544, 238–250. https://doi.org/10.1016/j.scitotenv.2015.11.060

ARTIGO 2 CA-Markov prediction modelling for the assessment of land use/land cover change in two sub-basins of the Tocantins-Araguaia River Basin

Manuscript edited according to standards of the scientific journal Soil Use and Management. This article is a preliminary version and, therefore, changes may appear to adapt it.

Wharley P. dos Santos[1]| Junior Cesar Avanzi[1,*]| Nilton Curi[1]| Salvador F. Acuña-Guzman[2,3]| Adnane Beniaich[4]

[1] Department of Soil Science, Federal University of Lavras (UFLA), Postal Code 37200-900, Lavras, MG, Brazil. *E-mail address*: wharleypereira@gmail.com; junior.avanzi@ufla.br (J.C. Avanzi); niltcuri@ufla.br

[2] Department of Physics, Federal University of Lavras, Lavras, 37200-900, Brazil. *E-mail address*: salvador.acuna@ufla.br

[3] University of Puerto Rico-Mayagüez. Department of Agricultural and Biosystems Engineering, Mayagüez, 00682, Porto Rico. *E-mail address*: salvador.acuna@upr.edu

[4]Mohammed VI Polytechnic University, UM6P, Marrocos. E-mail address: beniaich@gmail.com

*Corresponding author. Tel.: +55 35 38291639

E-mail address: junior.avanzi@ufla.br (J.C. Avanzi)

ABSTRACT

Understanding the land use/land cover (LULC) changes in tropical watersheds is major challenge ahead due to the enormous pressures of increased livestock and agricultural activities. The objective of this study was to analyze the LULC changes in two-midstream sub-basins of the Tocantins-Araguaia River basin for a period of 1997–2015 and to predict the LULC changes in short- and mid-term future scenarios (2030 and 2050). We used the Cellular Automata and Markov Chain (CA-Markov) model to predict the LULC changes in the Formoso and Sono sub-basins, and analyze their change patterns, based on biophysical and socio-economic LULC change drivers. The results show that agriculture and pasture areas would expand more largely in the Formoso River basin, while the native vegetation in the Sono River basin remains more stable in future scenarios. These results provide a reference base for further research about the response to the changing land use and land cover, helping for planning the future effects, and addressing political and social concerns that lead to sustainable development in the study areas.

Keywords: LULC, CA-Markov model, agricultural expansion, tropical watersheds, MapBiomas.

1 INTRODUCTION

Land is an important resource for the preservation of ecosystems and the promotion of agricultural activity throughout the world. Preserving this resource has been a challenge in the face of the pressures caused by climate change and the growing global demand for food and agriculture (FAO, 2018). The dynamics that involve changes in land use / cover and climatic variability can to some degree influence changes in hydrological responses in river basins, depending on the different agro-ecological environments present (Berihun et al., 2019).

Human activities have a strong influence on changes in land cover, constituting anthropogenic factors capable of promoting changes in vegetation on a local and regional scale over time (Pan et al., 2018), such as the conversion of natural vegetation to agricultural areas through deforestation and landscape fragmentation (S. N. de Oliveira, de Carvalho Júnior, Gomes, Guimarães, & McManus, 2017). Planted pastures and the introduction of extensive and mechanized cultivation lead to rates of removal of natural vegetation, enabling climatic variations through the response of precipitation and temperature over the landscape (Salazar, Baldi, Hirota, Syktus, & McAlpine, 2015).

The interaction dynamics between climate change and land use affect hydrological streamflow patterns at a local scale into a watershed (Sayasane, Kawasaki, Shrestha, & Takamatsu, 2016). In the tropical wooded areas, land cover change with forest fragmentation can alter the precipitation patterns (Debortoli et al., 2017; D. V. Spracklen, Baker, Garcia-Carreras, & Marsham, 2018; D. V. Spracklen, Arnold, & Taylor, 2012), exposing trees from edges of fragmented forest to sensitivity of precipitation change caused by displacement of the Intertropical Convergence Zone (ITCZ) (Albiero-Júnior et al., 2019). Furthermore, the fast-changing land use and cover rise the variability of rainfall, which makes soils more vulnerable to degradation due to a decrease of canopy and increase the direct impact of raindrops on the ground, and as a result of that, the surface runoff produced enters streams and rivers, loading

sediments from the soil erosion process. Tropical watersheds take an important place in relation to land use and land cover (LULC) changes, which correlate with the highest erosion losses due to the dominant cleared lands (Abdulkareem, Pradhan, Sulaiman, & Jamil, 2019), and the conversion of natural to agroecosystems can lead to transport and decomposition of soil organic carbon (SOC), depleting the SOC stock and increasing emission of greenhouse gases (GHGs) (Lal, 2019). Slash and burn farming and erosive processes are critics in the savanna –forest boundary in Brazil–, while forest species invest much more in leaf area and stem biomass, savanna species in the Brazilian Cerrado tend to distribute more biomass for roots and less for aerial structures (Hoffmann, 2005; Hoffmann & Franco, 2003; Paganeli, Dexter, & Batalha, 2020).

The biogeophysical and biogeochemical processes of the LULC change affect the climate in a local, regional, and global scale changing the chemical composition of the atmosphere and the physical parameters that determine the energy balance at the land surface (Deng, Zhao, & Yan, 2013). Those processes are vastly related to the increase of crop area and afforestation in tropical South America, not to mention that large areas of the Amazon rainforest are being clean-cut and burnt to agriculture (Mahmood & Pielke, 2017). In addition, it is estimated that around 39% of the Cerrado pastures are also currently degraded due to the low investment in soil conservation practices, coupled with rainfall patterns change (Pereira, Ferreira, Pinto, & Baumgarten, 2018).

The impacts of climate change on hydrological hazards have been assessed according to the influence of LULC change in tropical catchments (Fenta Mekonnen, Duan, Rientjes, & Disse, 2018; Näschen et al., 2019; Setyorini, Khare, & Pingale, 2017; Yira, Diekkrüger, Steup, & Bossa, 2016). Tocantins-Araguaia River Basin (TARB) is located in the central north of Brazil consisted of a large drainage network in which stand out the two major rivers Tocantins

and Araguaia. This watershed has a high vulnerability to LULC changes, and most of its environment is sensitive to climate change.

For this study, we aimed to analyze the LULC changes in two important sub-basins of the TARB, the Formoso and Sono sub-basins. Therefore, the two study areas are chosen to show the short- and medium-range impacts of agricultural and stock-raising development in the last agricultural frontier in Brazil. The two sub-basins are in contrast to their areas with natural vegetation cover, being one of them with prominence in ecosystems conservation and the other with large pasturelands and high land ownership concentration. These watersheds have large agroindustrial complexes, and the preservation of their natural resources is of great importance for the sustainable management of the soil. Cellular Automata-Markov (CA-Markov) model, by its efficiency and flexibility, was used to capture the trend and the spatial structure of the LULC categories in the study areas. The research work covers the development of LULC change analysis according to foremost the need to properly understand what impacts the farming activities will bring in short- and medium-future scenarios.

2 MATERIALS AND METHODS

2.1 Study area

The study area includes the Formoso and Sono sub-basins of the TARB and are located between 8°45'38" to 13°16'0"S latitude and 45°41'38" to 49°57'4"W longitude (Figure 1). The Formoso River basin (FRB), with a drainage area of 21,108 km², is located in the central TARB and has prominent livestock and agriculture, incorporating large irrigated agricultural projects (Figure 1a). The remaining natural vegetation cover in FRB mainly consists of savanna formations, riparian and gallery forests, and semi-deciduous seasonal alluvial forests (SEPLAN, 2012). On the Formoso sub-basin, Plinthosols, Ferralsols, Gleysols, and Acrisols are predominating soils. In general, the sub-basin soils are poorly drained, with drainage impediment and occasional floods during the rainy season.

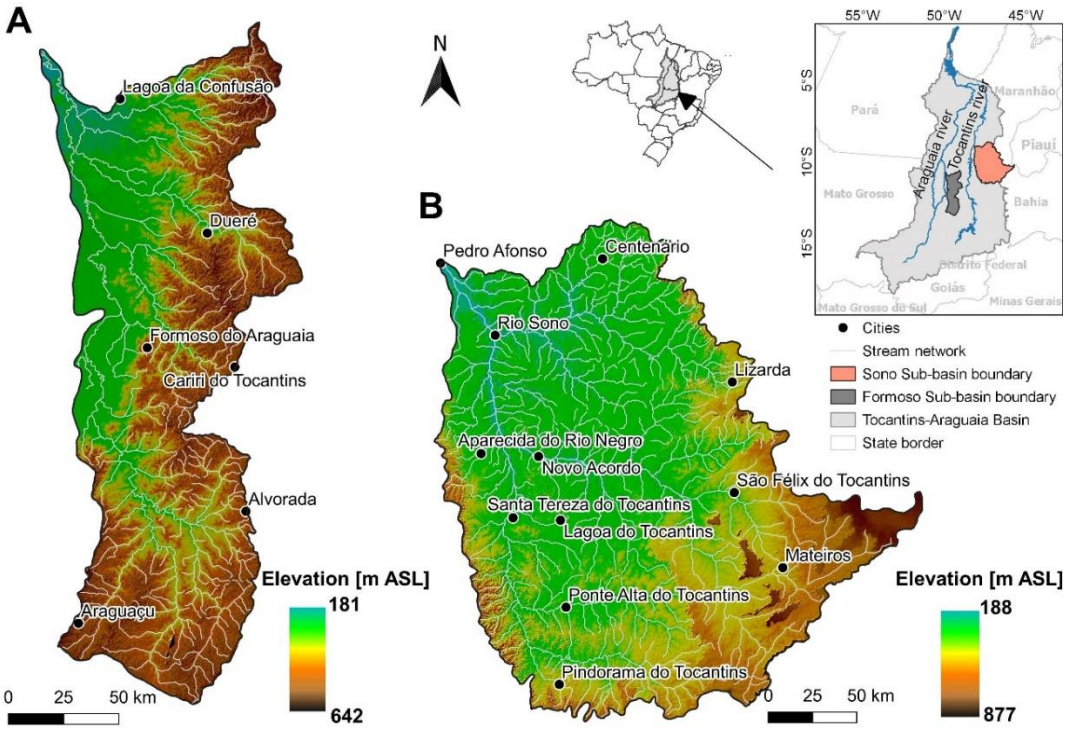

Figure 1 - Map of the Formoso (a) and Sono (b) sub-basins and their locations in the Tocantins-Araguaia River Basin (TARB).

The Sono River basin (SRB) (Figure 1b) has a drainage area of 45,728 km² and its main stream flows the east-northerly direction until it flows into the Tocantins River. With regards to relief, the Sono sub-basin has an undulating, even gently undulating landscape. The soils have a sandy texture with predominance of Arenosols, Plinthosols, Leptosols, Ferralsols and Acrisols. The vegetation is of the semi-deciduous and *campo cerrado* (savanna woodland) type.

2.2 Data Set

This analysis focused on two-midstream sub-basins in the Tocantins-Araguaia basin (Figure 1). The Cerrado biome occupies the area of the two sub-basins, with the Formoso Basin reaching the Cerrado-Amazon ecotone to the north. We considered land cover data provided by MapBiomas project (http://mapbiomas.org/), a highly credible source of classified and georeferenced land-use data based on LANDSAT that is available for the whole of Brazil at a 30-m resolution. MapBiomas was created by the System for Estimating Emissions of Greenhouse Gases of Brazilian Climate Observatory. The MapBiomas classification is generated from annual land cover and land use maps from an automatic classification routine applied to satellite images with high accuracy for the entire Cerrado biome (http://mapbiomas.org/pages/accuracy-analysis). MapBiomas 5.0 collection data classification was adapted to this study to allocate the most important classes in both watersheds. Since MapBiomas 5.0 collection 1997, 2006 and 2015 datasets have different number of classes, the land use classes for all three imageries were resampled and reclassified into seven broader and nuanced categories. Therefore, LULC categories for this study include: (1) forest, (2) savanna, (3) grassland, (4) pasture, (5) agriculture, (6) other lands, and (7) water. The MapBiomas classification legend was adjusted for this study. The original 30 × 30 m resolution data were aggregated to 100 × 100 m resolution to overlay the lower raster data resolution into the LULC modeling and allow CA-Markov modeling procedures. The LULC transition suitability was produced through biophysical and socio-economic variables (soil type, soil organic carbon

(SOC) stock, altitude, slope from DEM, rivers, streams, and other geographical data) (Table 1). These variables establish the best inherent suitability of each pixel for each LULC type in a time period in both sub-basins.

Table 1- Data source and description.

Data type	**Scale and resolution**	**Data source**
DEM	30 m × 30 m	Shuttle Radar Topography Mission (SRTM) produced by Consortium for Spatial Information (CGIAR-CSI)
Land use	30 m × 30 m	MapBiomas Collection 5.0 - Brazilian Annual Land Use and Land Cover Mapping Project (https://mapbiomas.org/)
Soil	1:1,500,000	Brazilian Agricultural Research Corporation (Embrapa Soils) - Brazilian Soil Classification System
		Brazilian Agricultural Research Corporation (Embrapa Soils) - Brazilian Soil Organic Carbon Stock map (0-30cm)
River network		National Water and Sanitation Agency (ANA) database https://metadados.ana.gov.br/geonetwork/srv/pt/main.home
Other geographical data		Roads - Ministry of Infrastructure (https://www.gov.br/infraestrutura/pt-br/assuntos/dados-de-transportes/bit/bitmodosmapas#maprodo)
		Cities and towns - Brazilian Institute of Geography and Statistics (IBGE) (www.ibge.gov.br)
		Rural settlements - National Institute for Colonization and Agrarian Reform (INCRA) (www.incra.gov.br)
		Nature Conservation Units - Ministry of the Environment (MMA) (www.mma.gov.br)
		Indigenous Lands - National Indian Foundation (FUNAI)
		(http://www.funai.gov.br/index.php/shape)
		Permanent Preservation Area (PPA) and Legal Reserves (LR) (http://www.car.gov.br/#/)

2.3 Markov Chain model

This model is a stochastic process fulfilling the Markov property, and is able to predict vegetation change (Balzter, 2000), based on the probability of transition, P_{ij}, between state i and j. Markov chain model is used to quantify transition probabilities of multiple land use/land cover in a finite number of states. Based on the conditional probability, the prediction of land use changes is explained by the following equation:

$$S_{(t,t+1)} = P_{ij} \times S_{(t)} \quad (1)$$

where S(t), S(t +1) are the land use status at the time of t or t +1; P_{ij} is the transition probability matrix in a state which is calculated as follows:

$$P_{ij} = \begin{bmatrix} P_{11} & P_{12} & \cdots & P_{1n} \\ P_{21} & P_{22} & \cdots & P_{2n} \\ \vdots & \vdots & \ddots & \vdots \\ P_{n1} & P_{n2} & \cdots & P_{nn} \end{bmatrix} \quad \left(0 \le P_{ij} \le 1 \text{ and } \sum_{j=1}^{N} P_{ij} = 1, (i, j = 1, 2, \ldots, n)\right).$$

2.4 CA model

Cellular Automata (CA) represent a type of model that focus on local interactions of cells with the cellular neighborhood. The CA model consists of a regular lattice with square cells, and global patterns generated by local actions that can change in time according to well-defined rules and subjected to the current state of a cell and its neighboring cells (Crooks, 2017). The CA model expression can be defined by:

$$S_{(t,t+1)} = f(S_{(t)}, N) \quad (2)$$

where *S* is the finite, discrete cellular states set, *N* is the cellular field, *t* is the time instant, *t +1* is the future time instant, and *f* is the transition rule of cellular states in local space. CA's transition rules use a 5 × 5 neighborhood to simulate LULC class in the future, and the cell size was set at 100 m × 100 m.

2.5 CA-Markov chain model

The Markov chain is able to control the temporal changes of LULC through the transition probabilities, while CA model controls the spatial changing, and it depends on either spatial characteristics or transition probabilities (Etemadi, Smoak, & Karami, 2018). Therefore, CA-Markov is an integrated model, which proves valuable to predict and simulate land use and land cover change over time (Kamusoko, Aniya, Adi, & Manjoro, 2009; Zhilong, Xue, Yili, & Jungang, 2017). The CA-Markov is modeled in software IDRISI, the Selva version (Eastman, 2012), through integrated functions of cellular automaton filter and transition area matrix of Markov processes, and is a widely-used tool for LULC simulation (Hyandye & Martz, 2017). The stage of spatial specification of land use changes is performed based on a collection of transition suitability maps for each land-use/land-cover category to produce the input for the CA model. In particular, each LULC transition suitability map comprises a collection of physical and socio-economic parameter maps (factors and constraints) using the Multiple-Criteria Evaluation (MCE) method (Eastman, 2012; Singh, Mustak, Srivastava, Szabó, & Islam, 2015). The suitability of each factor (e.g. elevation, slope gradient and road distances) is scored using MCE method in order to create factor suitability map with each pixel value standardized using fuzzy membership functions into 0–255 in byte, 0 representing unsuitable and 255 representing highly suitable area for a LULC class. The factors were weighted using Saaty's Analytical Hierarchy Process (AHP) in order to compound each LULC transition suitability map. The constraints (e.g. protected areas and water bodies) were standardized into a Boolean value (0 and 1), with 0 representing areas restricted for suitability analysis and 1 representing areas of potential suitability.

Land use/cover maps from 1997 and 2006 were used for model calibration and then the models were used to predict a land use/cover map for 2015. As a next step, the LULC map for 2030 and 2050 was simulated using models based on the 2006 and 2015 LULC maps. Since

CA-Markov model requires model calibration and validation, the model performance in predicting the LULC was assessed using Kappa coefficients in the VALIDATE module of the IDRISI software. Three statistics kappa were used: traditional kappa ($K_{standard}$), Kappa for no ability (K_{no}) and Kappa for location ($K_{location}$). Kappa for no ability (K_{no}) provides overall accuracy of the simulation, and represents an alternative to the standard Kappa, while $K_{location}$ and $K_{quantity}$ coefficients provide the level of agreement concerning the location and quantity between the reality map and simulated maps (R. G. Pontius, 2000; R. Gil Pontius, 2002). When the Kappa parameter values are above 0.80, the maps are in almost perfect agreement, and the CA-Markov model predictions can be regarded as fair and accurate (Viera & Garrett, 2005). When $0.75 \leq Kappa < 1$, the maps are in perfect agreement; if $0.5 \leq Kappa \leq 0.75$, it has a medium level of agreement; and if $Kappa \leq 0.5$, it has a rare agreement.

3 RESULTS

3.1. Land use changes

Based on the LULC maps in 2006 and 2015, each type of land use were used to project future changes from current patterns. The land use/cover transition probabilities and transition area matrix for the 1997–2006 and 2006–2015 periods (Figure 2), calculated based on each watershed, are shown in Tables 2 and 3. The observed LULC map of 2015 was then compared with the simulated LULC to evaluate the model performance.

According to transition probability matrix (Table 2), grasslands areas were more probable to undergoing no change in Sono River Sub-basin. In the Formoso River Sub-basin, the most stable LULC class included the pasturelands, with probability of no change greater than 70% (Table 3). On analyzing the transition probability matrix for the Sono River Sub-basin, it can be observed as the basin remains more protected in relation to the Formoso River

Sub-basin. In the Sono River Sub-basin, among the native vegetation classes, savanna and grasslands, registered the highest stability probabilities.

Table 2 - Land use/land cover changes transition probability matrix (P) in Sono River Sub-basin for the 1997-2006 calibration period.

	2006						
1997	**FO**	**SV**	**GL**	**PA**	**AG**	**OL**	**WT**
FO	0.624	0.332	0.003	0.038	0.001	0.000	0.002
SV	0.088	0.721	0.119	0.058	0.013	0.001	0.001
GL	0.001	0.182	0.780	0.013	0.022	0.002	0.000
PA	0.029	0.260	0.027	0.551	0.130	0.003	0.000
AG	0.004	0.036	0.139	0.053	0.739	0.028	0.000
OL	0.002	0.046	0.052	0.101	0.719	0.079	0.000
WT	0.310	0.148	0.020	0.001	0.000	0.001	0.521

FO = Forest, SV = Savanna, GL = Grassland, Pasture = PA, Agriculture = AG, OL = Other lands, WT = Water

Table 3 - Land use/land cover changes transition probability matrix (P) in Formoso River Sub-basin for the 1997-2006 calibration period.

	2006						
1997	**FO**	**SV**	**GL**	**PA**	**AG**	**OL**	**WT**
FO	0.630	0.300	0.002	0.055	0.000	0.000	0.013
SV	0.065	0.643	0.019	0.269	0.002	0.000	0.003
GL	0.003	0.287	0.516	0.158	0.028	0.000	0.009
PA	0.010	0.243	0.017	0.712	0.014	0.002	0.002
AG	0.007	0.114	0.022	0.490	0.365	0.000	0.003
OL	0.003	0.054	0.016	0.473	0.008	0.437	0.010
WT	0.144	0.165	0.028	0.037	0.007	0.000	0.619

FO = Forest, SV = Savanna, GL = Grassland, Pasture = PA, Agriculture = AG, OL = Other lands, WT = Water

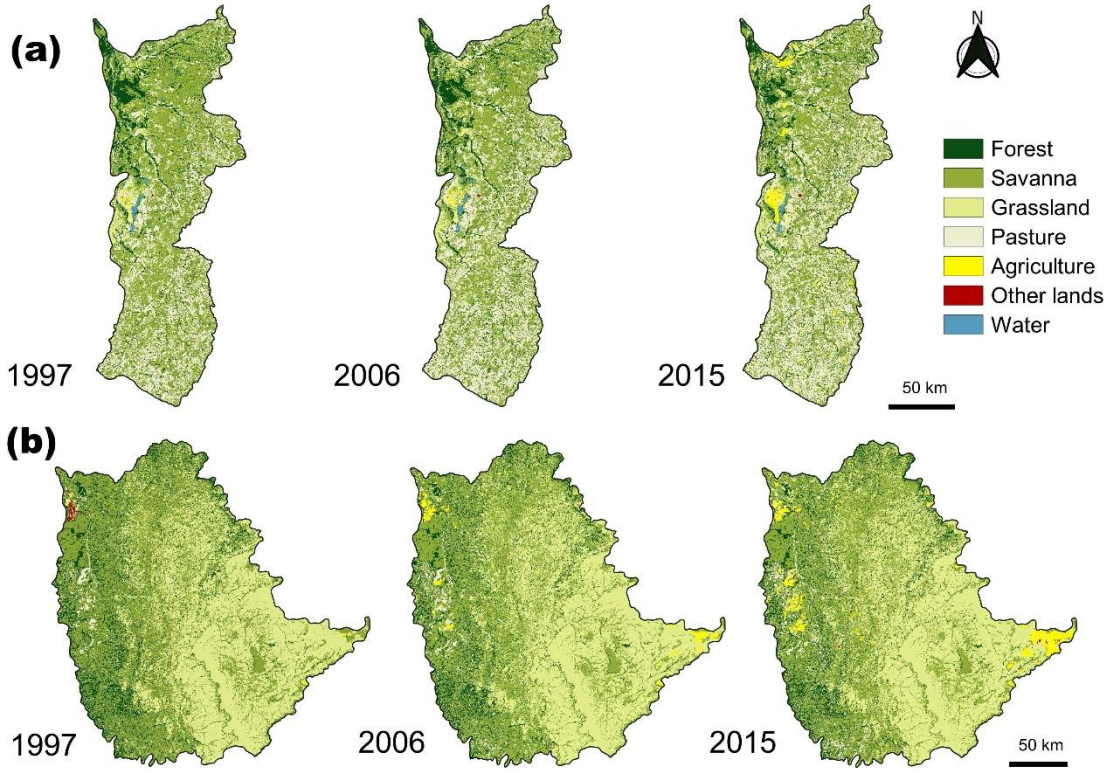

Figure 2 - Land use maps in calibration (1997-2006) and validation periods (2006-2015).

3.2 Validation of the CA-Markov chain model

Land use maps simulated in this study showed great match among the land use classes to Formoso and Sono River sub-basins. Changes in land use/land cover were simulated accurately over the given time period (Table 4). CA-Markov simulations using the 1996-2007 calibration data set had an overall Kappa above 0.8 for both watersheds, having achieved an adequate level of accuracy. The projected land use map for 2015 was compared with the actual land use to verify the validity in terms of quantity and location. The measures of quantity disagreement and allocation disagreement were useful to summarize the LULC categories. The simulated scenario for 2015 presented very similarly to the actual land use map, based on visual comparison (Figure 3).

Table 4. Summary of Kappa indices for model validation

Sub-basins	Kappa indices		
	$K_{standard}$	K_{no}	$K_{location}$
Formoso	0.8238	0.8587	0.8398
Sono	0.8693	0.8947	0.8889

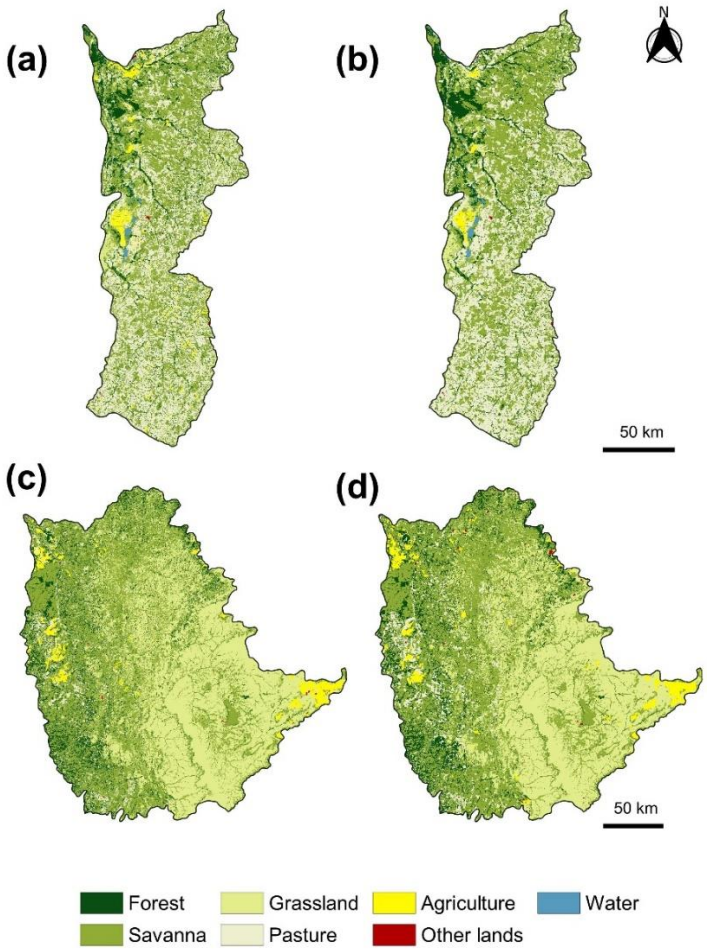

Figure 3 - Observed (right) and Simulated (left) Land use/land cover maps of the Formoso (a,b), and Sono (c,d) sub-basins for the year 2015.

The CA-Markov model is employed to predict future LULC in Formoso and Sono River sub-basins. Future LULC maps for 2030 and 2050 are predicted using the CA-Markov model based on the year 2015. The prediction of distribution of the LULC classes in 2030 and 2050 (Figure 4a, and 4b) shows a large expansion in agriculture and pasture in Formoso River Sub-Basin. It also shows increases in the same classes in Sono River Sub-Basin. The validation results indicate that the CA–Markov model simulations provide to be reliable for predicting future land use/land cover changes. These findings support the results found in different studies (Cunha, Santos, Silva, Bacani, & Pott, 2021; Gashaw, Tulu, Argaw, & Worqlul, 2017; Gidey, Dikinya, Sebego, Segosebe, & Zenebe, 2017).

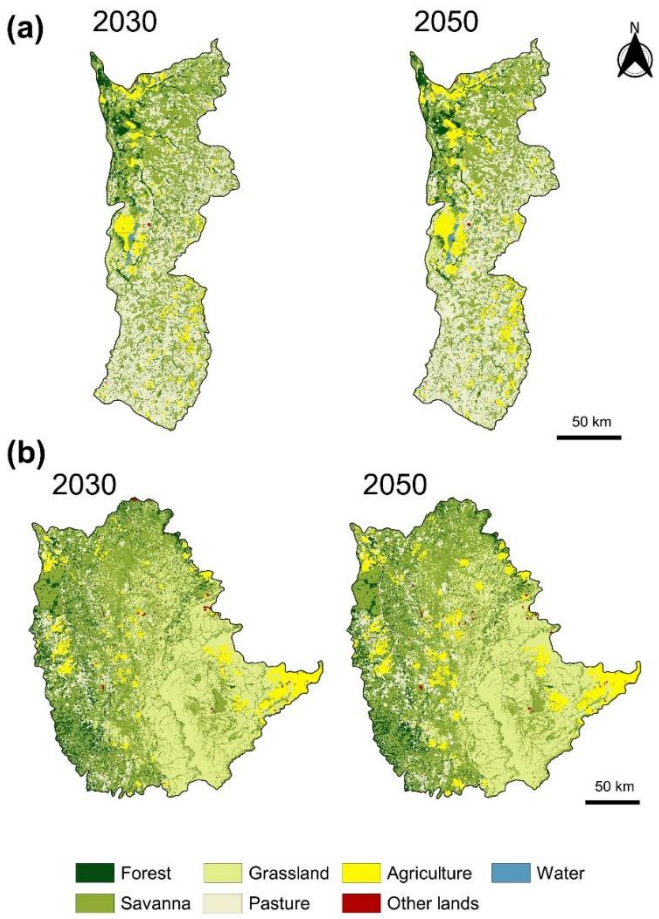

Figure 4 - Projected land use/land cover maps of the Formoso (a), and Sono (b) sub-basins for 2030 and 2050.

3.3 Change detection analysis

The LULC change analysis in this study has been divided into the following periods: 1997-2006, 2006-2015, and 1997-2015; as well as the future periods 2015-2030 and 2015-2050. Figure 5 shows the gains and losses in LULC categories for the both Formoso and Sono sub-basins respectively in the aforementioned periods.

The Formoso River Sub-basin shows the highest net gains of pasture land use category in savanna formation cover lands. From 1997 to 2015, the pasture land has gained 5.8% of area, while the savanna land has been lost 6.5% of area in the same period. For the remaining periods, the same behavior was noticed, with net increase above 1.9% of area in the Formoso River Sub-Basin for each nine-year LULC change period. In the Sono River Sub-basin, pasture land has the lowest amount of net gains in area, but cultivated lands have a considerable scale net gain, while observing, with regard to the expansion of agriculture in 1997-2015 period, the high increase in agriculture priority areas in Pedro Afonso and Mateiros municipalities. According to our predictions, pasture net gain is likely detected based on losses of grassland and savanna lands in SRB in the near and medium future, but in a larger area of savanna category in FRB.

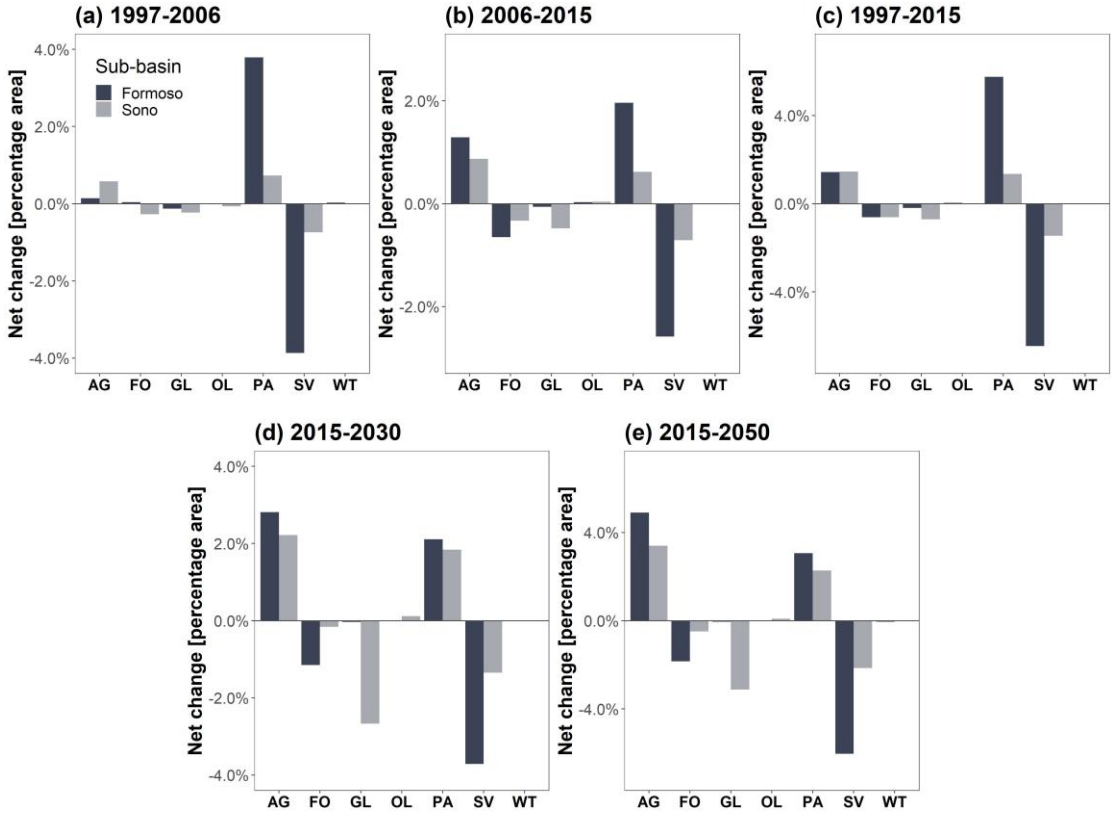

Figure 5 - Gains and losses in % of area of LULC by category in different time periods in Formoso River Sub-basin and Sono River Sub-basin. FO = Forest, SV = Savanna, GL = Grassland, Pasture = PA, Agriculture = AG, OL = Other lands, WT = Water.

4 DISCUSSION

The areas of different sub-basins show gains of pasture and agriculture in future predictions, with higher increase in pasture lands in the Formoso River Sub-basin and higher increase in agricultural lands in the Sono River Sub-basin in the future scenarios for 2030 and 2050. The conversion of others LULC types to agricultural lands in SRB is concentrated in the far east and northwest of the sub-basin. In SRB basin, the most prominent has been conversion of Cerrado areas to irrigated agriculture, highlighting soybean crops in the Pedro Afonso municipality. In addition to the high land suitability for crops in the Sono River basin, there is also a greater concern regarding the maintenance of protected areas. Since 1997, there has been an increase in protected areas located in the basin, in hard contrasting with the farming activities

on their border. The indigenous lands have a significant occupation in the SRB, in order to constitute a constraint areas facing increasing pressure of agriculture lands expansion. As to the cases in which land degradation prevails over environmental conservation areas, the Formoso River Sub-basin revealed itself as sub-basin with high problems remain concerned about the intensive agricultural activity over the years. Situated on the banks of the Formoso River, irrigated agriculture prevails in the floodplain areas (Morais, Nolêto Júnior, & Martins, 2017), comprising areas of low agricultural use, which still can offer risk to surface waters contamination by the growth of pesticide and fertilizer use (Guarda et al., 2020). Agriculture contributes significantly to the total collected in the State of Tocantins, standing out for the agricultural production in the Formoso do Araguaia and Lagoa da Confusão municipalities in the Formoso River Sub-basin (Tocantins, 2007).

The Formoso River Sub-basin presents areas characterized by high to very high natural vulnerability of water resources in the middle and low course (T. A. Oliveira, Viola, Mello, Giongo, & Coelho, 2015), aggravating the environmental impacts of land use change in this watershed. In order to expand the agriculture in Tocantins State, the Rio Formoso project was one of the first attempts to consolidate floodplains in watershed as large irrigated areas by the end of the '70s (Ajara, Figueiredo, Bezerra, & Barbosa, 1991). This project marked an important step of agricultural frontier pressure in the region, and how this is changing over time, is extremely critical to assessing the current land-use intensification.

Deforestation in Brazilian center-western Cerrado remains a recurrent issue and a serious concern. Nevertheless, the land-use intensification is coinciding with expansion of agricultural lands in agricultural frontier areas, which signalizes the necessity of the implementation of policies aimed at curbing the conversion of areas of native vegetation to agricultural lands (Barretto, Berndes, Sparovek, & Wirsenius, 2013). The analysis of the land use dynamism and the supporting information for sustainable planning are important to

understand which physical and political factors influence the conservation and degradation of native vegetation (Sawakuchi, Ballester, & Ferreira, 2013). In this regard, government control policies can lead to changes that directly affect land-use change, through specific land uses or better technologies that decrease production costs of commodities in expansionist agriculture and livestock, influencing forest conversion (Miccolis, Andrade, & Pacheco, 2014). It also includes the long-term implementation of a conservationist agriculture it is able to reduce the deforestation rates and enhance agricultural supply.

The advancement of agriculture in the Brazilian tropical savanna is expected based on the simulation and prediction of future scenarios in integrated models. This change is critical mainly in ecotones in transition to Cerrado, with agropastoral expansion having negative impacts on this native vegetation (Cunha et al., 2021). This biome has been impacted in the two sub-basins under study. Over recent decades, the Cerrado biome has lost area from agricultural and cattle ranching land expansion (Brannstrom et al., 2008; Grecchi, Gwyn, Bénié, Formaggio, & Fahl, 2014; Silva, Fariñas, Felfili, & Klink, 2006). This causes the Cerrado to be an increasingly threatened biome, with particular focus on tropical wetlands, which some areas are located in the Formoso River Sub-basin. The prominent land use in the Formoso River Sub-basin is agriculture, in on counterpoint to the prominent land use in Sono River Sub-basin, where the agriculture is prevailed together with large environmental conservation areas (Tocantins, 2011).

Options for managing such future land use changes and the related risk-mitigation measures in order to guarantee sustainable development and protect the environment are essential in short medium-term planning. Land use policy needs to take place in an organized and systematic manner, reaching the key areas of the national farming action plan, as exemplified e.g. by the sub-basins of Tocantins-Araguaia basin examined in this study.

Furthermore, the simulated maps of LULC serve as an instrument for forward planning the future effects of land use changes.

5 CONCLUSIONS

The land use/cover predictions showed a great performance using the CA-Markov modelling. According the transition probability matrix, the Sono River basin remains more protected, considering the predictions performed to the Formoso River basin. In the Sono River basin, the dominant native vegetation classes have high stability probabilities. The short- and medium-term LULC simulations show large expansion in agriculture and pasture in Formoso River basin. The land-use changes also have increased the farming lands in Sono River basin. The effects of land use changes on these two watersheds can introduce a strong impact of water erosion process, depending on soil management and environmental conservation conditions in the study areas. Understanding these effects can improve future land use planning and guarantee sustainable development in the short and medium term.

ACKNOWLEDGMENTS

This work forms a part of a study supported by the Coordination of Superior Level Staff Improvement (CAPES), the National Council for Scientific and Technological Development (CNPq). We would like to thank all the team involved in the Map-Biomas Project for providing the dataset used in this study. We gratefully acknowledge the U.S. Geological Survey (USGS) EROS Data Center responsible for archiving the SRTM 1 Arc-Second Global dataset.

ORCID

Santos, W.P. https://orcid.org/0000-0002-8077-2144

REFERENCES

Abdulkareem, J. H., Pradhan, B., Sulaiman, W. N. A., & Jamil, N. R. (2019). Prediction of spatial soil loss impacted by long-term land-use/land-cover change in a tropical watershed. *Geoscience Frontiers*, *10*(2), 389–403. https://doi.org/10.1016/j.gsf.2017.10.010

Ajara, C., Figueiredo, A. H., Bezerra, V. M. C., & Barbosa, J. G. (1991). O estado do Tocantins: reinterpretação de um espaço de fronteira. *Revista Brasileira de Geografia*, *53*(4), 5–48.

Albiero-Júnior, A., Camargo, J. L. C., Roig, F. A., Schöngart, J., Pinto, R. M., Venegas-González, A., & Tomazello-Filho, M. (2019). Amazonian trees show increased edge effects due to Atlantic Ocean warming and northward displacement of the Intertropical Convergence Zone since 1980. *Science of the Total Environment*, *693*, 133515. https://doi.org/10.1016/j.scitotenv.2019.07.321

Balzter, H. (2000). Markov chain models for vegetation dynamics. *Ecological Modelling*, *126*(2–3), 139–154. https://doi.org/10.1016/S0304-3800(00)00262-3

Barretto, A. G. O. P., Berndes, G., Sparovek, G., & Wirsenius, S. (2013). Agricultural intensification in Brazil and its effects on land-use patterns: An analysis of the 1975-2006 period. *Global Change Biology*, *19*(6), 1804–1815. https://doi.org/10.1111/gcb.12174

Berihun, M. L., Tsunekawa, A., Haregeweyn, N., Meshesha, D. T., Adgo, E., Tsubo, M., … Ebabu, K. (2019). Science of the Total Environment Hydrological responses to land use / land cover change and climate variability in contrasting agro-ecological environments of the Upper Blue Nile basin , Ethiopia. *Science of the Total Environment*, *689*, 347–365. https://doi.org/10.1016/j.scitotenv.2019.06.338

Brannstrom, C., Jepson, W., Filippi, A. M., Redo, D., Xu, Z., & Ganesh, S. (2008). Land change in the Brazilian Savanna (Cerrado), 1986-2002: Comparative analysis and implications for

land-use policy. *Land Use Policy*, *25*(4), 579–595. https://doi.org/10.1016/j.landusepol.2007.11.008

Crooks, A. (2017). Cellular Automata. In *International Encyclopedia of Geography: People, the Earth, Environment and Technology* (Vol. 26, pp. 1–9). https://doi.org/10.1002/9781118786352.wbieg0578

Cunha, E. R. da, Santos, C. A. G., Silva, R. M. da, Bacani, V. M., & Pott, A. (2021). Future scenarios based on a CA-Markov land use and land cover simulation model for a tropical humid basin in the Cerrado/Atlantic forest ecotone of Brazil. *Land Use Policy*, *101*(September 2020). https://doi.org/10.1016/j.landusepol.2020.105141

de Oliveira, S. N., de Carvalho Júnior, O. A., Gomes, R. A. T., Guimarães, R. F., & McManus, C. M. (2017). Landscape-fragmentation change due to recent agricultural expansion in the Brazilian Savanna, Western Bahia, Brazil. *Regional Environmental Change*, *17*(2), 411–423. https://doi.org/10.1007/s10113-016-0960-0

Debortoli, N. S., Dubreuil, V., Hirota, M., Filho, S. R., Lindoso, D. P., & Nabucet, J. (2017). Detecting deforestation impacts in Southern Amazonia rainfall using rain gauges. *International Journal of Climatology*, *37*(6), 2889–2900. https://doi.org/10.1002/joc.4886

Deng, X., Zhao, C., & Yan, H. (2013). Systematic modeling of impacts of land use and land cover changes on regional climate: A review. *Advances in Meteorology*, *2013*, 1–11. https://doi.org/10.1155/2013/317678

Eastman, J. R. (2012). IDRISI Selva Manual. In *Clark University*. Worcester, MA: Clark Labs., Clark University.

Etemadi, H., Smoak, J. M., & Karami, J. (2018). Land use change assessment in coastal mangrove forests of Iran utilizing satellite imagery and CA–Markov algorithms to monitor

and predict future change. *Environmental Earth Sciences*, *77*(5). https://doi.org/10.1007/s12665-018-7392-8

FAO. (2018). *The future of food and agriculture – Alternative pathways to 2050 | Global Perspectives Studies | Food and Agriculture Organization of the United Nations*. https://doi.org/Licence: CC BY-NC-SA 3.0 IGO

Fenta Mekonnen, D., Duan, Z., Rientjes, T., & Disse, M. (2018). Analysis of combined and isolated effects of land-use and land-cover changes and climate change on the upper Blue Nile River basin's streamflow. *Hydrology and Earth System Sciences*, *22*(12), 6187–6207. https://doi.org/10.5194/hess-22-6187-2018

Gashaw, T., Tulu, T., Argaw, M., & Worqlul, A. W. (2017). Evaluation and prediction of land use/land cover changes in the Andassa watershed, Blue Nile Basin, Ethiopia. *Environmental Systems Research*, *6*(1). https://doi.org/10.1186/s40068-017-0094-5

Gidey, E., Dikinya, O., Sebego, R., Segosebe, E., & Zenebe, A. (2017). Cellular automata and Markov Chain (CA_Markov) model-based predictions of future land use and land cover scenarios (2015–2033) in Raya, northern Ethiopia. *Modeling Earth Systems and Environment*, *3*(4), 1245–1262. https://doi.org/10.1007/s40808-017-0397-6

Grecchi, R. C., Gwyn, Q. H. J., Bénié, G. B., Formaggio, A. R., & Fahl, F. C. (2014). Land use and land cover changes in the Brazilian Cerrado: A multidisciplinary approach to assess the impacts of agricultural expansion. *Applied Geography*, *55*, 300–312. https://doi.org/10.1016/j.apgeog.2014.09.014

Guarda, P. M., Pontes, A. M. S., Domiciano, R. de S., Gualberto, L. da S., Mendes, D. B., Guarda, E. A., & da Silva, J. E. C. (2020). Assessment of Ecological Risk and Environmental Behavior of Pesticides in Environmental Compartments of the Formoso River in Tocantins, Brazil. *Archives of Environmental Contamination and Toxicology*,

79(4), 524–536. https://doi.org/10.1007/s00244-020-00770-7

Hoffmann, W. A. (2005). Ecologia comparativa de espécies lenhosas de cerrado e mata. In A. Scariot, J. C. Sousa-Silva, & J. M. Felfili (Eds.), *Cerrado: Ecologia, Biodiversidade E Conservação* (pp. 155–165). Brasília: Ministério do Meio Ambiente.

Hoffmann, W. A., & Franco, A. C. (2003). Comparative growth analysis of tropical forest and savanna woody plants using phylogenetically independent contrasts. *Journal of Ecology*, *91*(3), 475–484. https://doi.org/10.1046/j.1365-2745.2003.00777.x

Hyandye, C., & Martz, L. W. (2017). A Markovian and cellular automata land-use change predictive model of the Usangu Catchment. *International Journal of Remote Sensing*, *38*(1), 64–81. https://doi.org/10.1080/01431161.2016.1259675

Kamusoko, C., Aniya, M., Adi, B., & Manjoro, M. (2009). Rural sustainability under threat in Zimbabwe - Simulation of future land use/cover changes in the Bindura district based on the Markov-cellular automata model. *Applied Geography*, *29*(3), 435–447. https://doi.org/10.1016/j.apgeog.2008.10.002

Lal, R. (2019). Accelerated Soil erosion as a source of atmospheric CO2. *Soil and Tillage Research*, *188*, 35–40. https://doi.org/10.1016/j.still.2018.02.001

Mahmood, R., & Pielke, R. A. (2017). Land-Use/Cover Change and Climate. *International Encyclopedia of Geography: People, the Earth, Environment and Technology*, 1–11. https://doi.org/10.1002/9781118786352.wbieg0511

Miccolis, A., Andrade, R. M. T., & Pacheco, P. (2014). *Land-use trends and environmental governance policies in Brazil - Paths forward for sustainability*. Retrieved from http://www.cifor.org/library/5435/land-use-trends-and-environmental-governance-policies-in-brazil-paths-forward-for-sustainability

Morais, P. B. de, Nolêto Júnior, S., & Martins, I. C. de M. (2017). Análise de sustentabilidade do projeto hidroagrícola Javaés/Lagoa, no estado do Tocantins. *Cadernos de Ciência & Tecnologia*, *34*(1), 83–111.

Näschen, K., Diekkrüger, B., Evers, M., Höllermann, B., Steinbach, S., & Thonfeld, F. (2019). The Impact of Land Use/Land Cover Change (LULCC) on Water Resources in a Tropical Catchment in Tanzania under Different Climate Change Scenarios. *Sustainability*, *11*(24), 7083. https://doi.org/10.3390/su11247083

Oliveira, T. A., Viola, M. R., Mello, C. R., Giongo, M., & Coelho, G. (2015). Natural vulnerability of water resources in the Formoso River basin, Northern Brazil. *African Journal of Agricultural Research*, *10*(10), 1107–1114. https://doi.org/10.5897/AJAR2014.9370

Paganeli, B., Dexter, K. G., & Batalha, M. A. (2020). Early growth in a congeneric pair of savanna and seasonal forest trees under different nitrogen and phosphorus availability. *Theoretical and Experimental Plant Physiology*, *32*, 19–30. https://doi.org/10.1007/s40626-019-00164-8

Pan, N., Feng, X., Fu, B., Wang, S., Ji, F., & Pan, S. (2018). Increasing global vegetation browning hidden in overall vegetation greening: Insights from time-varying trends. *Remote Sensing of Environment*, *214*, 59–72. https://doi.org/10.1016/j.rse.2018.05.018

Pereira, O. J. R., Ferreira, L. G., Pinto, F., & Baumgarten, L. (2018). Assessing pasture degradation in the Brazilian Cerrado based on the analysis of MODIS NDVI time-series. *Remote Sensing*, *10*(11). https://doi.org/10.3390/rs10111761

Pontius, R. G. (2000). Quantification error versus location error in comparison of categorical maps. *Photogrammetric Engineering and Remote Sensing*, *66*(8), 1011–1016.

Pontius, R. Gil. (2002). Statistical methods to partition effects of quantity and location during comparison of categorical maps at multiple resolutions. *Photogrammetric Engineering and Remote Sensing*, *68*(10), 1041–1049.

Salazar, A., Baldi, G., Hirota, M., Syktus, J., & McAlpine, C. (2015). Land use and land cover change impacts on the regional climate of non-Amazonian South America: A review. *Global and Planetary Change*, *128*, 103–119. https://doi.org/10.1016/j.gloplacha.2015.02.009

Sawakuchi, H. O., Ballester, M. V. R., & Ferreira, M. E. (2013). The Role of Physical and Political Factors on the Conservation of Native Vegetation in the Brazilian Forest-Savanna Ecotone. *Open Journal of Forestry*, *03*(01), 49–56. https://doi.org/10.4236/ojf.2013.31008

Sayasane, R., Kawasaki, A., Shrestha, S., & Takamatsu, M. (2016). Assessment of potential impacts of climate and land use changes on stream flow: A case study of the Nam Xong watershed in Lao PDR. *Journal of Water and Climate Change*, *7*(1), 184–197. https://doi.org/10.2166/wcc.2015.050

SEPLAN. (2012). *Atlas do Tocantins: subsídios ao planejamento da gestão territorial.* Palmas: Secretaria do Planejamento e da Modernização da Gestão Pública do Estado do Tocantins.

Setyorini, A., Khare, D., & Pingale, S. M. (2017). Simulating the impact of land use/land cover change and climate variability on watershed hydrology in the Upper Brantas basin, Indonesia. *Applied Geomatics*, *9*(3), 191–204. https://doi.org/10.1007/s12518-017-0193-z

Silva, J. F., Fariñas, M. R., Felfili, J. M., & Klink, C. A. (2006). Spatial heterogeneity, land use and conservation in the cerrado region of Brazil. *Journal of Biogeography*, *33*(3), 536–548. https://doi.org/10.1111/j.1365-2699.2005.01422.x

Singh, S. K., Mustak, S., Srivastava, P. K., Szabó, S., & Islam, T. (2015). Predicting Spatial and Decadal LULC Changes Through Cellular Automata Markov Chain Models Using Earth Observation Datasets and Geo-information. *Environmental Processes*, *2*(1), 61–78. https://doi.org/10.1007/s40710-015-0062-x

Spracklen, D. V., Baker, J. C. A., Garcia-Carreras, L., & Marsham, J. H. (2018). The Effects of Tropical Vegetation on Rainfall. *Annual Review of Environment and Resources*, *43*(1), 193–218. https://doi.org/10.1146/annurev-environ-102017-030136

Spracklen, D. V., Arnold, S. R., & Taylor, C. M. (2012). Observations of increased tropical rainfall preceded by air passage over forests. *Nature*, *489*(7415), 282–285. https://doi.org/10.1038/nature11390

Tocantins. (2007). *Plano de Bacia Hidrográfica do rio Formoso – PBH rio Formoso, no Estado do Tocantins: Relatório Síntese*. Retrieved from www.semarh.to.gov.br

Tocantins. (2011). *Elaboração do Plano Estadual de Recursos Hídricos do Tocantins*. Retrieved from www.semarh.to.gov.br

Viera, A. J., & Garrett, J. M. (2005). Understanding interobserver agreement: The kappa statistic. *Family Medicine*, *37*(5), 360–363.

Yira, Y., Diekkrüger, B., Steup, G., & Bossa, A. Y. (2016). Modeling land use change impacts on water resources in a tropical West African catchment (Dano, Burkina Faso). *Journal of Hydrology*, *537*, 187–199. https://doi.org/10.1016/j.jhydrol.2016.03.052

Zhilong, Z., Xue, W., Yili, Z., & Jungang, G. (2017). Assessment of Changes in the Value of Ecosystem Services in the Koshi River Basin, Central High Himalayas Based on Land Cover Changes and the CA-Markov Model. *Journal of Resources and Ecology*, *8*(1), 67–76. https://doi.org/10.5814/j.issn.1674-764x.2017.01.009

ARTIGO 3 Vegetation dynamics and the relations with soil erosion potential by water under climate change in the Tocantins-Araguaia River Basin, Brazil

Norma NBR 6022 (ABNT 2018)

Wharley Pereira dos Santos[a], Junior Cesar Avanzi[a*], Nilton Curi[a]

[a] Department of Soil Science, Federal University of Lavras (UFLA), Postal Code 37200-900, Lavras, MG, Brazil. *E-mail address*: wharleypereira@gmail.com; junior.avanzi@ufla.br; niltcuri@ufla.br *Corresponding author: junior.avanzi@ufla.br (J.C. Avanzi)

Abstract

Changes in vegetation growth dynamics can be controlled by climate and human activity. In this case, soil erosion by water is a major threat to agricultural productivity, leading to a decrease in the vegetation cover response during the rainy season. A potential erosion risk-mapping model has been applied in this study aiming at evaluating the relationship with growing-season NDVI. We analyzed potential risk of soil erosion and NDVI change in the Tocantins-Araguaia River Basin from 1985 to 2005, using Revised Universal Soil Loss Equation (RUSLE) factors that describe most susceptible to soil erosion, and long-term seasonality trends in the GIMMS third generation (NDVI3g) record (1985–2005). The results show that potential erosion risk values above a level considered high are predominant in the study area. The highest decreasing growing-season NDVI values are presented northward in the watershed, followed by an increasing potential erosion risk values. Moderate negative correlations (max. r = -0.59) between NDVI and potential erosion risk were observed in the north and southwestward of the watershed. This study may help the governors and other stakeholders understand the importance of vegetation structure to make right management decisions and avoid land degradation.

Keywords: Growing-Season NDVI, Climate change, Soil erosion potential, RUSLE, Watershed.

1 INTRODUCTION

Recent change of vegetation growth and its influence on the response of environmental factors are indicators of changes in the environment affecting agricultural activity and the dynamism of a natural ecosystem. Therefore, it is important to understand the controlling factors of variation in vegetation cover, as well as to evaluate the interaction between climatic variables and vegetation cover (ZHANG et al., 2019).

Changes in vegetation cover are mainly the result of land use and land cover changes due to human activities (AROWOLO; DENG, 2018; KLEIN GOLDEWIJK; RAMANKUTTY, 2004; SONG et al., 2018). Against this background, soil erosion by water is one of the main threats to productivity in agricultural lands and the assessment of the potential for soil erosion by water is essential to measure the cost-effectiveness of soil conservation policies (PLAMBECK, 2020).

The relationship between land use change and climate change has been strongly discussed in studies with analyzes for recent centuries (DALE, 1997; NICHOLSON, 2001; OSTBERG et al., 2015). Changes in land cover caused by climate are particularly worrying in tropical regions, due to interactions with land use change at a local scale, and such changes are significant according to their temporality (LAMBIN; GEIST; LEPERS, 2003; LLOPART et al., 2018; SCHIELEIN; BÖRNER, 2018). In order to analyze the dynamism of changes in vegetation cover and the influence of the climate factor, remote sensing data such as the Normalized Difference Vegetation Index (NDVI) have been widely used (GU et al., 2018; JACQUIN; SHEEREN; LACOMBE, 2010; ZEWDIE; CSAPLOVICS; INOSTROZA, 2017). The NDVI can reflect the growth of surface vegetation during the rainy season, proving to be a sensitive indicator of land use and land cover change.

For this study, we aimed to analyze the relative importance between potential risk of soil erosion (Epot) and the growing-season NDVI in Tocantins-Araguaia basin. Therefore, the results can indicate the significant correlations between vegetation and climatic factors in the agricultural and stock-raising development areas into the watershed.

2 MATERIALS AND METHODS

2.1 Study area

Figure 1 - The Tocantins-Araguaia basin and the Amazonia and Cerrado biomes.

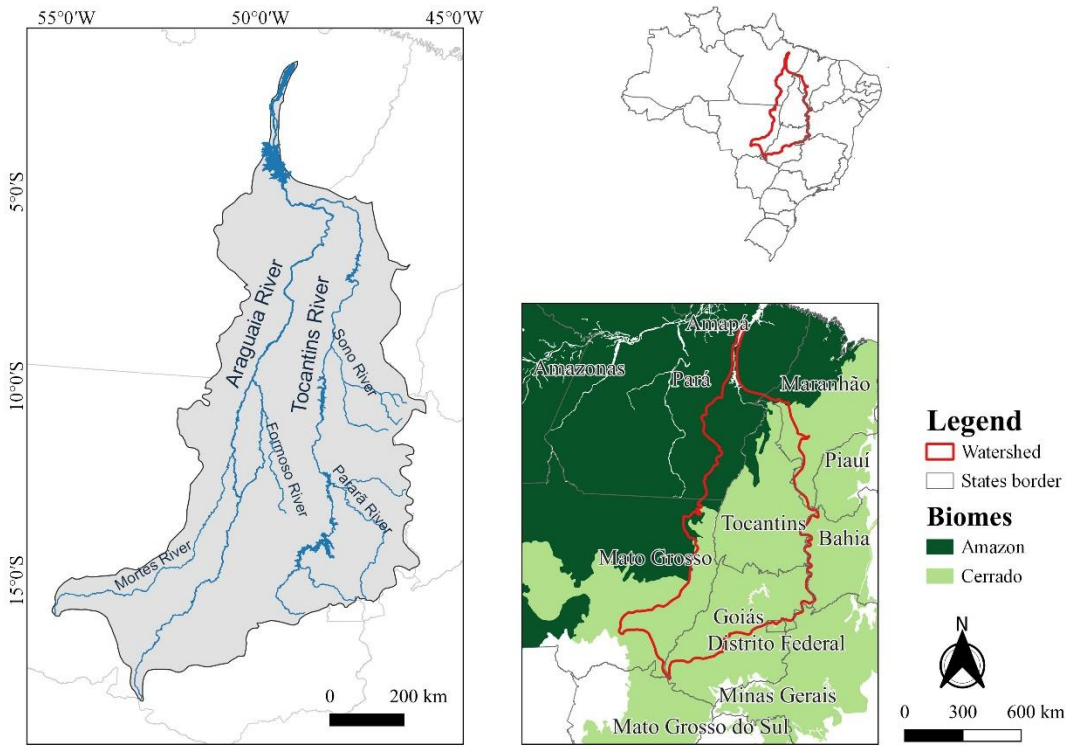

The Tocantins-Araguaia River Basin (TARB) is located in the central part of Brazil and it drains water from an area of 767,164 km² toward the northern coast (Fig. 1). The Tocantins River is the main river of the basin, and the Araguaia River is the large tributary river to the west. The watershed has a large drainage network, in which the Tocantins and Araguaia rivers allow a large extension navigation. The Amazon Biome predominates in the northwestern part

of the basin, while Cerrado Biome occupies the rest of the basin. The Cerrado Biome of the basin is inserted in the so-called MATOPIBA area (acronym for the names of the States of Maranhão, Tocantins, Piaui, and Bahia), which is one of the largest agro-industrial expansion zones in the world.

2.2 Data sources and pre-processing

2.2.1 GIMMS NDVI3g Dataset

The remote sensing dataset used to represent the vegetation change in this study is based on Global Inventory Modeling and Mapping Studies (GIMMS) 15-day composite NDVI3g v0 dataset (third generation from AVHRR sensors onboard the NOAA satellite series) with spatial resolution of 8 km × 8 km, which were acquired from Google Earth Engine (GEE). The NDVI3g v0 dataset has the longest time record and high quality. The maximum value composite method was used to generate the monthly NDVI (PIAO et al., 2011). The growing-season NDVI was calculated by the average monthly NDVI from October to April per year for the period 1985-2005. The GIMMS normalized difference vegetation index has been corrected for calibration, viewing geometry, stratospheric aerosols associated with volcanic eruptions (PINZON; TUCKER, 2014), and the NDVI3g v0 has been showed marked seasonality trends over large parts of the vegetated lands in the world for the period 1982–2013 (YE et al., 2021).

2.2.2 Potential risk of soil erosion dataset

In order to represent the soil erodibility (K-factor) in the watershed, we used a high-resolution (250 m cell size) spatially map across Brazil produced by Godoi et al. (2021). This factor was computed using the USLE nomograph with some essential soil properties, such as organic matter content, soil texture, soil structure, and permeability. The topographic factor was obtained using the SRTM digital elevation model (SRTM DEM) with a 30-m resolution data refinement over the entire Brazilian territory produced by SRTM/Topodata Project of National

Institute for Space Research (acronym in Portuguese: INPE) (DE MORISSON VALERIANO; DE FÁTIMA ROSSETTI, 2012). The rainfall erosivity factor, provided at 1km x 1km resolution, was calculated based on the overlapping baseline period of downscaling of four global climate multi-model ensemble of the Coupled Model Intercomparison Project (CMIP5) by the Eta regional climate model, named as Eta-BESM, Eta-CanESM2, Eta-HadGEM, and Eta-MIROC5, available in https://projeta.cptec.inpe.br and CORDEX-ESGF (DOS SANTOS et al., 2022).

2.3 Methods

2.3.1 Revised Universal Soil Loss Equation (RUSLE) and Potential risk of soil erosion

The USLE model was developed by Wischmeier and Smith (1978), and it's used to estimate the soil erosion in a plot of land with homogeneous characteristics. RUSLE, the revised version of USLE (RENARD et al., 1997) not only provides an estimation of soil loss at the plot scale, but also it is used to estimate the magnitude of soil erosion by water in watershed scale, spatializing water erosion, and delimiting high risk areas of water erosion in agricultural and forested watersheds. It is represented by the Eq. (1):

$$A = R\ K\ L\ S\ C\ P \quad (1)$$

A: Soil loss (Mg ha^{-1});
R: Rainfall erosivity factor (MJ mm ha^{-1} h^{-1});
K: Soil erodibility factor (Mg h MJ^{-1} mm^{-1});
L: Slope length factor (dimensionless);
S: Slope steepness factor (dimensionless);
C: Cover management factor (dimensionless);
P: Support practices factor (dimensionless).

Potential soil erosion risk (Epot) is the natural land susceptibility of erosion, irrespective of current land use or land cover. It is calculated from the physical parameters of the RUSLE – rainfall erosivity (R), soil erodibility (K), slope length (L) and steepness (S).

$$Epot = R\ K\ LS \qquad [Mg\ ha^{-1}\ year^{-1}] \qquad (2)$$

The separation of physical data from management data in the USLE is useful to indicate the potential improvement in soil erosion through changing management (SAMPSON, 1986).

The methodology followed for the development of rainfall erosivity factor values has been described before by dos Santos et al. (2022). The methodology used to estimate the topographic factor was based on the Desmet and Govers (1996) algorithm in the LS factor field-based modules of SAGA GIS.

2.3.2 Sen's slope and correlation analysis of the growing-season NDVI anomaly and potential soil erosion risk

We investigated the probable effects of record length on potential soil erosion risk and NDVI trends in Tocantins-Araguaia River Basin. The change over the period can be calculated by Sen's slope (SEN, 1968). Sen's estimator was used to determine the sign and magnitude of trend, *i.e.* change per unit time in Epot and growing-season NDVI time series. In other words, the slope coefficient determines the rate of increase or decrease in the trend and direction of change. This method is widely used to trend detection (BARVELS; FENSHOLT, 2021; HUANG; KONG, 2016; LIU et al., 2019; MUELLER; PFISTER, 2011; OĞUZ, 2019).

In addition, this study used linear correlation analysis to verify the relationship between the potential soil erosion risk and the growing-season NDVI. The Pearson correlation coefficient (r) between those two variables was calculated to assess the impact on vegetation dynamics of rainfall erosivity on soil and its interaction with the other factors concerned the

inherent risk of erosion. All images were resampled to overlay the lowest resolution of raster dataset provided.

3 Results

In assessing the potential risk of soil erosion, it can be seen from Figure 2a that values above a level considered high are predominant in the Tocantins-Araguaia basin. In the Tocantins River sub-basin, soil losses values above 600 Mg ha^{-1} $year^{-1}$ were observed in a large area. The greatest trends of Epot increase in the watershed were verified in its northwest portion (Fig. 2b), in natural areas of contact between the Cerrado and Amazon Biomes of great natural relevance.

Figure 2 - Average Annual potential risk of soil erosion (a) and Theil–Sen's slope for the annual data series during the period 1985–2005 (b).

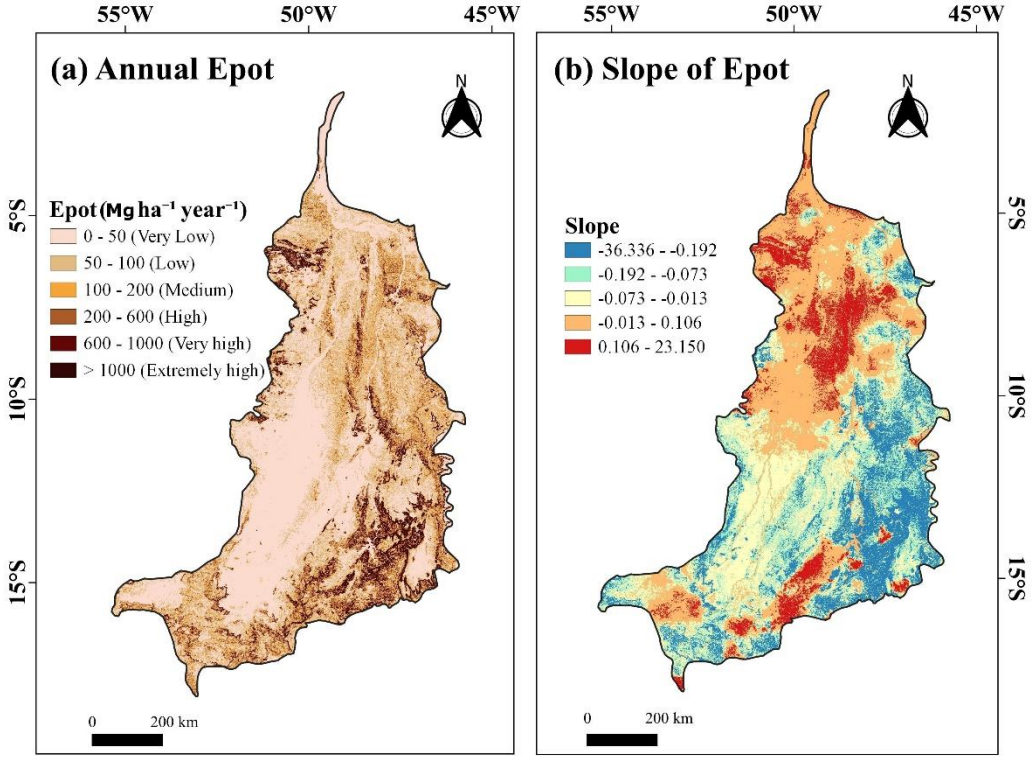

Classification of potential soil erosion risk based on Correa and Pinto (2012).

In the Tocantins-Araguaia basin scale, as shown in Figure 3a, the average annual values of growth-season NDVI showed the predominance of values above 0.6 in most of the

watershed, considering the period analyzed in the study. The average annual value of NDVI in the west of the watershed was very low, evidencing the characteristic predominance of soil exposed to sparse vegetation in the Sono River sub-basin, an important tributary of the Tocantins River on the right bank. The spatial distribution of the growing season NDVI in the TARB from 1985 to 2005 exhibited the largest decreases, almost exclusively concentrated in the north of the watershed with decreasing trend of mean NDVI at a rate above 0.001/yr (Fig 3b).

Figure 3 - Average growing-season NDVI (a) and Theil–Sen's slope for the NDVI trend during the period 1985–2005 (b).

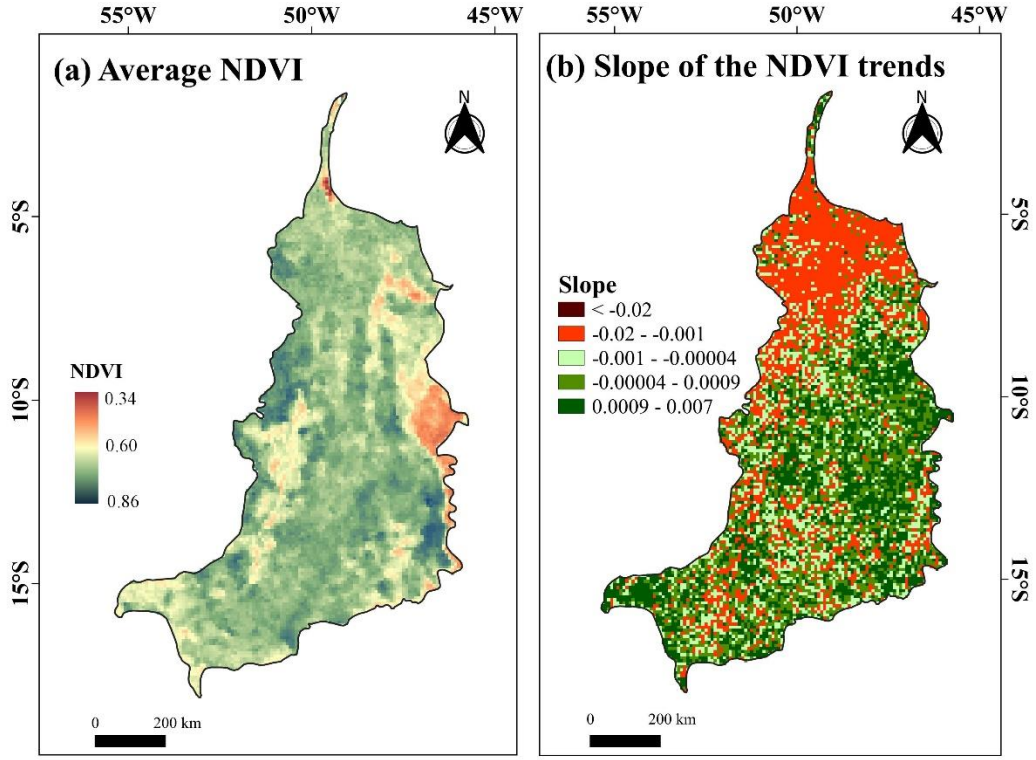

Analyzing Figure 4, we can verify the presence of alternating periods of reduction and increase in the growing-season NDVI values (Fig 4a) and the potential risk of soil erosion (Fig 4b) in the watershed. The period of greatest NDVI reduction in the time series between 1990 and 1991 was followed by the most drastic increase in the potential risk of soil erosion in the watershed. In contrast, the large decrease in Epot between 1989 and 1992 was followed by a

strong upward trend in NDVI. In this feedback process characteristic of the variables under analysis, the large increase in Epot between 1992 and 1995 forced a downward trend in the NVI until the end of the time series under study. The underlying premise of the analysis directs the degree of influence of the erosive potential of rainfall on the Epot according to significant changes in land use. The average values of the highest potential risk of soil erosion over the Tocantins sub-basin exceed at high to extremely high levels the average in the time series of the watershed.

Figure 4 - Mean growing-season NDVI time-series (a) and the mean potential risk of soil erosion time-series (b) in Tocantins-Araguaia basin.

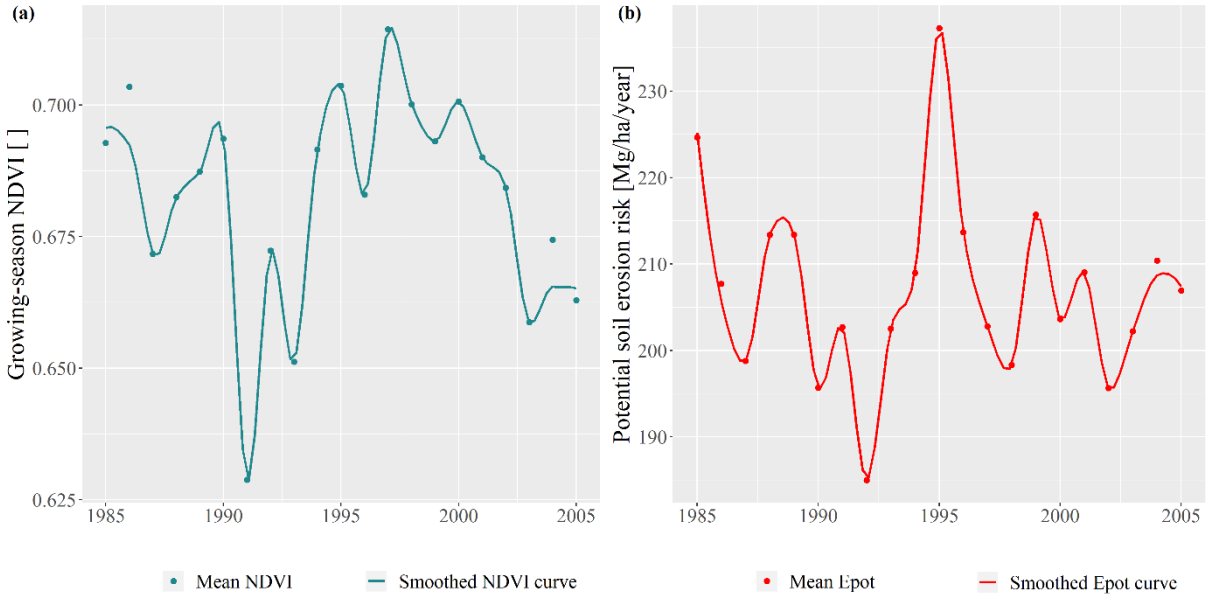

The inter-relationship between growing-season NDVI and the potential risk of soil erosion is represented in Figure 5 through the spatial distribution of the correlation coefficient (r) between Epot and NDVI during the years 1985-2005. Moderate negative correlations (max. r = -0.59) between NDVI and Epot were found in the north and southwestward of the watershed, agricultural frontier regions in Brazil. In contrast, other parts of the study region the decreasing trend in NDVI combined with a decreasing trend in Epot allowed the lowest positive values of r.

Figure 5 - Spatial patterns of correlation coefficients between growing-season NDVI and annual potential risk of soil erosion (Epot) over Tocantins-Araguaia basin during the period of 1985–2005.

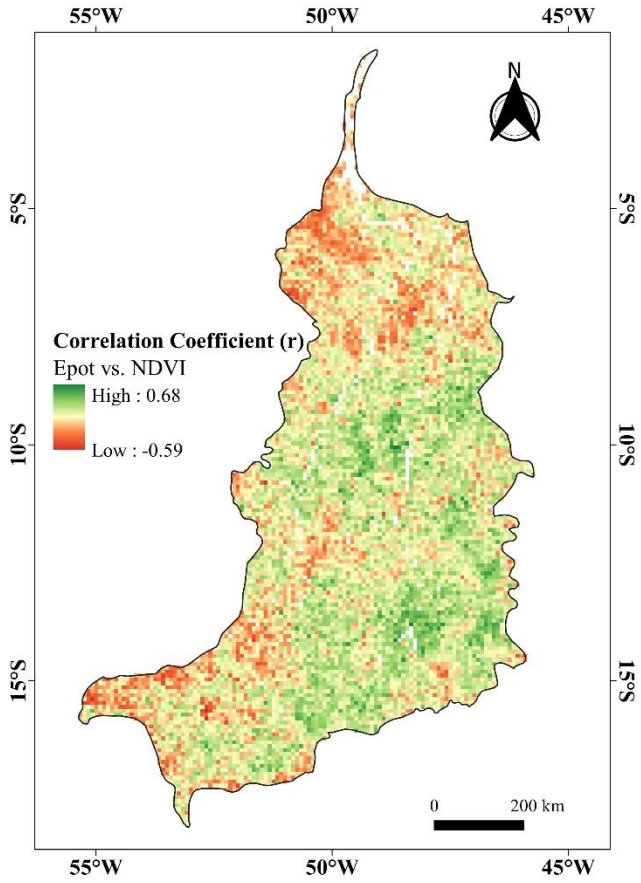

4 DISCUSSION

The Brazilian territory has expressive areas with high to very high susceptibility to water erosion; therefore, the natural erosion potential of soils in the study area is worrying, as it is highly influenced by high levels of rainfall erosivity, as presented by da Silva, Alcarde and Hitomi (2011) and Oliveira, Wendland and Nearing (2013). Land degradation in Cerrado pastures tends to exacerbate this concern even further, as the expansion of agricultural and pasture lands without a political direction for sustainable management in the states where the basin covers, can intensify deforestation and even lead to the abandonment of lands. Study performed by Pereira et al. (2018) a positive correlation was found between the negative slope

of the NDVI and the Human Development Index (HDI), which directs the axis of poverty and degradation further north of the Cerrado, where the MATOPIBA agricultural frontier region is located.

The most likely reason for the decreasing NDVI trend is the land degradation by the human activities, particularly as consequence of deforestation and overuse of pasture land in the northward of watershed. The northernmost region of the watershed includes lands of Amazon Biome, which has been impacted by forest degradation (MATRICARDI et al., 2020), combined with the intensification of the dry season and an increase in deforestation in the eastern Amazon (GATTI et al., 2021). It was clearly seen that the increasing of potential risk of soil erosion in these areas represent a strong influence of the land use change through deforestation. The loss in vegetation cover could either exacerbate the trend in rainfall erosivity indices, accelerating the soil erosion risk in agricultural frontier lands in Tocantins-Araguaia River Basin.

The assessment of soil erosion risk by water in heterogeneous soil conservation policies is important instrument for implementing control measures according to cost-effectiveness, however, in order to have an effective decision-making, other evaluations must be taken into account in large scale, *e.g.* establishing tolerance thresholds for soil loss and modelling sediment delivery (BISWAS et al., 2015; BATISTA et al., 2017; BORRELLI et al., 2018; PLAMBECK, 2020; ZHU et al., 2019). Despite the strong negative correlation between Epot and growing-season NDVI in agricultural lands, it represents the influence of climate change on the erosive potential of rainfall as a preponderant factor for the risk of soil erosion. In order to evaluate an interference of human activities on growing-season NDVI, other variables, *viz.* other vegetation indices that best describe the vegetation cover dynamics, to identify potential areas of land degradation at a regional scale (YENGOH et al., 2014; ZHONGMING et al., 2010).

This study informs the importance to analyzing the causes of land degradation based on evaluation of potential soil erosion risk and green vegetation cover change. It can be used as a direction to future land management strategies to be taken into account by policy-makers and stakeholders.

5 CONCLUSIONS

Moderate relationship was recorded between growing-season NDVI and climate erosivity change represented in the year-on-year change of the potential soil erosion risk. The highest decreasing NDVI values are observed northward in the watershed, followed by an increasing Epot in this region. Maximum negative correlations (r = –0.59) between growing-season NDVI and Epot are featured on north and southwestward of the watershed, where the agriculture and cattle-raising activities expansion is under development in Brazil. The assessment of soil erosion risk by water is important to soil conservation policies, and its relationship with NDVI could show that land degradation in fact is dependent on climate change and/or alterations due to human activity.

References

AROWOLO, A. O.; DENG, X. **Land use/land cover change and statistical modelling of cultivated land change drivers in Nigeria.** Regional Environmental Change, v. 18, n. 1, p. 247–259, 2018.

BATISTA, P. V. G. *et al.* **Modelling spatially distributed soil losses and sediment yield in the upper Grande River Basin-Brazil.** Catena, v. 157, p. 139-150, 2017.

BARVELS, E.; FENSHOLT, R. **Earth Observation-Based Detectability of the Effects of Land Management Programmes to Counter Land Degradation:** A Case Study from the Highlands of the Ethiopian Plateau. Remote Sensing, v. 13, n. 7, p. 1297, 29 mar. 2021.

BISWAS, H. *et al.* **Identification of areas vulnerable to soil erosion risk in India using GIS methods.** Solid Earth, v. 6, n. 4, p. 1247–1257, 2015.

BORRELLI, P. *et al.* **A step towards a holistic assessment of soil degradation in Europe:** Coupling on-site erosion with sediment transfer and carbon fluxes. Environmental Research, v. 161, n. September 2017, p. 291–298, 2018.

CORREA, E. A.; PINTO, S. A. F. S. **Avaliação do potencial natural de erosão da bacia**

hidrográfica do córrego Monjolo Grande (Ipeúna-SP). Revista Geonorte, v. 4, n. 2, p. 1356–1367, 2012.

DA SILVA, A. M.; ALCARDE, C.; HITOMI, C. **Natural Potential for Erosion for Brazilian Territory.** In: GODONE, D. (Ed.). . Soil Erosion Studies. London: InTech, 2011. p. 1–24.

DALE, V. H. **The relationship between land-use change and climate change.** Ecological Applications, v. 7, n. 3, p. 753–769, 1997.

DE MORISSON VALERIANO, M.; DE FÁTIMA ROSSETTI, D. **Topodata:** Brazilian full coverage refinement of SRTM data. Applied Geography, v. 32, n. 2, p. 300–309, mar. 2012.

DESMET, P. J. J.; GOVERS, G. **A GIS procedure for automatically calculating the USLE LS factor on topographically complex landscape units.** Journal of Soil and Water Conservation, v. 51, n. 5, p. 427–433, 1996.

DOS SANTOS, W. P. *et al.* **Projections of rainfall erosivity in climate change scenarios for the largest watershed within Brazilian territory.** CATENA, v. 213, n. August 2021, p. 106225, jun. 2022.

GATTI, L. V. *et al.* **Amazonia as a carbon source linked to deforestation and climate change.** Nature, v. 595, n. 7867, p. 388–393, 2021.

GODOI, R. DE F. *et al.* **High-resolution soil erodibility map of Brazil.** Science of The Total Environment, v. 781, p. 146673, ago. 2021.

GU, Z. *et al.* **Spatiotemporal variation in vegetation coverage and its response to climatic factors in the Red River Basin, China.** Ecological Indicators, v. 93, n. March, p. 54–64, out. 2018.

HUANG, S.; KONG, J. **Assessing Land Degradation Dynamics and Distinguishing Human-Induced Changes from Climate Factors in the Three-North Shelter Forest Region of China.** ISPRS International Journal of Geo-Information, v. 5, n. 9, p. 158, 2 set. 2016.

JACQUIN, A.; SHEEREN, D.; LACOMBE, J.-P. **Vegetation cover degradation assessment in Madagascar savanna based on trend analysis of MODIS NDVI time series.** International Journal of Applied Earth Observation and Geoinformation, v. 12, n. SUPPL. 1, p. S3–S10, fev. 2010.

KLEIN GOLDEWIJK, K.; RAMANKUTTY, N. **Land cover change over the last three centuries due to human activities:** The availability of new global data sets. GeoJournal, v. 61, n. 4, p. 335–344, 2004.

LAMBIN, E. F.; GEIST, H. J.; LEPERS, E. **Dynamics of Land-Use and Land-Cover Change in Tropical Regions.** Annual Review of Environment and Resources, v. 28, n. 1, p. 205–241, nov. 2003.

LIU, Q. *et al.* **Vegetation degradation and its driving factors in the farming-pastoral ecotone over the countries along belt and road initiative.** Sustainability (Switzerland), v. 11, n. 6, 2019.

LLOPART, M. *et al.* **Land Use Change over the Amazon Forest and Its Impact on the Local Climate.** Water, v. 10, n. 2, p. 149, 3 fev. 2018.

MATRICARDI, E. A. T. *et al.* **Long-term forest degradation surpasses deforestation in the Brazilian Amazon.** Science, v. 369, n. 6509, p. 1378–1382, 2020.

MUELLER, E. N.; PFISTER, A. **Increasing occurrence of high-intensity rainstorm events relevant for the generation of soil erosion in a temperate lowland region in Central Europe.** Journal of Hydrology, v. 411, n. 3–4, p. 266–278, dez. 2011.

NICHOLSON, S. E. **Climatic and environmental change in Africa during the last two centuries.** Climate Research, v. 17, n. 2 SPECIAL 8, p. 123–144, 2001.

OĞUZ, I. **ESTIMATION OF SOIL EROSION AND RIVER SEDIMENT YIELD IN A RURAL BASIN OF NORTH ANATOLIA, TURKEY.** Applied Ecology and Environmental Research, v. 17, n. 4, p. 7741–7763, 2019.

OLIVEIRA, P. T. S.; WENDLAND, E.; NEARING, M. A. **Rainfall erosivity in Brazil:** A review. CATENA, v. 100, p. 139–147, jan. 2013.

OSTBERG, S. *et al.* **Three centuries of dual pressure from land use and climate change on the biosphere.** Environmental Research Letters, v. 10, n. 4, p. 044011, 1 abr. 2015.

PEREIRA, O. J. R. *et al.* **Assessing pasture degradation in the Brazilian Cerrado based on the analysis of MODIS NDVI time-series.** Remote Sensing, v. 10, n. 11, 2018.

PIAO, S. *et al.* **Changes in satellite-derived vegetation growth trend in temperate and boreal Eurasia from 1982 to 2006.** Global Change Biology, v. 17, n. 10, p. 3228–3239, out. 2011.

PINZON, J.; TUCKER, C. **A Non-Stationary 1981–2012 AVHRR NDVI3g Time Series.** Remote Sensing, v. 6, n. 8, p. 6929–6960, 25 jul. 2014.

PLAMBECK, N. O. **Reassessment of the potential risk of soil erosion by water on agricultural land in Germany:** Setting the stage for site-appropriate decision-making in soil and water resources management. Ecological Indicators, v. 118, p. 106732, nov. 2020.

RENARD, K. G. *et al.* **Predicting Soil Erosion by Water:** A Guide to Conservation Planning with the Revised Universal Soil Loss Equation (RUSLE)Agriculture Handbook. Washington, DC, USA: [s.n.].

SAMPSON, R. N. **Erosion on range and forest lands:** impacts of land use and management practices. In: Soil conservation–assessing the national resources inventory. [s.l: s.n.]. p. 163–194.

SCHIELEIN, J.; BÖRNER, J. **Recent transformations of land-use and land-cover dynamics across different deforestation frontiers in the Brazilian Amazon.** Land Use Policy, v. 76, n. January, p. 81–94, jul. 2018.

SEN, P. K. **Estimates of the Regression Coefficient Based on Kendall ' s Tau.** Journal of the American Statistical Association, v. 63, n. 324, p. 1379–1389, 1968.

SONG, X. P. *et al.* **Global land change from 1982 to 2016.** Nature, v. 560, n. 7720, p. 639–643, 2018.

WISCHMEIER, W. H.; SMITH, D. D. **Predicting rainfall erosion losses** —a guide to conservation planning.U.S. Department of Agriculture, Agriculture Handbook. Washington, DC: [s.n.].

YE, W. *et al.* **Global trends in vegetation seasonality in the GIMMS NDVI3g and their robustness.** International Journal of Applied Earth Observation and Geoinformation, v. 94, p. 102238, fev. 2021.

YENGOH, G. T. *et al.* **The use of the Normalized Difference Vegetation Index (NDVI) to assess land degradation at multiple scales:** a review of the current status, future trends, and practical considerations. Lund, Sweden: [s.n.].

ZEWDIE, W.; CSAPLOVICS, E.; INOSTROZA, L. **Monitoring ecosystem dynamics in northwestern Ethiopia using NDVI and climate variables to assess long term trends in dryland vegetation variability.** Applied Geography, v. 79, p. 167–178, fev. 2017.

ZHANG, Y. *et al.* **Effects of climate change on lake area and vegetation cover over the past 55 years in Northeast Inner Mongolia grassland, China.** Theoretical and Applied Climatology, v. 138, n. 1–2, p. 13–25, 2019.

ZHONGMING, W. *et al.* **Stratified vegetation cover index:** A new way to assess vegetation impact on soil erosion. CATENA, v. 83, n. 1, p. 87–93, out. 2010.

ZHU, M. *et al.* **Spatial and temporal characteristics of soil conservation service in the area of the upper and middle of the Yellow River, China.** Heliyon, v. 5, n. 12, p. e02985, dez. 2019.